Faculty of Sciences
Department of Earth and Environmental Sciences
onkabetse.phuthego@studentmali.biust.ac.bw

HYDROLOGICAL MODEL CALIBRATION OF THE LIMPOPO RIVER BASIN IN BOTSWANA: AN APPLICATION FOR WATER RESOURCES PREDICTION UNDER THE CONTEXT OF CLIMATE CHANGE

by

ONKABETSE PHUTHEGO
Student ID number: 12 000 452
BSc (Earth & Environmental Science) (BIUST)

A Thesis Submitted to the Faculty of Sciences in Partial Fulfilment of the Requirements for the Award of the Degree of Master of Science in Environmental Science by Botswana International University of Science and Technology

Supervisor(s):

Dr. Sithabile Tirivarombo

Department of Earth and Environmental Science

Faculty of Science

BIUST

tirivarombos@biust.ac.bw

October, 2022

Table of Contents

BOTSWANA INTERNATIONAL UNIVERSITY OF SCIENCE & TECHNOLOGY

POSTGRADUATE SCHOOL

Declaration Regarding the Work and Copyright

DECLARATION REGARDING THE WORK AND COPYRIGHT

Candidate: ONKABETSE PHUTHEGO

Student ID: 12000452

Thesis Titled: Hydrological model calibration of the Limpopo river basin in Botswana: an application for water resources prediction under the context of climate change

I, ONKABETSE PHUTHEGO, certify that the Thesis is all my own original work and that I have not obtained a degree in this University or elsewhere on the basis of any of this work.

Signed: -- Date: 22nd October 2022

Primary Supervisor

I, DR. SITHABILE TIRIVAROMBO the Candidate's **Primary Supervisor**, hereby confirm that I have inspected the above titled thesis and, to the best of my knowledge, it is based on the original work of the candidate.

Signed: -- Date: 22nd October 2022

Abstract

The 21st century is faced with various climate related problems, amongst them water stress brought about by increased frequency of extreme hydrological droughts Freshwater resources are sensitive to variable climates and are bound to be strongly impacted by climate change. This in turn has negative impacts on both the quantity and quality of water resources required to meet human and environmental demands. Apart from climate driven factors, other forces contributing to the impairment of water resources availability include but are not limited to population growth, rapid urbanization, various land use activities and water pollution.

Africa is considered one of the most vulnerable continents by virtue of an inherently variable climate and because of low adaptive and coping capacities. The consequences of high climatic variability and climate change are likely to be felt more severely in arid and semi-arid regions such as Botswana, where water resources are scarce and most livelihoods rely entirely on rain fed agriculture for sustenance. Equitable and sustainable water allocation in such regions requires appropriate and timely water management strategies that can adequately account for the available water resources. Such strategies should be well informed by scientific findings as well as availability of reliable hydrological records. However, most regions especially in southern Africa are characterised by hydrological data paucity mainly because of inconsistent monitoring or due to lack of resources to carry out the monitoring programme.

Deficiencies in hydrological data can partly be addressed by calibrating a hydrological model which can then be used to simulate future hydrological conditions in a catchment. If the calibrated model responds well to the catchment specific characteristics and processes it can then be used as a baseline proxy for data upon which, certain hydrological variables can be predicted. Moreover, a well calibrated and validated model gives the assurance that the model can reliably represent the catchment hydrological characteristics at any given time. If prediction can be reliably carried out, data on some of the missing variables can be derived as this may be the case in data sparse regions. Hydrological modelling therefore becomes more important for solving problems related to climate variability and change on the one hand and addressing water and food security on the other hand. Hence, once calibrated model can be used for various water use scenarios and for predicting water availability in the future. The predictive model outputs can be used to inform decision making in water resources management particularly where the catchment is ungauged or lacks quality hydrological data

The main aim of this study was to calibrate a hydrological model for the sub-basins of the Limpopo River located in Botswana. As an example of model application, the calibrated model was then used to predict streamflow in the future (2025 -2050) under the context of climate change. To further validate the calibrated model, two drought indices were compared consisting of the Standardized Streamflow Index (SSI, generated from simulated streamflow) and the Standardised Precipitation Evapotranspiration Index (SPEI).

The study applied a three-fold process where, firstly the semi-distributed Pitman hydrological model was set up and calibrated for the sub-basins in the study area. Second, by coupling with downscaled and bias corrected Global Climate Model

(GCM) datasets, the calibrated model was then used to predict streamflow in the future under the context of climate change. The GCMs consisted of the Representative Concentration Pathway 4.5 and were extracted from the Coordinated Regional Climate Downscaling Experiment (CORDEX). Finally, a comparative analysis of drought was performed using the SSI and SPEI.

The Pitman model has been successfully calibrated for the Limpopo sub-basins in Botswana. This can be inferred from the statistical objective performance functions where both the Nash-Sutcliffe coefficient of efficiency (CE) and the coefficient of determination (R^2) were > 0.5 while the percent bias was <20 % on average. Generally, streamflow is expected to decrease in the near future on average by ≥25%. Despite slight differences in the frequency of occurrence of future droughts, this study revealed a close positive correlation between the streamflow derived drought index (SSI) and SPEI. There were no significance differences at the 95% confidence interval between SSI and SPEI, thus further reinforcing the capability of the calibrated model to simulate future hydrological conditions in the Limpopo sub-basins of Botswana. The study concludes that the calibrated model can adequately represent the hydrological response characteristics in the study area and can therefore be used to inform decision making in managing the basin's water resources. The calibrated model can also be applied to predict different hydrological variables. Nonetheless, it is always necessary to acknowledge predictive uncertainty when simulating hydrological components under future conditions of climate change.

Acknowledgements

Firstly, I would like to thank the Almighty for giving me the opportunity and strength to undertake this research study to its completion.

I would like to express my sincere gratitude to my supervisor Doctor Sithabile Tirivarombo for all the support, technical guidance and prompt feedback she provided throughout the entire course of my research. Through her guidance and support, she has helped me improve the depth of my knowledge in hydrological modelling and appreciate the concept more. Her patience and constructive criticisms have helped in achieving my goal.

I would also like to extend my gratitude to the Botswana International University of Science and Technology (BIUST) for providing both the financial assistance and a favourable environment to carry out my research.

I am extremely grateful to the Department of Water and Sanitation, Ministry of Agriculture Development and Food Security, Water Utilities Corporation and Department of Meteorological Services, Botswana for providing me with the data that was required to carry out this research.

I would like to acknowledge every individual who has provided a word of suggestion and encouragement to making this research a success and thank you to my colleagues who made it easier during the tough times of my study period at BIUST.

Lastly, I would like to thank my family and friends for their patience, sacrifices and emotional support they provided throughout the course of my study.

LIST OF TABLES

List of Figures

Chapter 1

Introduction

1.1 Background of the study

Water forms a fundamental basis for ecosystem sustainability while at the same time, it is a medium through which the effects of a changing climate are experienced. Rainfall and temperature are the most common variables that can be used to indicate any changes in climate (Jacobsen et al., 2005; Broader, 2011). Higher than normal average temperatures and variations in precipitation, together with other climatic variables are projected to affect the availability of water resources in various ways. Impacts include changes in rainfall distributions, soil moisture, streamflow and groundwater recharge. Flood and drought events are predicted to occur more frequently due to global climate change and this may have adverse impacts on water resources availability (Talafre and Knabe, 2009). Scientific evidence shows that freshwater resources are highly vulnerable to the impacts of climate variability and climate change (Mbaye et al., 2015). These consequences are felt more in arid and semi-arid regions of the world as such Botswana may face challenges of surface water availability in the face of global climate change. Due to a low adaptive capacity Africa is considered one of the most vulnerable continents to the effects of climate variability and climate change. It is reported that an estimated 300 million people have already been affected by water shortages (Eriksen et al., 2008; WWAP, 2009). The impacts of climate variability and climate change are worsened by the fact that a larger proportion of the population in southern Africa depends entirely on rainfed agriculture for sustenance. Continued efforts to minimize risk to climate related vulnerabilities require adequate planning and long-term management of freshwater resources.

However, one of the drawbacks to effective and sustainable development of water resources in southern Africa is lack of reliable baseline information, particularly hydroclimatic data.

Climate variability and climate change alter the hydrological regime resulting in changes in precipitation, runoff, soil moisture and evapotranspiration (Collier et al., 2008; Kundzewicz, 2008). The severe effect imposed by a changing climate on water resources tends to amplify the impacts of other stresses such as those resulting from changing economic activity, land-use change and urbanization. For example, during the 1970s Africa experienced a considerable decrease in rainfall such that rain-fed agriculture was negatively impacted while seasonal flooding of wetlands was reduced and poverty levels spiked across the region (Mbaye et al., 2015). Climate predictions indicate a change in rainfall and increased variability across the continent. For example, Hernes et al. (1995) postulated an increase of 1.6°C in temperature by the year 2050 whereas Ragab and Prudhomme (2002) predicted an average temperature increase of 1.5°C to 2.5°C in southern Africa and an increase of 2.5°C to 3°C in the northern parts of Africa by 2050. Due to climate change, arid and semi-arid lands are likely to increase in areal extent by 5-8% by the 2080s, resulting in depletion of water resources thus causing drier areas to be highly impacted by the slightest decrease in rainfall (Collier et al., 2008; Batisani and Yarnal, 2010). De Wit and Stankiewicz (2006) report that by the end of the twenty-first century 25% of Africa's surface water may be threatened due to reductions in perennial drainage. It is therefore clear that proper water resources planning and management strategies are required in arid and water scarce regions of the world.

To understand catchment hydrology and to be able to predict water resources in a catchment, a hydrological modelling approach has been adopted in this study. Hydrological models have proven to be primary tools that can be used to generate continuous estimates of hydrological data and other variables especially in areas that are data scarce. Models mimic the real-world system and are therefore expected to bring out results that are close to reality (Devi et al., 2015). A rainfall-runoff model consists of a series of equations that estimate runoff as a function of several parameters used to characterise a watershed (Sorooshian et al., 2008). There are different hydrological models each of which are classified according to the runoff generation mechanism that the model employs (Tessema, 2011). Hydrological models are used to predict the impacts of different water use scenarios and climate change on water resources. For example, to determine the impact of climate change on water resources the hydrological model is force, driven with data from global climate models (GCMs) using different scenarios. The incorporation of climate model information into a hydrological model therefore suggests a connection between current climate variability and water-related management which will aid in adapting to longer climate change impacts.

1.2 Problem statement

Botswana is characterised by a semi-arid type of climate, with low annual rainfall amounts. Furthermore, the country experiences low surface runoff with shallow water storages, since the dams have large surface areas that expose the available water to high temperatures thus high rates of evaporation (McJannet, 2008). These conditions contribute to water scarcity especially in a country that relies heavily on rainfed agriculture. Prolonged dry seasons as result of climate change are expected to amplify and propagate water related challenges into the future. Therefore, a need arises to provide information on potential future changes in the hydrological regime which will aid decision-makers in developing better management, mitigation and adaptation strategies that guarantee equitable and sustainable access to water. To do this, good quality time series datasets are required upon which a baseline can be created for future predictions. However, most of southern Africa is characterised by data paucity and thus calibrated hydrological models become ideal tools for hydrological predictions.

1.3 Significance of the study

There are numerous gaps in knowledge when dealing with water management in a catchment. This may be due to lack of adequate hydrometric data, for example, some basins are ungauged and some lack observational data. Such limitations can be an impediment to the proper management of water resources. Calibrated hydrological models can be used to address the limitations of data paucity at the local scale. There is an intricate relationship between water resources and climate implying that most catchment hydrological processes are climatically driven. Therefore, the need arises for improved understanding of climate related issues with respect to the hydrological regime at scales relevant to decision making. This study calibrates a hydrological model for the Limpopo sub-basins in Botswana. The calibrated model is then applied to evaluate the impacts of future climate change on streamflow. The results of the study can be used to assist decision makers on how best to plan and manage water resources especially in ungauged catchments and in view of global climate change. The application of hydrological modelling also deepens our knowledge on catchment specific hydrological processes.

Most of the southern African region is characterised by hydrological data paucity. This may be attributed to various reasons such as inconsistent monitoring and insufficient resources. Insufficient data complicates the prediction of water resources for the future.

1.4 Objectives of the study

The focus of this study was to calibrate a hydrological model for the sub-basins of the Limpopo in Botswana and use the calibrated model to predict water availability in the future under the context of climate change. The specific objectives of the study are as follows:

i. **Calibrate a hydrological model for the sub-basins of the Limpopo that lie in Botswana.**

   The modified Pitman monthly rainfall-runoff model is calibrated for the sub-basins in the study area. Since the model is a physically based model; founded on a thorough understanding of physical processes and the application of fundamental hydrodynamic laws, the parameter estimations are guided by the physical processes of the catchment.

ii. **Simulate streamflow in the Limpopo sub-basins under future climate change scenarios.**

   To understand the impacts of a changing climate on water resources, the calibrated hydrological model is force driven with climate model data from different GCMs to simulate future streamflow.

iii. **Assess the occurrence of historical and possible future droughts (in the face of climate change.**

   Semi-arid regions like Botswana are prone to extreme hydrological events, where droughts tend to be recurring phenomenon. Droughts have drastic effects on regions that are already water scarce. This study assesses historical droughts and determines future droughts under the context of climate change. To achieve this, the Standardized Precipitation Evapotranspiration Index (SPEI) is used.

iv. **Perform a comparative analysis of the Standardised Streamflow Index (SSI) and Standardised Precipitation Evapotranspiration Index (SPEI).**

This process further validates the performance of the calibrated hydrological model by comparing droughts generated from streamflow simulated by the calibrated model to those generated by SPEI.

1.5 Expected outcome

This research aims to enhance the understanding of hydrological processes at the catchment scale. It will enable the application of hydrological modelling at the operational levels and under different water use and climate change scenarios. Furthermore, the study can be used as a preliminary to inform possible management and adaptation strategies for integrated water resources management.

Chapter 2

Literature review

2.1 Introduction

Water plays a crucial role towards sustaining the ecological and developmental needs for humans and the biophysical environment. However, both surface and groundwater resources are under threat from over abstraction and from various sources of pollution (Lentswe and Molwalefhe, 2020). These threats have negative impacts especially in arid and semi-arid areas where groundwater is the primary source of water. Also during prolonged dry periods when shallow moisture reserves are depleted, groundwater plays a crucial role in sustaining the ecosystem and watershed needs (Grafton and Hussey, 2011). The Global Risk Perception Survey conducted in 2015 reported that water scarcity would present the largest impact on society in the next 10 years (World Economic Forum, 2015). Better management strategies are therefore required to safeguard and sustain the scarce water resources while at the same time preserving the hydrological regime of a catchment (Zakaria, 2010; Teutschbein, 2013). These strategies should be able to strike a balance between a growing population's need for water while at the same time assisting in decision making by using water resources tools which allow for estimation and allocation of the predicted water resources (Loucks et al., 2005).

2.1.1 Threats to global water resources

The 21st century is faced with various problems, some of which are caused by natural events while others are caused by anthropogenic activities. Excessive water use by the various water users is one factor that elevates stress on water resources causing demand to fall short of supply (Agarwal et al., 2000). Water scarcity is likely to be worsened by a rapidly growing population and the water use patterns of a modern population while on the other hand rapid urbanisation and climate change are contributing factors to increasing water scarcity (Donnelly and Cooley, 2015). According to the World Bank (2016), rapid population growth and increasing development have reduced the global freshwater availability per capita per year from 13 360.32 m^3 to 5 925.67 m^3 between 1962 and 2014. Water pollution aggravates water scarcity in the sense that polluted water is not fit for any use. The World Assessment Program asserts that globally, two million tonnes of human waste are discharged into water courses daily while the global nitrogen pollution from fertilisers has increased by 20% (Harris, 2015).

Even though demographic, economic, and technological development are the major threats to water resources, climate variability and climate change have also contributed to water resources vulnerability. Climate related changes affect the spatial and temporal distribution of rainfall with consequent impacts on the timing of runoff (Cosgrove and Loucks, 2015). Hydrological systems are rendered sensitive to changing climatic conditions such that most of the effects of a changing climate will be felt through changes in the water cycle (Bates et al., 2008; Chiew et al., 2009). Streamflow is an important indicator of a catchment's response to climate variability and climate change. Climate change worsens the threats to water resources by increasing the frequency of extreme flood and drought events due to increased temperature and evapotranspiration rates (Cramer et al., 2014). For example, a decrease of 10 to 30% in streamflow is expected due to future climate change over some dry regions at mid latitudes and dry tropics (Raneesh, 2014).

2.1.2 Climate varriability and climate change

Climate variability refers to fluctuations or variations in the mean state of climate while climate chage refers to long-term changes in temperature and weather patterns (IPCC, 2013). Changes in climate may be brought about by variations in the solar cycle or by anthropogenic activities such as burning of fossil fuels which in turn emit greenhouse gases. Climate variability occurs at decadal and annual scales and can result in short term extreme events like floods, droughts, or tropical storms. These events can have major effects on a country's economy especially where economic related activities such as agriculture may be sensitive to the fluctuations in weather and climate. Globally, it is anticipated that future climate change would have more negative effects on freshwater systems. Botswana is a good example of a developing country where climate variability has a marked influence on the country's economy. For instance, the contribution of the agricultural sector to the economy fell from 42.7% at independence to 1.9% in 2008 (Southern African Development Community, 2011) which may partly be attributed to climate variability amongst other causes.

Variability can be attributed to natural internal processes within the climate system such as volcanic eruptions, El Niño and La Niña events. External processes also have an influence on variability and these are largely contributed from anthropogenic activities some of which lead to enhanced greenhouse gase effect. In Africa, the most signifacant source of climate variability is the seasonal migration of the Intertopical Convergence Zone (ITCZ), emanating from the solar radiation input which varies from summer to winter (Broccoli et al., 2006; Baumberg et al., 2015). The ITCZ is an area of low pressure centered on average around six degrees north of the Equator where the Northeast Trade Winds meet the Southeast Trade Winds (Nielbock, 2017). Seasonal variations resulting from differential heating or cooling of the hemisphere shift the ITCZ such that when the northern hemisphere is warm the ITCZ shifts northward and when the southern hemisphere is warm, the ITCZ shifts southward (Tallaksen and Van Lanen, 2004; Ambrosino et al., 2011). These variations are accompanied by changes in trade winds and an asymmetric response of the Hardley circulation while there is a shift in the sub-tropical high pressure belt as well as the jet stream (Vellinga and Wood, 2002; Bitz and Chiang, 2005; Broccoli et al., 2006).

Atmospheric and oceanic circulations also transfer moisture and heat around the planet thus affecting climatic patterns of variability at different spatial and temporal scales. Ocean-atmospheric interactions when combined with variations in sea surface temperatures (SSTs), influence climate thus contributing significantly to climate variability (Gleick, 2000; Hoell, 2017). The link between oceanic and atmospheric events arises from the El Nino/Southern Oscillation (ENSO) which is caused by the existence of the "Bjerknes feedback" mechanism (Deppenmeier et al., 2016). Human activities also enhance greenhouse gas concentrations in the atmosphere thus leading to climate change. Over time, anthropogenic greenhouse gas emissions have increased because of rapidly increasing population and economic growth. According to IPCC (2015) fossil fuel combustion and industrial processes which emit CO_2 contributed about 78% of the total greenhouse gases between 1970 and 2010. Properties of the Earth’s surface such as chemical composition and the dynamics of the atmosphere also influence climate variability (Laprise, 2008).

2.1.3 Droughts

Drought is a prolonged period of abnormally low rainfall, leading to shortage of water (Tallaksen and Van Lanen, 2004; Belayneh et al., 2016). Drought has an impact on ecosystems, human livelihoods and the economy (Heim, 2002; Vogt et al., 2011). Crop production is the most vulnerable to the effects of drought and this may compromise a region's food security. Therefore a good understanding of the characteristics of drought at different spatial and temporal scales is required for efficient water management strategies (Kermen and Onuşluel, 2018).

There are four types of drought according (Van Loon, 2015). Meteorological drought is defined as a lack of or reduction of precipitation over a region for a specific period. It is characterised by below-average precipitation and above-average temperatures, and it frequently precedes and drives other types of droughts. Agricultural drought, refers to a period when there is a lack of moisture in the soil, resulting in lower agricultural production and plant development. Hydrological drought is caused by deficits in precipitation over a longer period of time. These droughts affect surface and subsurface water supplies and they reduce the amount of streamflow and groundwater levels. Lastly, a socioeconomic drought refers to insufficient water resources supply to meet economic demand.

Drought monitoring and quantification are essential components of an effective water management strategy. Drought indices are operational definitions for droughts, they monitor and quantify droughts (Kermen and Onuşluel, 2018). The indices are derived from meteorological data such as precipitation and temperature while some are streamflow based. Among the meteorologically derived indices are the Standardised Precipitation Index (SPI) originated by Mckee et al. (1993), the Standardised Precipitation Evapotranspiration Index (SPEI, Vicento-Serrano et al., 2012), the Palmer Drought Severity Index (PDSI) developed by Palmer (1965) and the Effective Drought Index (EDI, Buyn & Wilhite, 1999). Streamflow derived drought indices include the Standardised Drought Index (SDI, Nalbantis and Tsakiris, 2009) and the Standardized Streamflow Index (SSI, Telesca et al., 2012). The procedures for calculating SPI, SPEI, SDI and SSI are statistically similar and the indices are calculated by transforming monthly streamflows into z-scores (Vicento-Serrano et al., 2012).

2.2 Rainfall-runoff modelling

Runoff plays a major role in balancing the hydrological cycle (Figure 2.1) by returning excess precipitation to the oceans and determining how much water becomes streamflow (Sitterson et al., 2017). In the management of a catchment's water resources, surface runoff is important for monitoring water quality and quantity, flood forecasting and for understanding ecosystem relationships in the aquatic environment (Huffman et al., 2011). Runoff is generated by two mechanisms namely, saturation excess and infiltration excess (Davey, 2008). Some of the parameters that determine the amount of surface runoff are rainfall and soil characteristics, land cover and land use, hillslope and vegetation (Yang et al., 2015). Modelling runoff provides a better understanding of hydrologic phenomena and how changes affect the hydrological cycle. Insight is gained on catchment response and yields, estimation of available water and water resources forecasting (Vaze, 2012). The hydrological modelling process provides a framework to appreciate the relationship between climate, human interaction and water resources (Leavesley, 1994; Jothityangkoon et al., 2001; Xu, 2002).

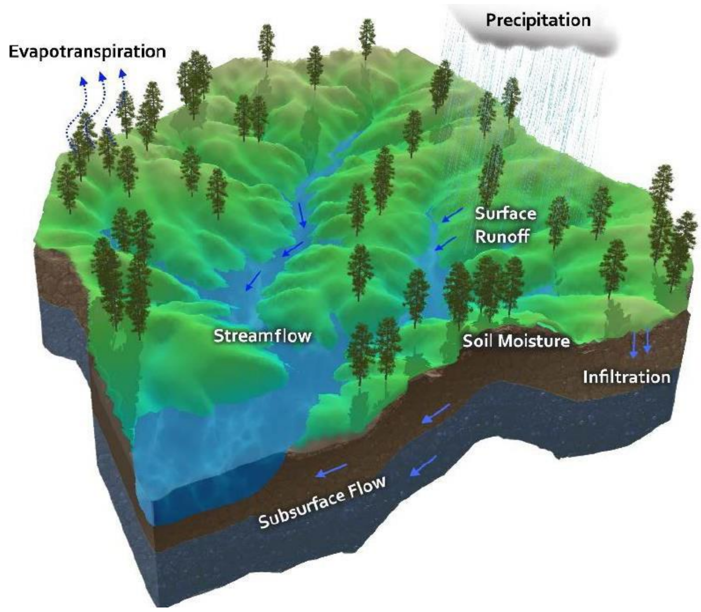

Figure 2.1: The different components of a hydrological cycle *Source: Sitterson et al. (2017)*

Different tools are used to provide an efficient management of water resources and among them are databases containing information based on aspects such as environmental, physical, social, political, economic as well as water supply and usage (Zeinalie et al., 2021). Adequate and reliable hydrological datasets are required to assist proper management of water resources. However, inconsistent monitoring and insufficient resources have caused hydrological data paucity in some regions. Hydrological or rainfall runoff models are some of the tools used to address this limitation. Hydrological models are a set of equations aimed at estimating runoff as a function of various parameters used to describe watershed characteristics such as precipitation, interception, evapotranspiration and infiltration (Devi et al., 2015). They mimic a real-world situation and reflect the catchment's runoff response to climate and anthropogenic forcing (Sorooshian et al., 2008).

2.2.1 Hydrological model classification

The need for models that reflect a certain level of complexity and understanding of catchment scale hydrological processes has resulted in the development of multiple hydrological models with various degrees of assumption and simplification (Aghakouchak and Habib, 2010; Oosthuizen et al., 2018). Different categories of hydrological models exist based on the manner in which they calculate runoff and on the purpose for which each model was developed (Singh, 1995). Each model has its own unique characteristics due to different parameter inputs. The nature of physical principles applied in the formulation of the model determines the category of the model (Refsgaard, 1996; Devi et al., 2015). Models can either be classified based on model structure or on spatial processes.

Structural models

The structure of a model determines how runoff is calculated (Singh, 1995). Based on model structure there are empirical, conceptual, and physically based models (Dooge, 1959; Binley et al., 1991).

Empirical models

Also referred to as observation-oriented models, empirical models are data driven models that acquire information from existing data and are confined to the range of observed data (Devi et al., 2015; Sitterson et al., 2017). These models make use of mathematical equations derived from concurrent input and output time series data and do not consider the physical basin characteristics and processes thus they have no physical connection to the catchment (Sitterson et al., 2018). The models exhibit a non-linear relationship between inputs and outputs and not much is known about the internal processes that control how runoff results are determined, in other words they are based on the black box concept (Beven, 2012; Granata et al., 2016). An advantage of these models is that a small number of input parameters are required. Also, they are easy to use, cost effective, simple to implement and have a faster run time (Devi et al., 2015; Sitterson et al., 2018). The models have limitations in that they cannot calculate the distribution of runoff values between upstream and downstream areas because of a few parameters. At the same time some effects of catchment change cannot be adequately represented (Tessema, 2011).

Conceptual models

Conceptual models were developed in the 1960s because of enhanced computing power which allowed the use of simplified linkages to generate an integrated representation of the terrestrial phase of the hydrological cycle (Wheater, 2008). These models make use of some aspects of physical processes together with a mathematical description of the catchment response. Semi-empirical equations are used, and model parameters are evaluated both from field data and through calibration. They are made up of a series of interconnected reservoirs that reflect the physical elements in a watershed. The water balancing concept is employed where water reserves are replenished by rainfall, infiltration, and percolation, and emptied by evaporation, runoff, and drainage, among other processes (Vaze, 2012; Devi et al., 2015). The models have a simple model structure and are easy to calibrate, however, they do not consider spatial variability within a catchment (Sitterson et al., 2017).

Physically based models

Physically based models are also known as mechanistic models or process-based models. An understanding of the physics related to catchment hydrological processes is applied in developing the models (Vaze, 2012). Mathematical equations that are physically based are used to represent multiple parts of real hydrologic responses in the catchment. The models can be regarded as mathematically idealized representations of real-world processes that make use of temporally and spatially dependent state variables (Devi et al., 2015; Sitterson et al., 2018). Water balance equations, conservation of mass and energy, momentum, and kinematics are among the general physics laws and principles applied to the models (Sitterson et al., 2018). These models can be applied to ungauged catchments if the physical parameters are known, and the effects of catchment change can be explicitly represented. However, the need for large amounts of data limits their usage (Uhlenbrook et al., 2004).

Spatially based models

Another way of classifying rainfall-runoff models is to use the spatial configuration within a catchment. Spatially based models are generated based on parameters as a function of space and time. Information consisting of variations in geology, soils, vegetation, topography and geology is required while consideration is also given to how the runoff generated is routed across the catchment (Beven, 2012). The models are categorised into lumped, semi-distributed, and fully distributed models (Kampf and Burges, 2007).

Lumped models

Lumped models do not consider the spatial variability within a catchment, the catchment is regarded as a single homogenous unit and model inputs are averaged over the entire catchment (Rinsema, 2014). For example, uniform precipitation and average soil moisture storage are applied across the entire catchment. The drawback is that this may result in over-or under-parameterization (Rinsema, 2014; Tessema, 2011).

Distributed models

Distributed models consider the spatial variability by dividing a catchment into smaller units each of which have their unique set of parameters (Rinsema, 2014). The strength of these models comes from the fact that the basin hydrological processes are linked to the physical basin properties. However, these models are data intense and require a very long run time (Moradkhani and Sorooshian, 2008; Tessema, 2011).

Semi-distributed models

These models utilise a combination of lumped and distributed parameters (Pechlivanidis et al., 2011). Input data is made up of averaged catchment data together with specific sub-catchment data (Sitterson et al., 2017).

Even though model development is well advanced, selecting an effective modelling system for integrated management applications remains a challenge. Key constraints in model application include considerable data requirements. Also, the process may be time consuming and not cost effective as several elements related to the model structure must be considered, such as process description, numerical discretization and effective parameterization (Tessema, 2011; Youssef, 2015).

2.2.2 Hydrological model application

A generalized schematic for choosing a modelling approach is presented in Figure 2.2 (Anderson and Woessner, 1992; Refsgaard, 1996). The following steps are summarized from Tessema (2011).

i. Define the purpose of the application to assist in determining which modelling system is best suited to solving the problem at hand.

ii. Build the conceptual model by determining the complexity of the model based on the specific purpose or need. This is done by identifying the system boundaries, data collection, literature reviews and field visits of the study area.

iii. Choose the mathematical model from existing codes, adjusted by adding components to an existing one, or created entirely from scratch.

iv. Model set up, this involves a preliminary selection of parameter values from the input data and the initial conditions are defined after which model calibration is performed followed by model validation. Calibration is the process of determining the best set of parameters that will allow the model to accurately recreate the observed data. Validation is carried out to prove the calibrated model's ability to simulate acceptable results.

v. The performance of the model is assessed by comparing the model output to the observed data. The process visually compares the simulated and observed stream flow hydrographs, while also using the goodness-of-fit criteria/ statistical measurement tools. The correlation coefficient (R), coefficient of determination (R^2), Nash-Sutcliffe Efficiency (NSE), Root Mean Square Error (RMSE), and Mean Absolute Error (MAE) are used to assess the performance of model calibration and validation (Santhi et al., 2001; Moriasi et al., 2007; Aghakouchak and Habib, 2010; Othman et al., 2021) using equations.

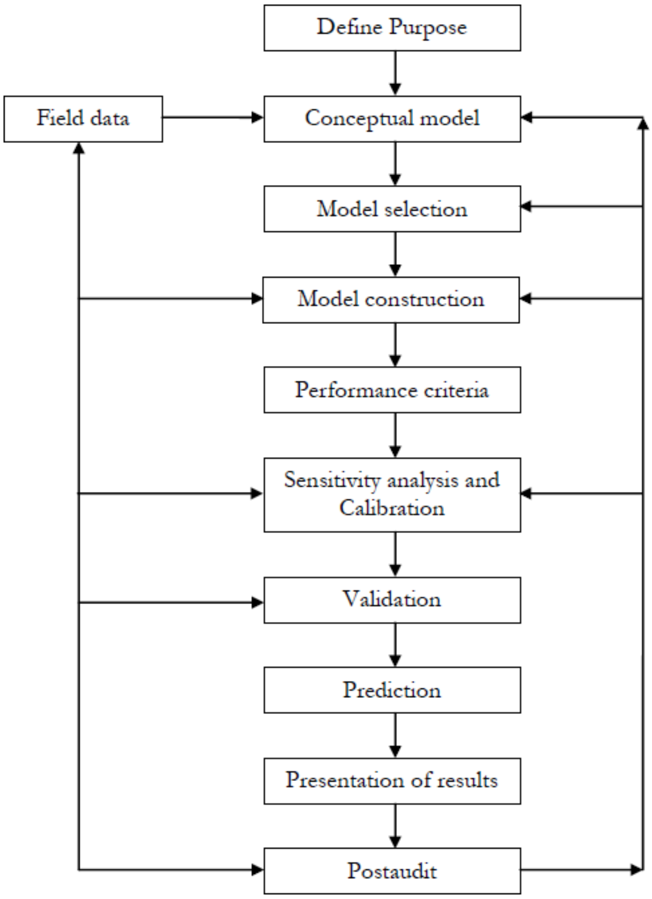

Figure 2.2: Schematic for hydrological model application. Modified after Anderson and Woessner (1992) and Refsgaard (1996)

2.2.3 Calibration and validation of hydrological models

Models are calibrated to reproduce catchment-scale responses of streamflow to rainfall, and to other parameters such as evaporation, soil moisture storage, and groundwater recharge. Using either manual or automatic calibration, the process involves estimating or predicting parameter values and comparing them to observed values until a close fit is obtained (Wheater, 2008; Devi et al., 2015). In so doing a representative hydrological behaviour of the catchment of interest is achieved. According to Othman et al. (2021) calibration is used to lessen the gap between the observed and simulated hydrographs. During the calibration process the parameters are altered to ensure the acceptable correlation between observed and simulated flows and to get a good fit. Calibration can be performed manually or automatically or by combining both methods (Singh, 1995).

Manual Calibration

Manual calibration involves adjusting model parameters in successive model runs until the model output closely matches the observed data (Pechlivanidis et al., 2011). This process is, however, time-consuming and requires the modeller to be experienced to achieve sound and reasonable calibrations (Xu, 2002). This therefore requires the modeller to have extensive knowledge of model structure and its conceptualisation as well as the physical basin characteristics. As such, it is possible that different modellers may generate different outcomes (Sorooshian et al., 2000; Wheater, 2002).

Automatic Calibration

This process involves the use of computer algorithmns to search the parameter space through execution of multiple model runs (Madsen, 2000; Vrugt et al., 2003). The algorithms speed up the calibration process by using confidence intervals that minimize differences between modeled and observed data (Xu, 2002). Thus the objective of this process is to speed up the calibration process at the same time eliminating the subjective human that is relied upon in the manual calibration approach (Boyle et al., 2000). However, automatic calibration works well when used together with manual calibration (Mwelwa, 2004; Pechlivanidis et al., 2011).

Model Validation

According to Henriksen et al. (2003), model validation is the process of demonstrating that a calibrated site-specific model is capable of making reasonably accurate predictions outside the calibration period. Validation tests the performance and the robustness of the calibrated model. In other words, validation verifies that the calibrated parameter values may be utilized to recreate events or environmental conditions outside the calibrated time series. A good validation shows that the calibrated model can replicate the catchment response characteristics without changing the calibrated parameter values when simulation is carried out in adifferent period or in a diffferent area. Model validation should be assessed operationally and conceptuallly. Operationally, a determination is made if simulated values agree with observed values while conceptually it is determined if theory and the assumptions upon which the model is premised are justifiable (Kerr and Goethel, 2014).

2.2.4 Uncertainty in hydrological modelling

Rainfall-runoff models provide an over-simplification of the basin physical processes therefore the models are fraught with some degree of uncertainty (Sitterson et al., 2017). Factors that contribute to predictive uncertainty include inadequate knowledge or poor understanding of the complex hydrological dynamics, climatic variability and input data issues. According to Knutti (2008) parameter uncertainty arises if the values used in the parameterisations are not adequately constrained by the observed evidence. Devac and Dhanya (2017) state that the main source of error in hydrological modelling is the uncertainty in determining model parameters because of a mismatch between model complexity and the available data. Therefore, uncertainty in hydrological modelling emanates from model structure uncertainty, input-output data uncertainty and uncertainty in the estimation of parameters (Beven, 2005; Knutti, 2008).

Model structural uncertainty arises from assumptions made in formulating the model and from the simplified representation of processes that take place in the real-world. The complexity of the underlying hydrological processes has also resulted in poor or insufficient knowledge of the processes and consequently the use of inappropriate assumptions for model conceptualisation and mathematical formulations (Liu and Gupta, 2007). Input data uncertainty arises from errors in measuring climatic variables and the observed streamflow. Vrugt et al. (2005) state that limited and infrequent monitoring, as well as sparse gauging networks also contribute to input data uncertainty. On the other hand, model parameter uncertainty arises from the way the parameters are estimated either through regionalization or prior methods (Liu and Gupta, 2007).

Water resources have often been managed under conditions of uncertainty in the past decades. With increased computer use and improved understanding of processes, hydrologists now acknowledge uncertainty in hydrological modelling, thus decision making can be better informed (Benke et al., 2011). A number of approaches can be applied to reduce uncertainty in hydrological modelling (Shrestha et al., 2009). Uncertainty is dealt with through a probability distribution function which is calculated using a probabilistic rather than a deterministic approach (e.g. Kavetski et al., 2006). A parameter distribution type (e.g. normal or uniform distribution) is then determined, which in turn is applied to generate a large number of possible parameter sets. A choice of the most suitable model structure is made and the different parameter sets are forced onto the hydrological model to generate ensembles of predicted flows through random and independent sampling techniques such as the Monte Carlo approach (Kapangaziwiri et al., 2009).

2.2.5 Modelling the impacts of climate change on water resources

Model projections of the Earth's climate provide important data for predicting climate change impacts and assessing policy decisions (Goodall et al., 2013). The predicted change in climate change is anticipated to affect the hydrological cycle on a global scale, thereby intensifying the uneven distribution of water resources (Huntington, 2006). As such the need for integrating information from climate-model projections and observed hydro meteorological data is vital to develop strategies that promote adaptation to climate change (Raucher, 2011).

Global climate models (GCMs) can be used to forecast future climate change based on assumptions about how greenhouse gas concentrations will vary in the future (Teutschbein, 2013). They simulate the complex interactions between the atmosphere, ocean and biosphere. Global and regional climate models are used for climate change modelling under various emission scenarios known as the Representative Concentration Pathways (RCPs, Van Vuuren, et al., 2011). These scenarios describe specific emission trajectories and the subsequent radiative forcing. There are four different emission pathways; RCP2.6, RCP6, RCP4.5 and RCP8.5 whose concentrations are projected to the year 2100 (Van Vuuren et al., 2007; Van Vuuren et al., 2011)

The RCP2.6 emission pathway illustrates literature-based scenarios that result in extremely low greenhouse gas concentrations. It is expected that by mid-century the radiative forcing may reach a level of 3.1 W/m^2 after which it may drop to 2.6 W/m^2 by 2100. The RCP 4.5 pathway proposes that the total radiative forcing will stabilize shortly after 2100 but may not exceed the long-run radiative forcing target level (Wise et al., 2009). The RCP6 scenario projects that the total radiative forcing may stabilize at 6.0 Watts per square meter (Wm−2) by the year 2100. The RCP8.5 is the worst-case scenario in which greenhouse gas emissions increase over time (Riahi et. al., 2007)

Although incorporating information from climate-model projections with the hydrological data is vital for future projections it has its own limitations. The GCMs simulate climate processes at a coarse scale, therefore there is need to downscale them so that they can match the relevant spatial scales for cathment hydrological modeling (IPCC, 2007; Hegerl, 2007). Downscaling thus scales down the global information to local and regional scales (Hewitson and Crane, 1996). There are different downscaling approaches. Statistical downscaling establishes statistical correlations between large-scale climatic information and regional variables (Wilby et al., 2006). On the other hand, dynamical downscaling uses regional climate models (RCMs) for limited regions with boundary conditions based on GCM simulations. This approach resolves atmospheric processes while maintaining consistency with the driving GCM such that internally consistent output variables are produced (Wilby et al., 2002).

Chapter 3

Study area and data sources

3.1 Study area

The Limpopo River spans a distance of 1 750 km and drains an area of 412 000 km^2. The river is riparian to four countries namely Botswana, Mozambique, South Africa and Zimbabwe. The respective country's areal contributions to the basin are 19%, 21%, 45% and 15% (Figure 3.1). The main river rises in the mountains that divide South Africa from Botswana and Zimbabwe, it then flows into Mozambique before entering the Indian Ocean at Xai-xai (World Meteorological Organization, 2012). In Botswana, Gaborone the capital city and Francistown the second largest city are in the Limpopo River basin. Most of Botswana's population lives in the South and South-Eastern parts of the country. In 2012 about 60% (1 197 314 people) of the country's population was reported to reside in the Limpopo Basin (LIMCOM, 2013). There are six sub-basins of the Limpopo in Botswana namely, Shashe, Motloutse, Lotsane, Mahalapye, Bonwapitse and Notwane (Fig 3.1).

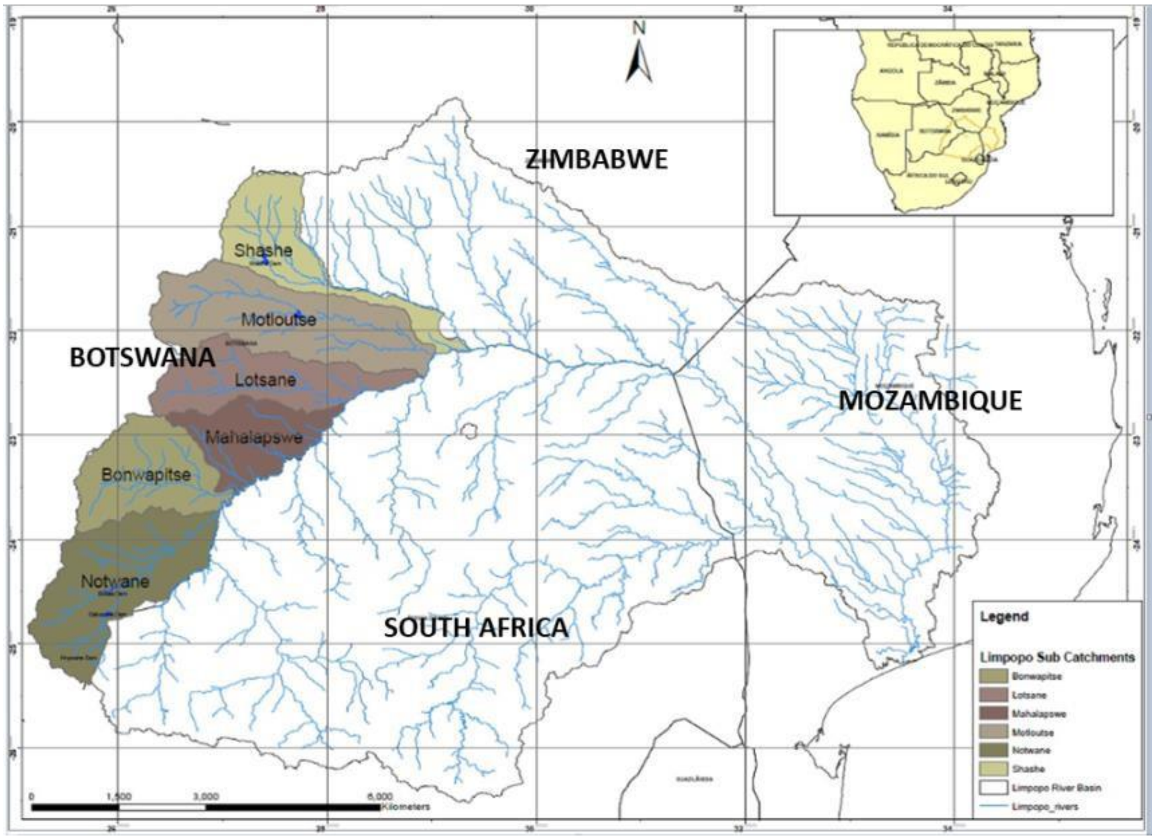

Figure 3.1: Botswana sub catchments within the Limpopo basin
Source: *Zhu and Ringler (2010); DWS (2018)*

3.1.1 Climate

The climate of Limpopo River basin is driven by a series of diverse air masses which include the dry continental tropical, marine western Mediterranean and the equatorial convergence zone (GOB-MMRWA, 1991; Schulze, 1997; Unganai, 1998). As a result, the climate varies from the western part of the basin, characterised by a temperate climate to a subtropical climate at the river mouth in the Mozambique (LRAK, 2011). Rainfall is highly seasonal in nature extending from October to April and peaking in February. Across the basin there is a significant variation in the seasonal distribution of rainfall. For example, the western part which is the most arid region in the basin receives a mean annual rainfall of 200mm. On the other hand, the southern middle part of the basin receives an annual mean rainfall of 1500 mm. The eastern part near the Indian

Ocean experiences an average of 600 mm of rainfall per annum. Irrespective of the amount of rainfall received the number of days with rainfall per year hardly exceeds fifty percent thus the rainfall season is short (WMO, 2012).

Botswana receives an average annual rainfall ranging from about 650mm in the extreme northeast (Chobe District) to less than 250mm in the extreme southwest (Kgalagadi District). Specifically, the Limpopo sub-basins in Botswana receive an annual rainfall ranging from 160 to 477mm (Figure 3.2). Mahalapye and Lotsane sub-basins receive an annual rainfall average of 350mm to 450mm.The average annual rainfall in Shashe sub- basin ranges from about 400mm to above 600mm but sometimes rainfall amounts as low as 200 can be experienced. The Notwane and Bonwapitse sub-basins receive an annual average rainfall of 160 to 318mm (LBPTC, 2010).

Botswana is a semi-arid country characterised by a cold winter experienced from June to August, with low temperatures of about 0°C to 4°C mainly during the night and early mornings. Summer occurs from November to April with a temperature range of 30°C to 40°C (NWMP, 2006). On average the Limpopo basin temperature ranges between 23 °C and 32°C (Figure 3.3). Seasonal temperatures are high during summer with a range of 17.8°C to 20.8°C while the winter season experiences the lowest temperatures ranging from 4.4°C in the southern part of the basin around Notwane, Bonwapitse, Mahalapye and Lotsane to 9.0°C in the Motloutse and Shashe sub-basins.

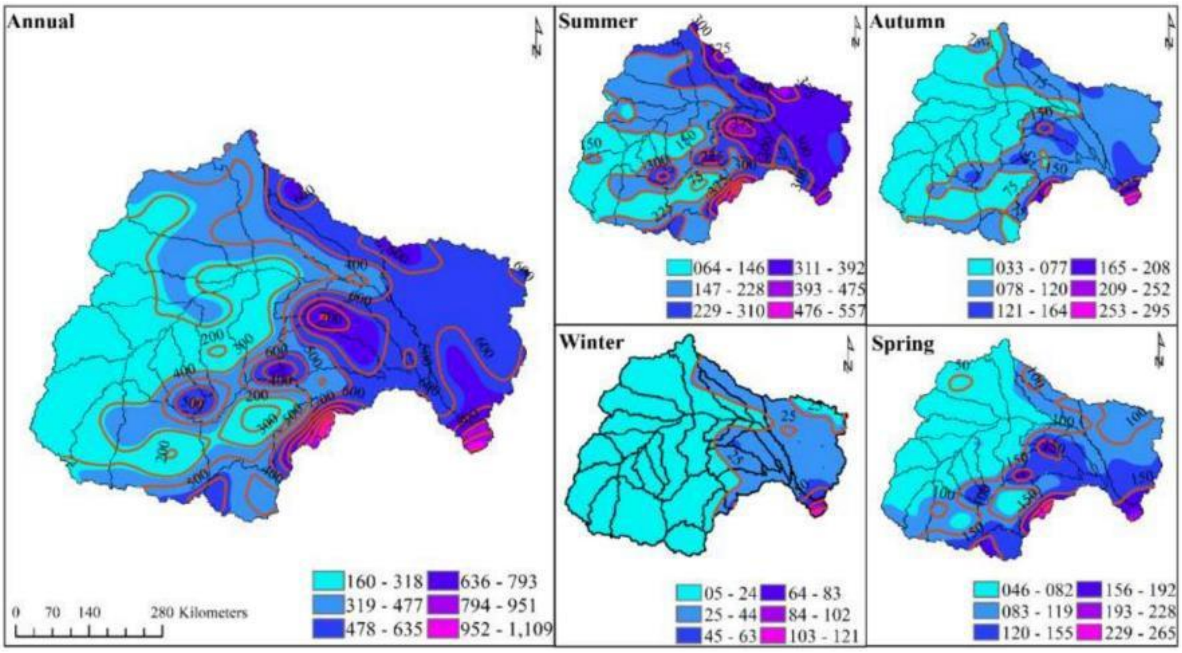

Figure 3.2: Mean annual and seasonal rainfall from 1979 to 2013 in the Limpopo River Basin
Source: *Mosase and Ahiablame (2018)*

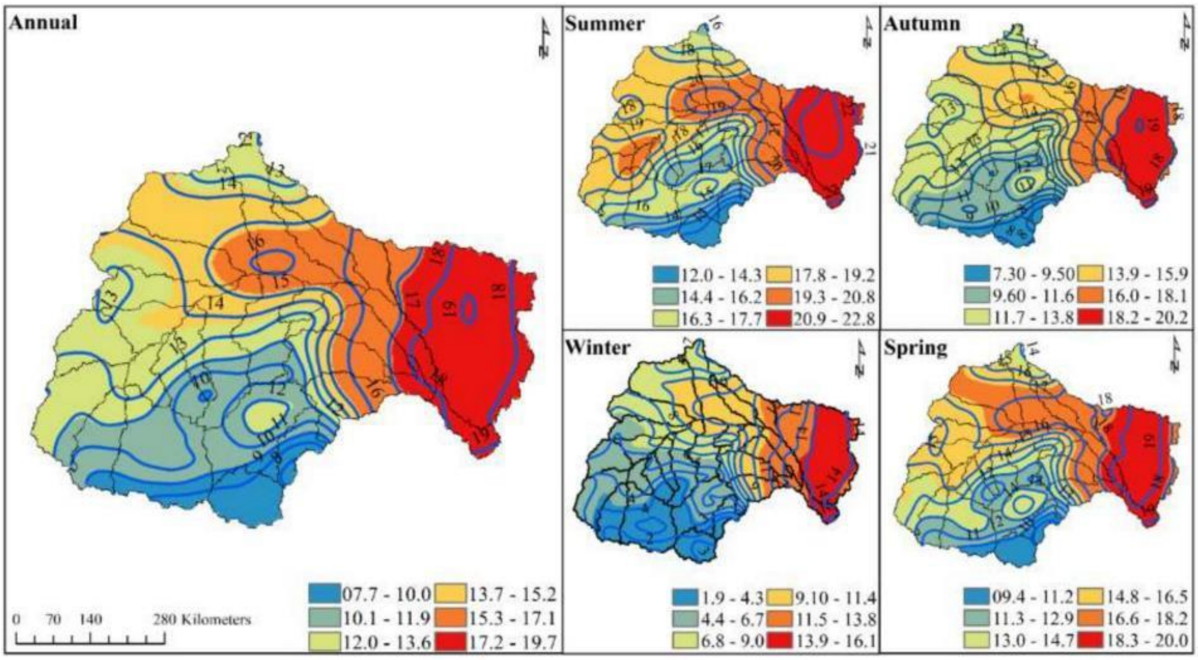

Figure 3.3: Mean annual and seasonal minimum temperature from 1979 to 2013 in the Limpopo River
Source: *Mosase and Ahiablame (2018)*

3.1.2 Hydrology

The six sub-basins of the Limpopo in Botswana with their respective areas (FAO, 2004) are: Bonwapitse (9 904 km^2), Lotsane (9 748 km^2), Mahalapye (3 385 km^2), Motloutse (1 953 km^2), Notwane (1 853 km^2) and Shashe (12 070 km^2). The respective mean annual runoff contributions from the different sub-basins are 81Mm^3 , 86Mm^3, 22Mm^3, 86Mm^3, 62Mm^3 and 288Mm^3 (FAO, 2004) .The Limpopo basin's freshwater resources are estimated at an annual average of 4 800 to 5 200 Mm^3 distributed in rivers, lakes and aquifers (Alemaw et al., 2008). Out of all the Limpopo basin countries, Botswana has the least dense stream network (Figure 3.4) which indicates the arid conditions that prevail in the country (LRBM, 2013). Within the Botswana sub-basins there are nine major dams totalling a full combined capacity of 915.7Mm^3 (WUC, 2019). The Gaborone, Bokaa and Nnywane dams located in the Notwane sub-basin have a total capacity of 164.93 Mm^3. The Lotsane dam has a full capacity of 42.5Mm^3. The Shashe sub-basin has the largest combined full dam capacity of 514.27Mm^3 contributed by the Ntimbale, Shashe and Dikgatlhong dams. The Letsibogo and Thune dams are found within the Motloutse sub-basin with a total combined full capacity of 194 Mm^3.

Figure 3.4: Stream network in the Limpopo basin *Source: LRBM (2013)*

3.1.3 Geology and Topography

The geology of the Limpopo River basin (Figure 3.5) consists mainly of the Kalahari Craton which encompasses the Kaapvaal craton, the Zimbabwe craton and the Limpopo Belt. The Archaean Craton, the Karoo System and the Bushveld Igneous Complex are also found in the basin. The Limpopo Mobile Belt runs east-west from the Kaapvaal craton to the Zimbabwe craton covering a significant section of the Limpopo River basin (Schlüter, 2006; Chinoda et al., 2009). Argillites, fluvial sandstones, and mudstones dominate the lower part of the basin (Ashton et al., 2001; Chinoda et al., 2009). The basin's landforms are mostly undulating plains, with medium and low gradient mountains and hills interspersed towards the west while a coastal plain and valley floor are dominant in the east (CGIAR, 2003)

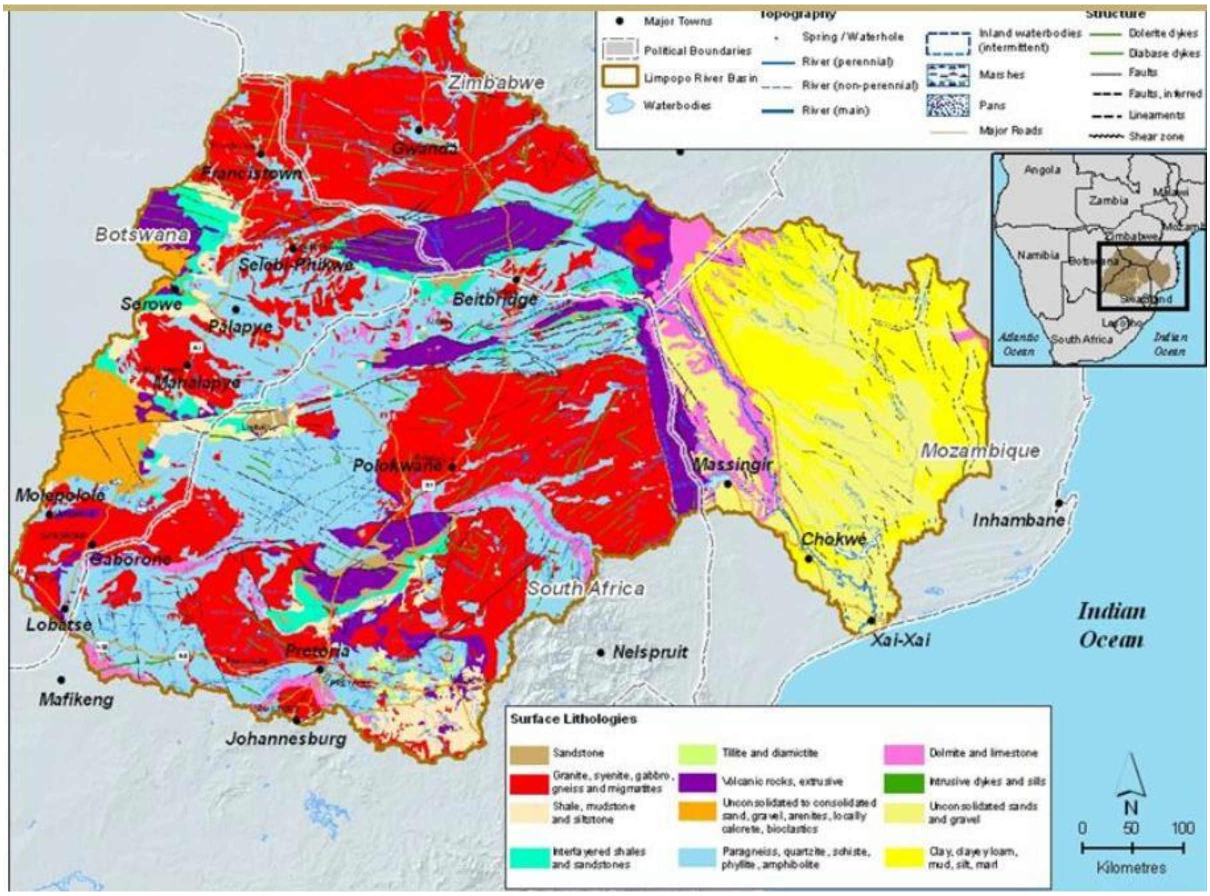

Figure 3.5: Surface lithology of the Limpopo River basin Source: *SADC (2010)*

3.1.4 Soils

The dominant soils within the Botswana sub-basins (Figure 3.6) include arenosols and luvisols. Arenosols are sandy in texture while luvisols are characterised by humus that has accumulated on the surface of a heavily eroded layer of clay and minerals that contain iron. In addition, shallow leptosols are found in the northern sub-basins, they are shallow soils that form from numerous parent materials and are found over continuous gravelly rock and soils (FAO ISRIC, 2003).

3.1.5 Land use in the Limpopo Basin

The Limpopo River basin (Figure 3.7) is mainly covered with Savannah Grassland. In addition, tropical and subtropical grasslands as well as shrub lands are found in the Botswana sub-basins. Over and above this, the Notwane sub-basin contains deserts and xeric shrub lands (WWF, 2010).

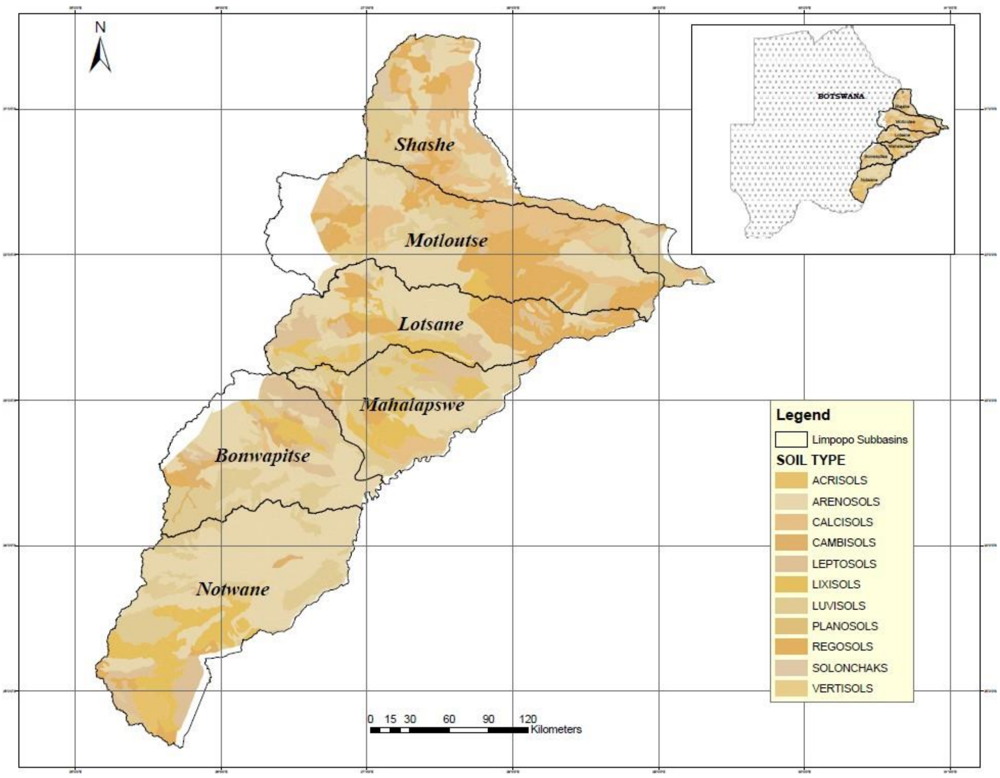

Figure 3.6: Soil types within the Limpopo sub-basins Source: *DWS (2018)*

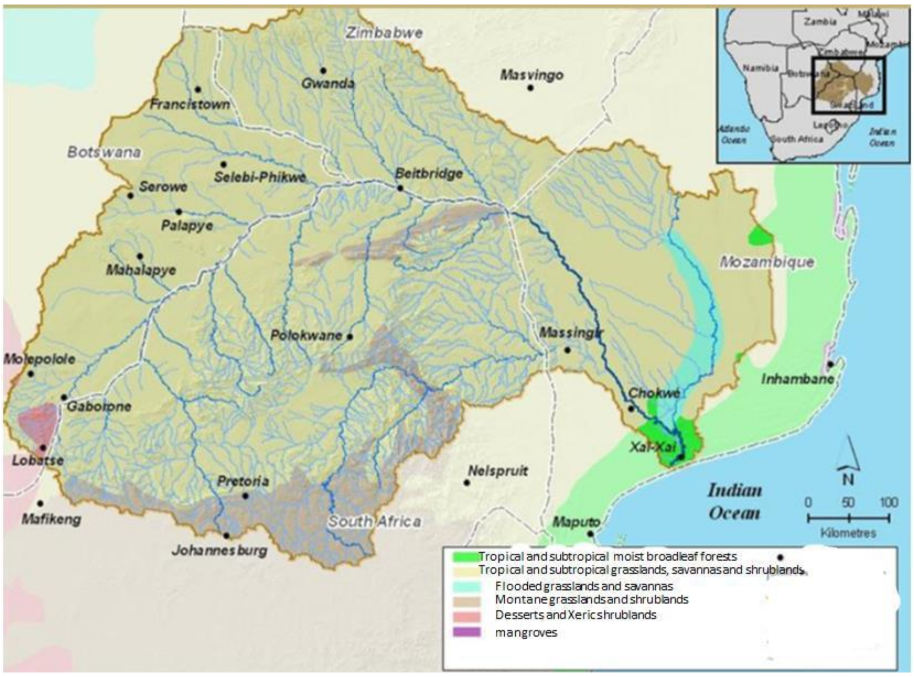

Figure 3.7: Terrestrial biomes of the Limpopo River Basin Source: *WWF (2010)*

The Limpopo basin in Botswana is mainly used for pastoral and arable farming (Figure 3.8). Residential land and forest plantations account for just over 20% of Botswana's land area (FAO, 2003).

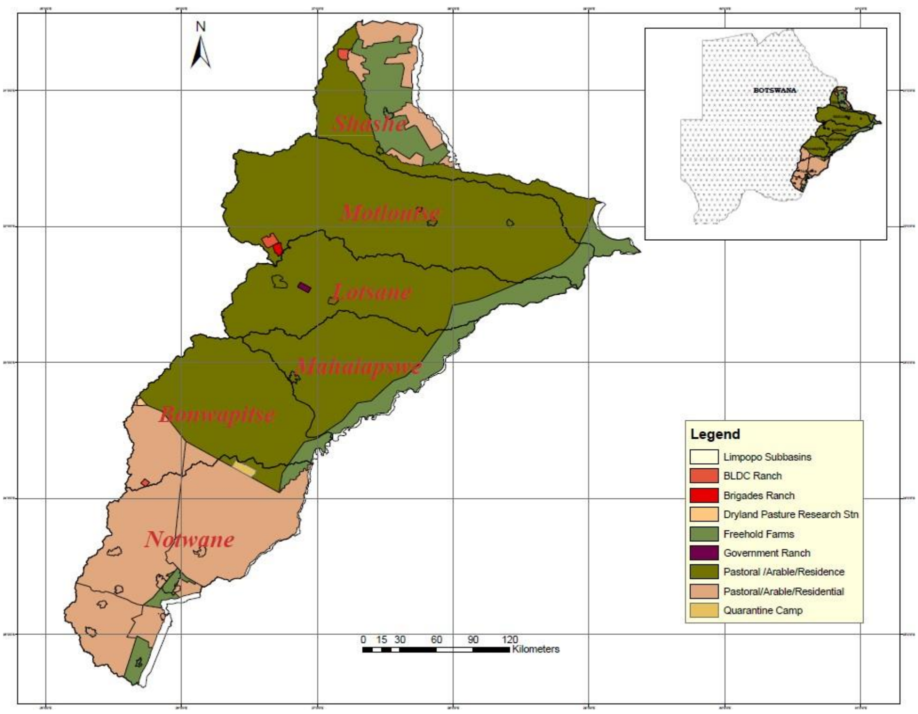

Figure 3.8: Main Land Use types in the Limpopo sub basins Source: *DWS (2018)*

3.2 Data Sources

Rainfall and temperature datasets were obtained from the Department of Meteorological Services and the Department of Water and Sanitation in Botswana. To complement the observed rainfall, timeseries datasets were also obtained from the Climate Research Unit (CRU) of the University of East Anglia (Harris et al., 2020). The CRU data (1901 to 2018) consists of 0.5° rainfall grids derived by interpolating monthly climate anomalies from extensive networks of local weather station observations. The angular-distance weighting (ADW) method was used for interpolation. The advantage of the ADW method is that it provides an easy way to trace and link each gridded value to the input observations. Runoff timeseries datasets were provided by Department of Water and Sanitation in Botswana. The datasets were complemented by runoff data from the Global Runoff Data Centre (GRDC, 2003), this was in case of missing data or short timeseries. Potential evapotranspiration data were downloaded from the International Water Management Institute's World Climate portal (IWMI, 2020). The data sets are based on Penman-Montieth evapotranspiration estimations, which calculate evaporation from open water surfaces based on climate variables such as daylight, temperature, humidity, and wind speed.

Bias corrected GCM datasets for both temperature and rainfall under the Representative concentration pathway RCP4.5 were obtained from the Swedish Meteorological Hydrological Institute's Coordinated Regional Climate Downscaling experiment initiative (Giorgi et al., 2009; Jones et al., 2011). According to the Intergovernmental Panel on Climate Change (IPCC), RCP 4.5 is a moderate emission scenario where emissions are expected to peak around the year 2040 and then decline. This scenario is ideal for Botswana as the country does not exhibit any high emissions and does not have many industries such that the likelihood of high emissions is minimal. The GCM datasets are available at 0.44° grids and were downscaled using the distribution-based scaling method (DBS, Yang et al., 2010). The WATCH-Forcing-Data-ERA-Interim data (WFDEI, Weedon et al., 2014) was used as the reference dataset. WFDEI provides interpolated half degree gridded meteorological variables whose dataset covers the period 1979–2014. The Regional Climate Models (RCMs) used in this study consist of CLMcom and RCA4 which are driven by four Global Climate Models (GCMs) namely, CNRM-CERFACS-CNRM-CM5, ICHEC-EC-Earth, MOHC-HadGEM2-ES and MPI-M-MPI-ESM-LR.

Chapter 4

Methodological approach

4.1 Introduction

This chapter describes the methods carried out to fulfil the objectives of the study. A five-step process was implemented consisting of setting up the hydrological model for the study area, generating the model parameter space, model calibration and validation, predicting the hydrological impacts of future climate change and hydrological drought analysis. The sections that follow describe the Pitman hydrological model that was used in this study together with the steps followed to fulfil the objectives of the study.

4.2 The Pitman model

Most of the models that have been applied in southern Africa address region-specific needs which involve estimating water resources availability and assessing impacts on water resources. The Pitman model, a conceptual and semi-distributed monthly time step rainfall-runoff model is among some of the widely used models in the region (pitman, 1973; Hughes, 1997). The model was originally developed by Pitman (1973) and later modified to include groundwater-surface water interactions by Hughes and Forsythe (2006). The model structure consists of storages associated with the core hydrological processes at the catchment scale. These include surface and subsurface processes, groundwater storage, discharge and routing processes as well as water use activities that take place at the basin scale (Bharati & Gamage, 2010). The modified version of the model has been used with success in various applications. For example, Hughes et al. (2006) used the model to calibrate Okavango basin while Kapangaziwiri (2008) used the model to estimate parameters for a wide range of selected basins in the region. The structure of the modified Pitman model is depicted in Figure 4.1.

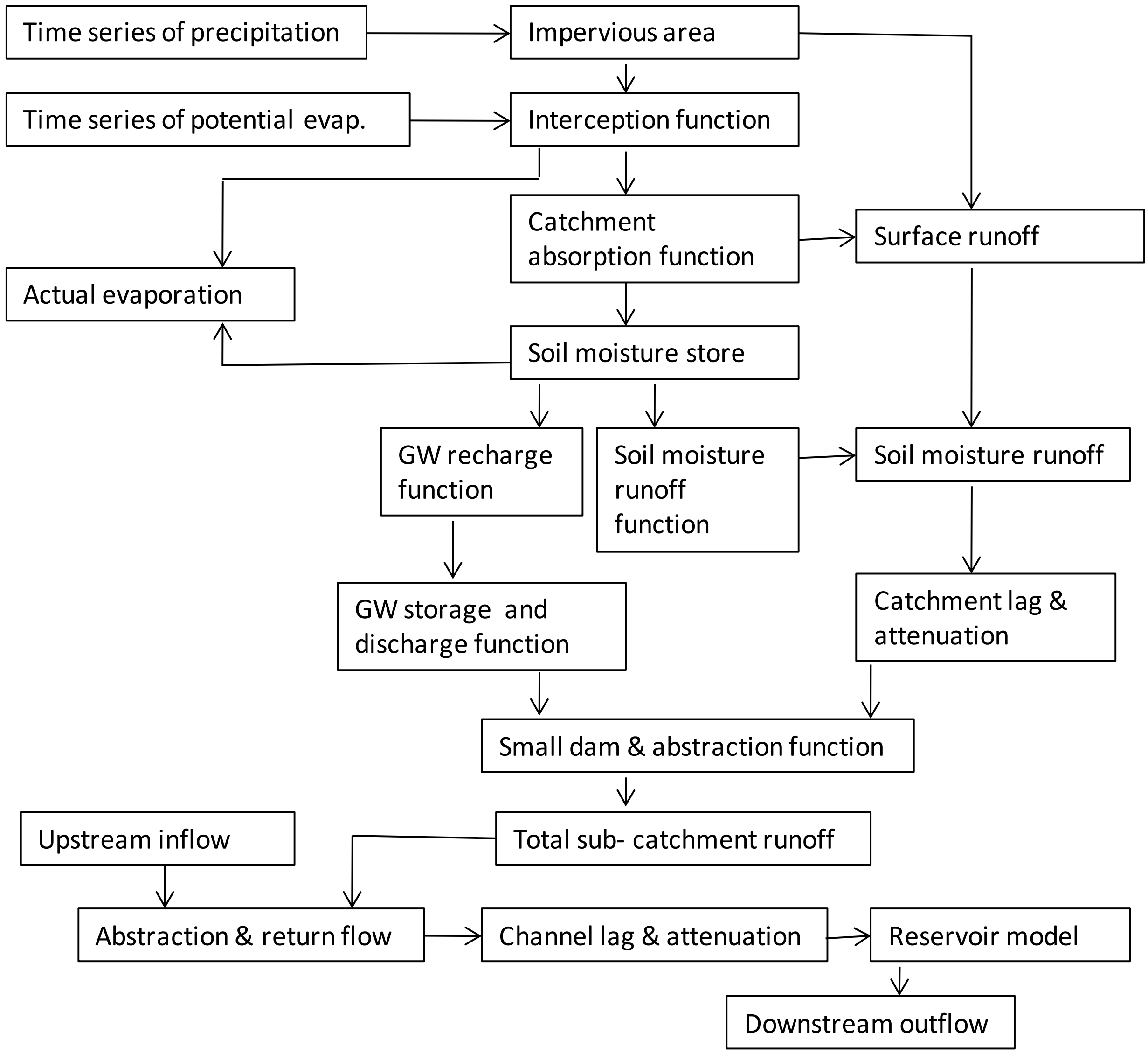

Figure 4.1: Flow diagram of the modified version of the Pitman model (Hughes et al., 2006)

The main Pitman model parameters and their descriptions are described below and summarized in Table 4.1. The primary input parameters of the model include a time series of monthly rainfall, monthly distributions of potential evaporation and catchment area.

Rainfall distribution function (RDF): This parameter is used to distribute the monthly rainfall depths into four periods where, lower values represent evenness of distribution of rainfall with an increase in the monthly rainfall total (Mwelwa, 2004; Hughes et al., 2006), for this study a range of 0.6 to 1 is used as the sub basins are within a semi-arid environment.

Interception storage parameters (PI1 and PI2): Two interception storage parameters are presented in the model. The parameter PI1 represents interception from natural vegetation (type 1) and PI2 for plantation vegetation (type 2).

Surface runoff parameters (ZMIN, ZMAX and ZAVE): The model defines three sources of surface runoff: runoff from impermeable surfaces, from excessive infiltration, and from excessive moisture storage. Three surface runoff parameters control the absorption capacity of the basin in response to different rainfall rates. The parameter ZMIN represents a minimum sub-basin absorption rate, ZMAX represents a maximum sub-basin absorption rate and ZAVE represents a mean sub-basin absorption rate. The parameter AI represents the proportion of the basin that is impermeable, and it is used in the calculation of runoff from the impervious surfaces.

Soil moisture storage and runoff parameters (ST and FT): The interflow runoff rate at storage ST is defined by the parameter FT, the maximum rate of interflow runoff given in mm/ month. If ST is exceeded in any month, the excess also contributes to runoff as saturation excess runoff. The power function POW represents power of moisture storage- runoff equation.

Evapotranspiration from the soil moisture store (R): this parameter is used to define the relationship between the ratio of actual evapotranspiration to potential evapotranspiration and the current level of soil moisture storage, it ranges between 0 and 1. Evapotranspiration losses are expected to be different between the two vegetation types and a parameter FF is used as an evapotranspiration scaling factor for vegetation type 2.

Groundwater recharges parameters (SL, GW, and GPOW): the parameter SL represents minimum moisture storage below which no GW recharge occurs. The parameter GW represents the maximum groundwater recharge rate. GPOW parameter defines the power of the relationship between the current soil moisture store and recharge which helps to quantify the recharge at different moisture levels.

Groundwater discharge parameters (DDENS, T, S, GW slope and R). The parameter DDENS (km/km^2) represents the ratio of total channel length to the basin area. The transmissivity parameter T (m^2/d) represents the product of the thickness of the saturated aquifer and its permeability. Storativity (S) signifies the aquifer's capacity to hold water. The GW slope parameter defines the regional groundwater gradient influencing the drainage from an upstream to a downstream sub-basin. The riparian strip factor (R) is given as a percentage of the total slope element width over which the evapotranspiration process is active; its function is to control the evaporation losses from the groundwater storage through areas in the margins of the channel.

Routing parameters (TL and CL): The parameter TL is a sub-basin routing parameter which represents the runoff time lag as it relates to the surface and soil moisture runoff components. The parameter CL is a channel routing parameter that is used for large basins where attenuation, even at the monthly scale is possible (Hughes et al., 2006).

Table 4.1 List of the Modified Pitman Model parameters Hughes et al., 2006)

Parameter	Units	Parameter description
RDF		Rainfall distribution factor, controls the distribution of total monthly rainfall over four model iterations
AI	Fraction	Impervious fraction of the sub-basin
PI1 and PI2	Mm	Interception storage for two vegetation types
AFOR	%	% area of sub-basin under vegetation type 2
FF	Fraction	Ratio of potential evaporation rate for Veg2 relative to Veg1
PEVAP	Mm	Annual sub-basin evaporation
ZMIN	mm month^{-1}	Minimum sub-basin absorption rate
ZAVE	mm month^{-1}	Mean sub-basin absorption rate
ZMAX	mm month^{-1}	Maximum sub-basin absorption rate
ST	Mm	Maximum moisture storage capacity
SL	Mm	Minimum moisture storage below which no GW recharge Occurs
POW		Power of moisture storage-runoff equation
FT	mm month^{-1}	Runoff from moisture storage at full capacity (ST)
GPOW		Power of moisture storage-GW recharge equation
GW	mm month^{-1}	Maximum groundwater recharge at full capacity (ST)
RSF	%	Controls the riparian evaporation losses from GW storage
R		Evaporation-moisture storage relationship parameter
TL	Months	Lag of surface and soil moisture runoff
CL	Months	Channel routing coefficient
D.Density	km km^{-2}	Drainage density
T	m^{2}d^{-1}	Groundwater transmissivity
S	Fraction	Groundwater storativity
GW Slope	Fraction	Initial groundwater gradient
A,B		Parameters in non-linear area-volume relationship
ResCap	Mm^{3}	Reservoir capacity
DEAD	%	Dead storage
INIT	%	Initial storage
Res 1-5	%	Reserve supply levels (% full capacity)
ABS	Mm^{3}	Annual abstraction volume
COMP	Mm^{3}	Annual compensation flow volume

4.3 Hydrological model set up

The hydrological model was set up in Spatial and Time Series Information Modelling software (SPATSIM). The software is an integrated data management and modelling software package developed at the Institute for Water Research at Rhodes University (Hughes and Forsyth, 2006). SPATSIM provides tools for managing and manipulating data, setting up and running hydrological models as well as data analysis. The software is executed in a GIS spatial interface that connects to a database of attribute data and has a wide range of data presentation and analysis tools. The Delphi programming language in conjunction with ESRI Map objects are employed to give the spatial data interface. All attribute information relevant to spatial elements (point, line, or polygon) is saved in Paradox data tables. Spatial data is accessed through shapefiles. The spatial data is also accessed through four data dictionaries; all references to the shapefiles that are used, as well as the unique field identifiers, are found in dictionary 1, while dictionary 2 comprises of references to the SPATSIM attributes and their data types. In the SPATSIM database tables, data dictionary 3 indicates where attribute-linked information can be found and dictionary 4 connects the records in the spatial data with the records in the SPATSIM attribute data tables. Other data about specific spatial elements can be retrieved via linked database tables.

Figure 4.2 shows the main screen of SPATSIM consisting of five menu items namely features, attributes, procedure, application and help. The shapefiles are loaded into the software through features. To each shapefile there are attributes where data for the spatial components are found. When adding the data, the type of attribute should be specified. Internal data processing methods are specified under procedures while the model run option is found under the application menu item. The simulation time series results are displayed through the inbuilt time series software (TSOFT).

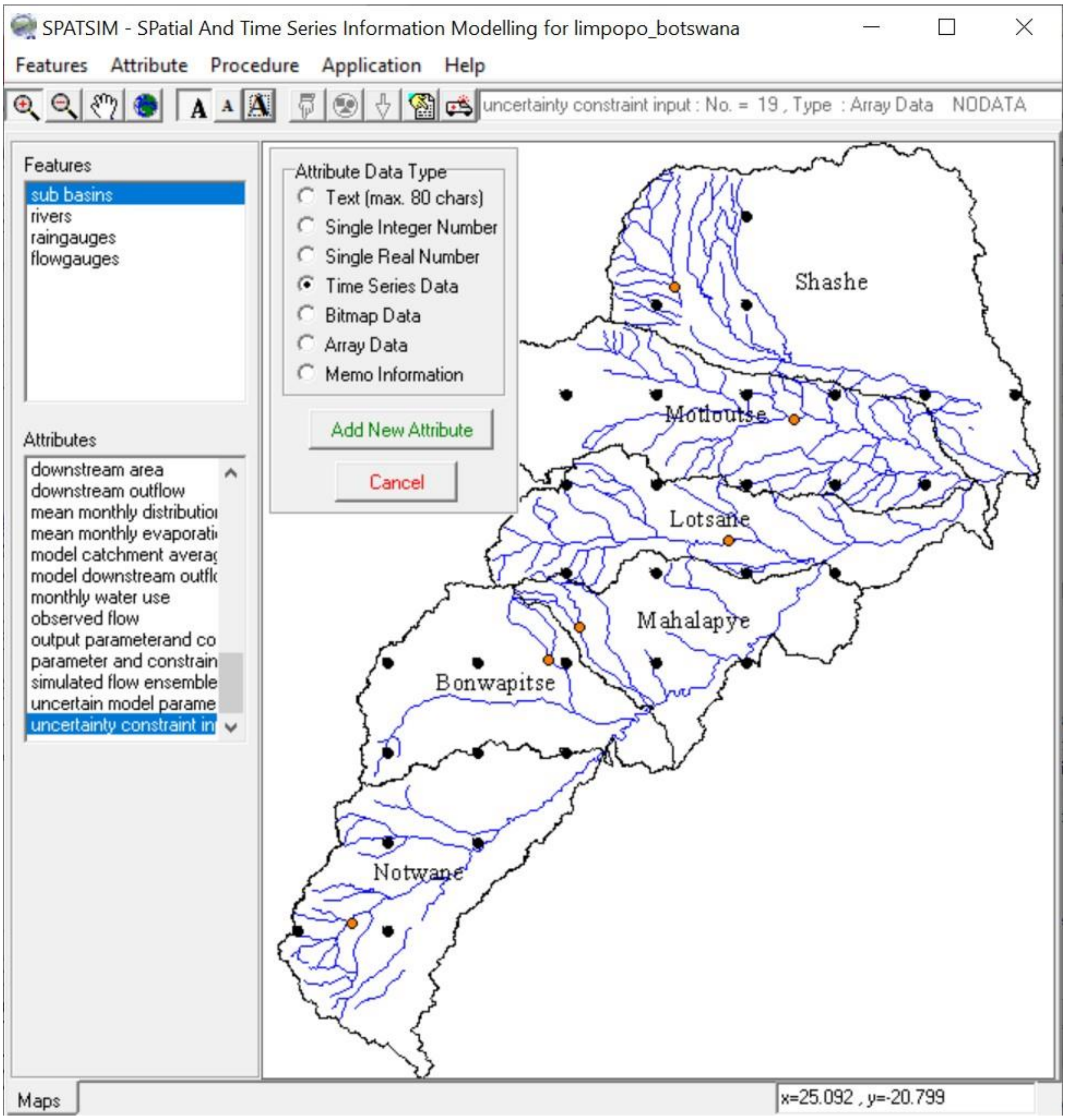

Figure 4.2: SPATSIM interface and model set up for the Limpopo sub-basins in Botswana

4.3.1 Generation of catchment averaged rainfall in SPATSIM

Catchment averaged rainfall, which offers an average rainfall amount for a set of point data within the catchment, is preferable for regional water resource assessments. Interpolation is carried out for this process. Weighted average rainfall data is generated from point rainfall data using downstream area attribute then selecting 'Procedure' then moving onto 'Point to area' menu item. Navigation to the area for which the average rainfall is to be calculated is done then clicking onto it, a search area which defines the radius for the calculation is highlighted (Figure 4.3).

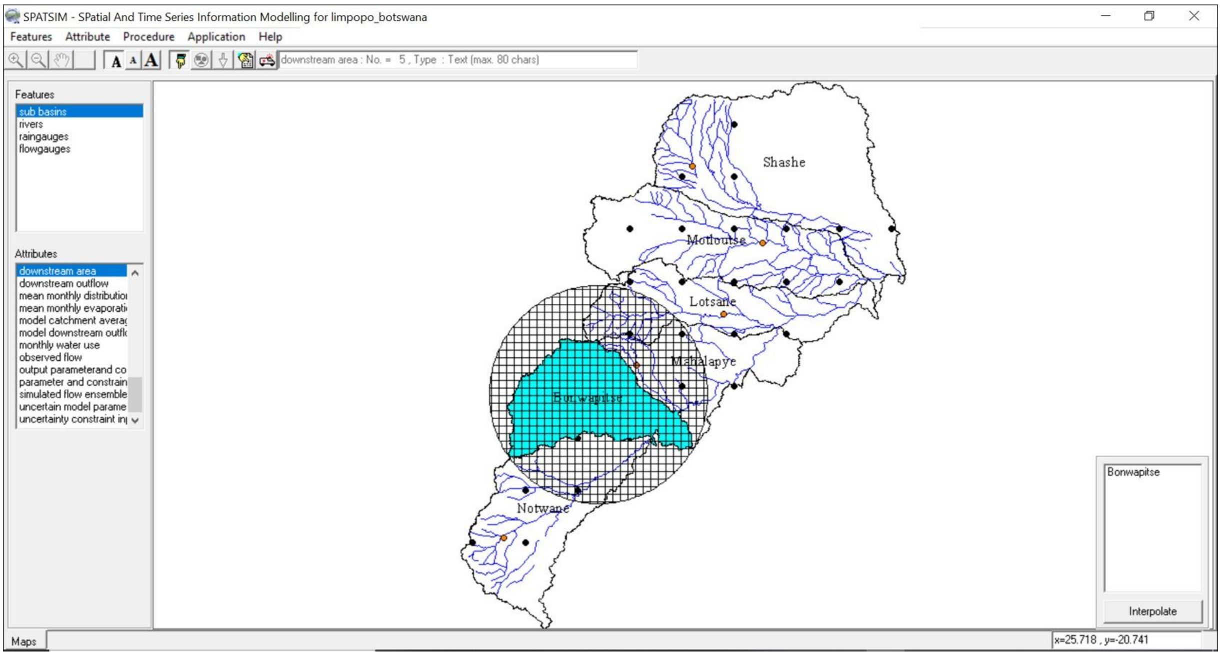

Figure 4.3: Defining an interpolation radius for calculation of basin average data

4.4 Generating the model parameter space

Any model is associated with uncertainty. For example, estimating model parameters is one of the primary sources of uncertainty. There is also model structural uncertainty (Gupta et al., 2012). Therefore, an uncertainty framework should be used in conjunction with the hydrological model to assess and quantify the uncertainty (Hughes et al., 2010). To constrain the parameters, initial ranges of minimum and maximum values are assigned. These ranges are guided by the physical basin properties normally obtained from field observations as well as prior knowledge of the basin processes and from available literature. Model runs are done through the uncertainty version of the model where the range of parameter values is used to create an ensemble of outputs. To choose the closest parameter space a Monte Carlo approach is used, where parameters of each sub basin are independently sampled. The process incorporates a uniform distribution in which both the mean parameter and standard deviation are stated, and the minimum and maximum values of the parameters are specified, thus constraints to all ranges are established (Figure 4.4). The results together with the goodness of fit statistics are viewed through the timeseries software (TSOFT) which is provided in the model.

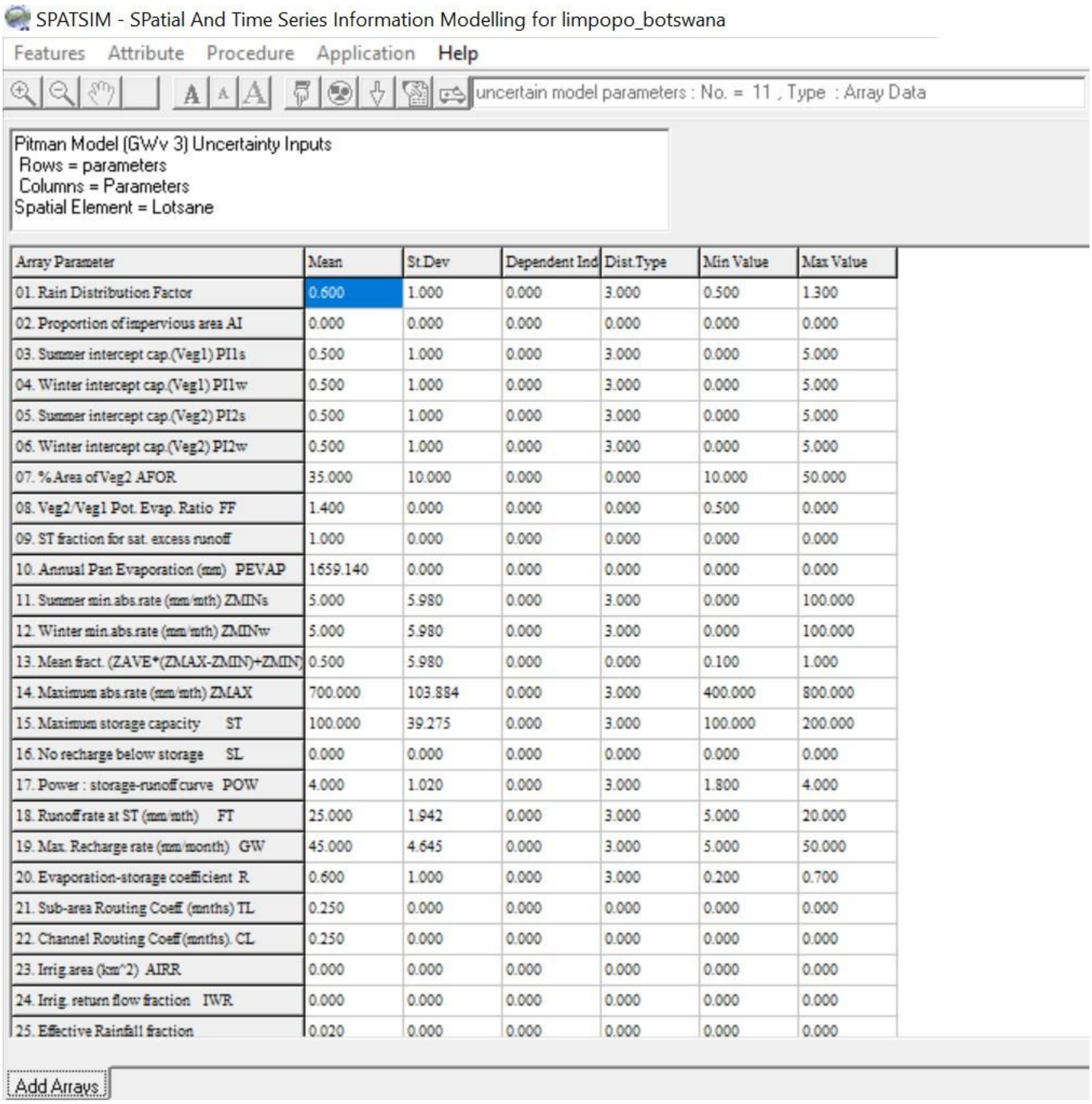

Array Parameter	Mean	St.Dev	Dependent Ind	Dist.Type	Min Value	Max Value
01. Rain Distribution Factor	0.600	1.000	0.000	3.000	0.500	1.300
02. Proportion of impervious area AI	0.000	0.000	0.000	0.000	0.000	0.000
03. Summer intercept cap.(Veg1) PI1s	0.500	1.000	0.000	3.000	0.000	5.000
04. Winter intercept cap.(Veg1) PI1w	0.500	1.000	0.000	3.000	0.000	5.000
05. Summer intercept cap.(Veg2) PI2s	0.500	1.000	0.000	3.000	0.000	5.000
06. Winter intercept cap.(Veg2) PI2w	0.500	1.000	0.000	3.000	0.000	5.000
07. % Area of Veg2 AFOR	35.000	10.000	0.000	0.000	10.000	50.000
08. Veg2/Veg1 Pot. Evap. Ratio FF	1.400	0.000	0.000	0.000	0.500	0.000
09. ST fraction for sat. excess runoff	1.000	0.000	0.000	0.000	0.000	0.000
10. Annual Pan Evaporation (mm) PEVAP	1659.140	0.000	0.000	0.000	0.000	0.000
11. Summer min.abs.rate (mm/mth) ZMINs	5.000	5.980	0.000	3.000	0.000	100.000
12. Winter min.abs.rate (mm/mth) ZMINw	5.000	5.980	0.000	3.000	0.000	100.000
13. Mean fract. (ZAVE*(ZMAX-ZMIN)+ZMIN)	0.500	5.980	0.000	0.000	0.100	1.000
14. Maximum abs.rate (mm/mth) ZMAX	700.000	103.884	0.000	3.000	400.000	800.000
15. Maximum storage capacity ST	100.000	39.275	0.000	3.000	100.000	200.000
16. No recharge below storage SL	0.000	0.000	0.000	0.000	0.000	0.000
17. Power : storage-runoff curve POW	4.000	1.020	0.000	3.000	1.800	4.000
18. Runoff rate at ST (mm/mth) FT	25.000	1.942	0.000	3.000	5.000	20.000
19. Max. Recharge rate (mm/month) GW	45.000	4.645	0.000	3.000	5.000	50.000
20. Evaporation-storage coefficient R	0.600	1.000	0.000	3.000	0.200	0.700
21. Sub-area Routing Coeff (mnths) TL	0.250	0.000	0.000	0.000	0.000	0.000
22. Channel Routing Coeff (mnths). CL	0.250	0.000	0.000	0.000	0.000	0.000
23. Irrig.area (km^2) AIRR	0.000	0.000	0.000	0.000	0.000	0.000
24. Irrig. return flow fraction IWR	0.000	0.000	0.000	0.000	0.000	0.000
25. Effective Rainfall fraction	0.020	0.000	0.000	0.000	0.000	0.000

Figure 4.4 Illustration of a physically based parameter space within the uncertainty framework of the model

4.5 Calibration and validation

Calibration refers to the process of estimating model parameters. The process ensures that the resultant parameters generate a simulated streamflow with the best fit to the observed streamflow hydrograph. Calibrations are done automatically and manually. The parameters sets are assigned initial values (maximum and minimum) that are guided by the physical basin properties. The calibration process followed the approach of Hughes et al. (2010) and is summarised in the following steps.

I. Assigning initial parameter ranges (minimum and maximum values) based on the physical basin properties.
II. Apply the Monte Carlo probabilistic sampling approach to generate ensembles from the total parameter space using the uncertainty version of the model
III. Use the statistical objective functions to establish behavioural parameter sets for which a model performance whose Nash Sutcliffe coefficient of efficiency CE > 0.5 and percent bias within a range of ± 10% are regarded as acceptable (Hughes et al., 2011).
IV. Finally perform manual calibration to fine tune and improve the parameters for each of the sub-basins.

Validation ensures that the values of the calibrated parameters can be used to reproduce situations or events outside of the calibrated time series. When simulation is carried out in a different period or in a different location, a good validation demonstrates that the calibrated model can mimic the catchment response characteristics without modifying the calibrated parameter values. During the validation process, time series data is entered into the model without having to alter the already calibrated parameters and a model run is performed. A successful validation demonstrates that the calibrated model can replicate the catchment response characteristics when simulation is run during a different period or in a different location without changing the values of the calibrated parameter.

4.6 Assessing the model performance

In assessing the model performance, three statistical objective functions are used and these are calculated in SPATSIM. The objective functions consist of the coefficient of determination (R^2) which is defined as the amount of variance in the observed data that is explained by the simulated data. R^2 ranges between 0 and 1. Poor correlations have values closer to 0 while reasonably good correlations show values closer to 1 indicating that all the variabilities in the observed data have been incorporated in the simulated values (Mwelwa, 2004). R^2 is given as follows:

$$R2= [\Sigma (Q_0-\overline{Q_0}) * (Q_s-\overline{Q_s})]^2 \;/\; [\Sigma(Q_0-\overline{Q_0})^2 * (Q_S-\overline{Q_S})]^2 \qquad (4.1)$$

Where, Q_0 is observed discharge, $\overline{Q_0}$ is the mean of observed discharge, Q_S is the simulated discharge and $Q_{S(m)}$ represents the mean of simulated discharge. One of the shortcomings of the R^2 is it's over sensitiveness to outliers and it is also insensitive to the systematic differences between the observed and simulated values (Legates and McCabe, 1999). The Nash Sutcliffe coefficient of efficiency (CE, Nash and Sutcliffe, 1970) is sensitive to systematic error and is thus a better statistic than R^2. CE measures the variance of the observed data as described by the model and takes on the values less than 0, representing an unwanted outcome where the observed mean is deemed the better predictor than the model to a value of 1 which implies a perfect match between the observed and simulated values. Big differences between CE and R^2 suggest a systematic error. CE is calculated as follows:

$$CE=1-[(Q_0-\overline{Q_S})^2 \;/\; (Q_0-\overline{Q_0})^2] \qquad (4.2)$$

The third statistical objective is the percentage error which is defined as the difference between the approximate value and the exact value in respect to the exact value (Helmenstine, 2020). Analysing how closely the measured value corresponds to an actual value is the goal of determining the percent error. To determine the % error, the relative error is multiplied by 100 and expressed as follows.

$$\% \text{ error} = ((\text{Approximate value-exact value})/ \text{ exact value})) *100 \quad (4.3)$$

4.7 Climate change assessment

Most estimates of climate change are produced using global-scale models, which generate changes that are expected to occur over many years and into the foreseeable future. The weakness of the global climate models is that atmospheric details like cloud cover airborne particles and localised pollution sources are not represented yet they have an impact in climate at local scale (Cooney, 2012), thus the need for downscaling. Eight GCM model outputs of temperature and precipitation under RCP 4.5 are used in this study. The models include CM5 CLMcom, CM5 RCA4, EARTH CLMcom, EARTH RCA4, ES CLMcom, LR CLMcom and LR RCA4. (Giorgi, et al., 2009; Jones et al., 2011; Gnitou et al., 2019). The GCM datasets were downscaled using the Distribution-Based Scaling approach under the initiative of the Swedish Meteorological Hydrological Institute's CORDEX initiative (Giorgi et al., 2009; Jones et al., 2011). The downscaling technique involves converting large-scale GCM data to smaller regional scales where observed and simulated frequency distributions are matched by assuming variable-dependent theoretical distributions (Yang et al., 2010). The downscaled GCM outputs are then imported into the calibrated model to simulate the future hydrological conditions in a basin.

Changes in monthly streamflow, precipitation and temperature relative to the historical conditions are given as percent deviations of the long term mean values for the different variables (Tan et al., 2020) and calculated as follows:

$$\%\ \text{Change} = \frac{(\text{future mean} - \text{historical mean})}{\text{Historical mean}} * 100 \qquad (4.4)$$

4.8 Hydrological Drought

To understand the spatial and temporal variability of water resources in the study area, a hydrological drought analysis was performed at the 12-monthly timescale. The Standardized Precipitation Evapotranspiration Index (SPEI), which considers both precipitation and the effect of temperature on droughts has been applied. Since climate change predictions postulate a temperature rise in the 21st century SPEI is an appropriate index as it incorporates temperature into its calculation. SPEI is a multiscalar drought index that measures drought severity according to its intensity and duration. In this study, SPEI was generated using the SPEI package (Bergueria et al., 2014) found in R software package. SPEI is calculated based on the non-exceedance probability of the differences between precipitation and potential evapotranspiration. (PET). For this study PET was calculated using the Thornthwaite method (Thornthwaite, 1948). The difference (D_i) between monthly precipitation and monthly PET is given as follows:

$$D_i = P_i - PET_i \qquad (4.5)$$

The SPEI is calculated as standardized values of f(x) according to Abramowitz et al. (1965)

$$SPEI = W - \frac{C_0 - c_1 w + c_2 w2}{1 - d_1 w + d_2 w2 + d_2 w3} \qquad (4.6)$$

$$w = \sqrt{-2\,\mathrm{In}(p)} \qquad (4.7)$$

For P≤0.5 where P is the probability of exceeding a determined Di value and P= 1-f(x).

C_0=2.515517, C_1=0.802853, C_2=0.010328, d_1=1.432788, d_2=0.189269, d_3=0.001308.

The SPEI drought categories and classes (Mckee et al., 1993) are shown in Table 4.2

Standardized Streamflow Index (SSI)

The SSI is a statistically based drought index that is based on monthly streamflow over a lengthy period. It is applied to identify anomalies in observed streamflow. The index is often calculated for a monthly accumulation period, however longer periods such as 3-12 months can be used to track the cumulative water deficit over the hydrological year. For this study a period of 12 months was used to account for hydrological droughts. The index is calculated using seasonal streamflow amounts with their long-term mean and standard deviation. Streamflow data simulated for the future (2025 to 2050) was used to generate the SSI under the R software package. The procedure involves determining the probability density function for the selected streamflow time series, after which the streamflow data is normalized using the gamma function. Once the cumulative distribution function F(x) is identified, the SSI values can be calculated as z-scores, following the procedure of Guttman (1999). The index is computed by dividing the difference between the normalized seasonal streamflow and its long-term seasonal mean by the standard deviation. SSI is given as follows:

$$\mathrm{SSI}= \frac{x_{y}-x_{\check{y}}}{\sigma} \qquad (4.8)$$

Where X_y is the seasonal streamflow amount, $X_{\check{y}}$ is the long-term seasonal mean and σ is its standard deviation. The classifications of SPEI and SSI are presented in Table 4.2.

Table 4.2 SPEI and SSI categories and drought classes

SPEI Values	Category	SSI Value	Category
≥2.00	Extremely wet	≥2.00	Extremely wet
1.5 to 1.99	Very wet	1.50 to 1.99	Severely wet
1.00 to 1.49	Moderately wet	1.00 to 1.49	Moderately wet
-0.99 to 0.99	Near normal	0.00 to 0.99	Mildly wet
-1.00 to 1.49	Moderately dry	0.00 to -0.99	Mild drought
-1.5 to 1.99	Severely dry	-1.00 to 1.49	Moderate dry
≤-2	Extremely dry	-1.50 to -1.99	Severe dry
		≤-2	Extreme drought

Chapter 5

Results and Discussion

5.1 Calibration

This section presents the hydrological model calibration results for the different sub-basins of the Limpopo in Botswana. The modelling process consisted of gathering information on the physical basin characteristic which would help in constraining the parameter space before importing the data into the modified Pitman model for calibration.

5.1.1 Assigning the initial parameter space

The Pitman model parameters were described in Chapter 4. The ST, AFOR and PEVAP parameter values were fixed based on the unique characteristics of the sub basins. The parameters TL, CL, GPOW and SL were fixed at 0.25, 0, 3.5 and 0 respectively as recommended in literature (e.g. Hughes et al., 2009). Initial ranges for the main parameters were assigned using the physical basin properties and guidelines outlined in Kapangaziwiri (2008) as follows.

- High values of RDF are expected in semi-arid sub basins
- High values of ZMIN and ZMAX values are assigned for coarse textured soils and low values for fine textured soils.
- Basins with a large variation in soil properties exhibit large differences in the ZMIN and ZMAX values.
- Low infiltration capacities of soils are associated with low values of ZMIN and ZMAX, which are assigned to arid basins with thin soils.

- Parameters PI1 and PI2 are guided by the proportion of vegetated area, where low values are assigned to grassland and bush areas and large values are assigned to dense forest or managed plantations.
- The ST parameter is guided by the moisture holding capacity of soils within a sub basin, in which high values are assigned to highly fractured unsaturated zones and deep soils while low values are assigned to areas with thin soils
- The FT parameter is partly guided by soil characteristics and influenced by topology. High FT values are assigned for high gradient and high relief, whereby the runoff rate is increased in steep gradient areas and low values assigned to low gradient areas.
- The parameter GW is influenced by the ST parameter in combination with the underlying geology, soil structure and texture, fracturing and secondary weathering.
- The R parameter is guided by the relationship between soil and evapotranspiration where high values are assigned to areas of less dense vegetation and low values are expected for deep rooted vegetation.

5.1.2. Individual sub-basin characteristics for assigning initial parameter values

For the RDF parameter, a parameter range of 0.5 to 1.0 was assigned to all the sub-basins because the study area is in a semi-arid region where the parameter value is expected to be high. It is worth noting that the soil moisture store (ST) is made up of two parts (the soil and unsaturated components). In the unsaturated zone under the soil, fractured formations have the ability to store moisture in cracks and fissures. Because much of southern Africa is underlain by fractured rock structures (Kapangaziwiri, 2008), the ST parameter must account for the moisture storage capacity of these fissures thus a parameter range of 120 mm to 200 mm was assigned. Also worth noting is that the presence of different soil types accounts for the difference in the calibrated amount of moisture in each sub basin as soil porosity differs. Transmissivity and storativity from previous studies (Sitoe and Qwist-Hoffman, 2013) have been used for the parameter estimations. Transmissivity (m^2 d^{-1}) is a product of permeability and saturated aquifer thickness, while the storativity is a measure of the capacity of the aquifer to store water.

Bonwapitse

The predominance of deep Kalahari sands implies an ST parameter range of 120 to 200 mm. Subtropical grasslands, savanna shrub lands and scattered trees are dominant in the catchment area. The sandy texture and the presence of vegetation allows for absorption rates of ZMIN (50.5 to 150 mm/month) and ZMAX (200- 800mm/month).

Lotsane

The sub basin is dominated by Luvisols. Though with good drainage, the soils are shallow thereby limiting root penetration and may cause water logging thus the ST value was set at a range of 100 mm-200 mm, which is also characteristic of semi-arid areas. The high elevation of 625 m to 1 380 m above sea allows for a high FT range of 5 to 30 mm/month. Though always associated with poor groundwater conditions, there are some Karoo age sedimentary basins overlain by volcanic sequences thus the GW parameter can be estimated at a medium range of 15 to 50 mm/month.

Mahalapye

The sub basin is mostly covered by lixisols, underlain by loamy sand suggesting high ST values (120 mm to 200 mm). Subtropical grasslands and savanna shrublands dominate the sub basin, in addition there are lixisols which limit vegetation growth, as clays crack suggesting low absorption rate values. Therefore, the ZMIN and ZMAX values range between 5 to 50mm/month and 200 to 400 mm/month respectively. The sub basin mainly comprises of granite and gneissic rocks with the occurrence of Karoo age sedimentary basins underlain by volcanic sequences together with the Fractured Waterberg, Palapye, Soutpansberg groups (Environmentek CSIR, 2003), which are known to provide a low groundwater yields. However, with the presence of Karoo basins which have proven to be good aquifers a medium range of 15 to 50 mm/month was allocated for the GW parameter.

Motloutse

The sub basin is made up of subtropical grasslands and savanna shrublands suggesting high absorption rate values. However, the presence of luvisols (high clay content) implies medium absorption rates of the range of 5 to 20 mm/month for ZMIN and 400 to 700mm/month for ZMAX as well as a medium ST value range of 120 to 200mm (within the semi arid limits). Within the catchment, groundwater is found in crystalline basement rocks, the Karoo strata and alluvial deposits, these are sand river aquifers that form shallow unconfined aquifers (SMEC/EHES, 2006; Lentswe and Molwalefhe, 2020). Thus, the GW parameter was set at a range of 15 to 50 mm/month.

Notwane

Almost 50% of the sub basin is covered by the Arenosols and Acrisols,Leptsols,Regosols and Lixisols. Therefore, an ST value ranging between 120 to 200mm is assigned. The sub basin is covered by deserts and xeric shrub lands together with savanna shrublands (WWF, 2010), by virtue of being sparse there are possibilities of high runoff suggesting a ZMIN range of 25 to 150mm/month and ZMAX ranging from 400 to 800mm/month. The huge difference between the 2 parameters is caused by the different types of vegetation within the sub basin. The groundwater yields are generally low

(Environmentek CSIR, 2003) due to the presence of underlying sedimentary rocks that have low porosity thus the GW parameter was set at 15 to 50 mm/month.

Shashe

The different soil types that are found within the area include Luvisols, associated with good drainage and forming on flat or gently sloping landscapes and the Leptosols, which are characterised as free draining soils (Nachtergaele, 2010) therefore the ST parameter range is set at 120 to 200 mm/month. The hydrolithological units found in the sub basin consist of the Fractured Waterberg, Palapye, Soutpansberg groups as well as the Central Zone of the Limpopo Mobile Belt, made up of granite and gneissic rocks all of which have low groundwater yields in general (Moseki, 2013). The GW parameter was therefore assigned a range of 5 to 20 mm/month. The assigned parameter ranges for all the sub- basins are presented in Table 5.1.

5.2 Model calibration and validation results

The calibration and validation results for all the six sub-basins are presented in this section. Table 5.2 shows a summary of the model performance statistics while the final calibration parameters are presented in Table 5.3. Different simulation periods were used for the various sub-basins based on availability of the time series data of good quality at the different gauging stations. Statistical objective functions consisting of the coefficient of determination (R^2) and coefficient of efficiency (CE) as well as the percent bias (PBIAS) were used to assess the performance of the model. For all the sub-basins the R^2 and CE values are greater than 0.5 and the percentage bias between lies within a range of ± 10%.

Table 5.1 Initial parameter ranges assigned for the 6 sub-basins

Parameter	Shashe		Motloutse		Lotsane		Mahalapye		Bonwapitse		Notwane	
	Min	Max	Min	Max	Min	Max	Min	Max	Min	Max	Min	Max
RDF	0.5	1	0.5	1	0.5	1	0.5	1	0.5	1	0.5	1
ZMIN	5	30	5	20	5	50	5	50	50.5	150	25	150
ZMAX	400	600	400	700	400	800	200	400	400	800	400	800
ST	120	200	120	200	120	200	120	200	120	200	120	200
POW	1.8	2	1.8	3	1.8	4	1.8	2	1.8	4	1.8	3.5
FT	1	5	5	35	5	30	1	5	5	20	3	5
GW	5	20	15	50	5	50	15	50	5	20	15	50
R	0.2	0.7	0.2	0.7	0.2	0.7	0.2	0.7	0.01	0.7	0.2	0.7
D.DENS	0.2	0.5	0.2	0.5	0.2	0.5	0.2	0.5	0.2	0.5	0.2	0.5
T	5	20	5	30	5	30	5	20	5	30	5	30
S	0.001	0.008	0.001	0.008	0.001	0.008	0.001	0.008	0.001	0.008	0.001	0.008
GW slope	0.001	0.01	0.001	0.01	0.001	0.01	0.001	0.01	0.001	0.01	0.001	0.01
RSF	0.2	0.8	0.2	0.8	0.2	0.8	0.2	0.8	0.2	0.8	0.2	0.8

Table 5.2 summary of the model performance for the six sub basins

Sub-basin	Period	Months	R^2	CE	PBIAS (%)
Bonwapitse	Calibration	120	0.834	0.809	14
	Validation	84	0.776	0.511	0.85
Lotsane	Calibration	255	0.771	0.761	14
	Validation	77	0.944	0.918	16
Mahalapye	Calibration	243	0.736	0.725	15
	Validation	72	0.788	0.783	23
Motloutse	Calibration	135	0.741	0.78	15
	Validation	108	0.97	0.893	15
Notwane	Calibration	84	0.836	0.732	17
	Validation	59	0.736	0.726	21
Shashe	Calibration	133	0.871	0.849	14
	Validation	64	0.771	0.701	5

Table 5.3 shows the final calibrated parameters obtained in this study. The differences among the sub-basins can be attributed to different physical basin properties as well as varying catchment response characteristics.

The time series plots for the various sub-basins are displayed in Figures 5.1 to 5.6. For the Bonwapitse sub-basin (Figure 5.1), the high flow simulations are satisfactory whereas the low flows are frequently over and under simulated. The simulated flows compare very well with the observed flows giving CE and R^2 values of 0.809 and 0.834 respectively while the percent bias of 14% suggests an acceptable simulation (Table 5.2).

Table 5.3: Final calibrated parameters for the 6 sub basins

Parameter	Bonwapitse	Lotsane	Mahalapye	Motloutse	Notwane	Shashe
RDF	0.9	0.6	0.955	1	0.9	0.9
PI1s (mm)	3	0.5	2	4	3	2
PI1w (mm)	1.5	0.5	1.5	4	3	1.5
PI2s (mm)	2	0.5	2	4	3	2
PI2w (mm)	1.5	0.5	1.5	4	3	1.5
AFOR%	20	35	30	20	30	30
PEVAP(mm)	1638.4	1659.1	2135	2288.7	2461.3	1882.6
ZMINs(mm/month)	50.5	5	5	10	25	25
ZMINw(mm/month)	50.5	5	5	10	25	25
ZMAX(mm/month)	750	700	200	600	800	570
ST(mm)	180	100	119.7	100	120	119.7
POW(mm/month)	1.8	4	1.9	3	2.5	1.9
FT(mm/month)	10	25	3.1	35	8	3
GW(mm/month)	4	45	20	5	15	20
R	0.01	0.6	0.2	0.2	0.4	0.2
TL(months)	0.2	0.2	0.2	0.25	0.3	0.25
CL(months)	0	0	0	0	0	0
GPOW	3.5	3.5	3.5	3.5	3.5	3.5
D.DENS	0.4	0.4	0.4	0.4	0.4	0.4
T(m2/d)	30	25	15.739	4.5	30	15.7
S	0.001	0.001	0.008	0.001	0.001	0.008
GW slope	0.01	0.001	0.01	0.01	0.01	0.01
RSF	0.4	0.5	0.2	0.3	0.5	0.2

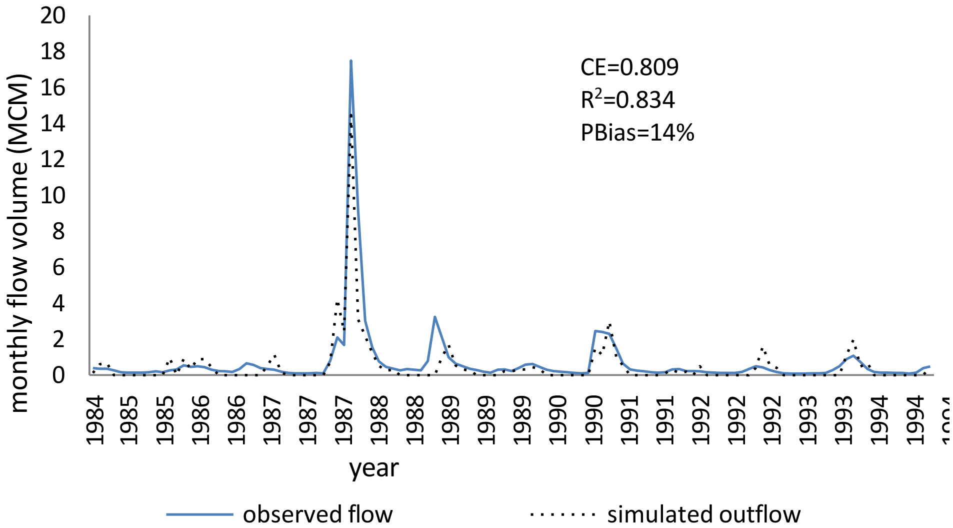

Figure 5.1: Observed and simulated monthly flows for Bonwapitse

For the Lotsane sub basin (Figure 5.2), the simulated low flows show a close fit with the observed flows in magnitude and pattern of the time series. On the other hand, the high flows are frequently under and over-estimated. Nonetheless, the calibration generated an R^2 value of 0.771 and CE value of 0.761 with a percent bias value of 19% suggesting an acceptable simulation.

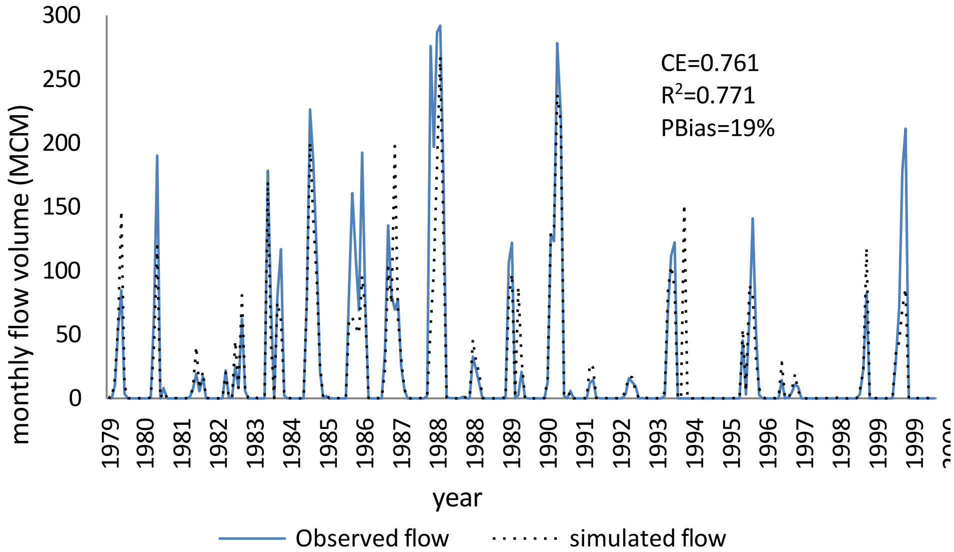

Figure 5.2: Observed and simulated monthly flows for Lotsane

The Mahalapye sub basin (Figure 5.3) is generally characterised by low flows which complicated the calibration process. This resulted in over-simulation of the very low flows while the high flows were often under-simulated. However, the simulated flows compare well with the observed flows as indicated by CE and R^2 values of 0.725 and 0.736 respectively while the percent bias was 15%.

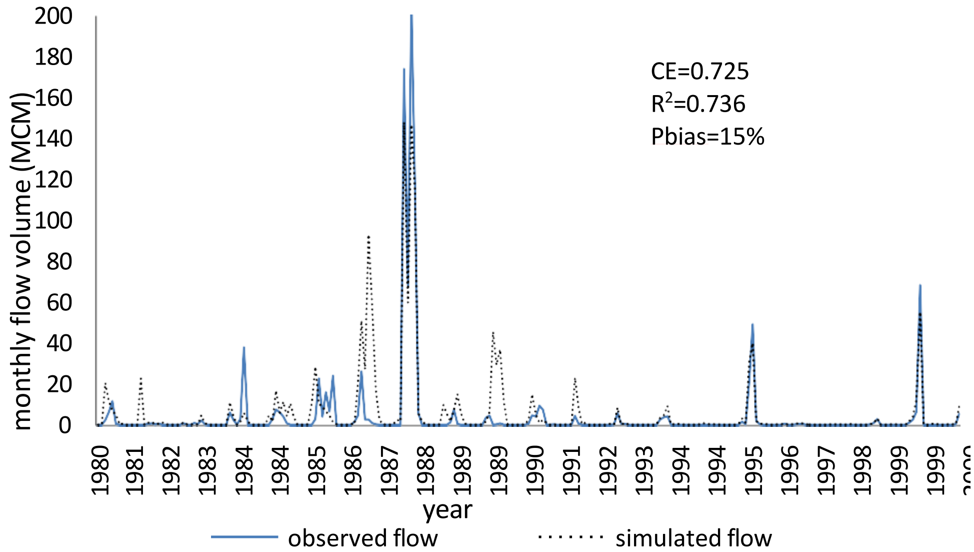

Figure 5.3: Observed and simulated monthly flows for Mahalapye

For the Motloutse sub basin (Figure 5.4), despite over-and under-simulation of the high flows an R^2 value of 0.741, a CE value of 0.741 and a percent bias of 15% were obtained. For Notwane sub basin (Figure 5.5), the low flows are slightly over simulated while the high flows around 2011 and 2013 periods are slightly over simulated. The simulated flows compare well with the observed flows giving the CE and R^2 values of 0.732 and 0.836 and a percent bias of 17%.

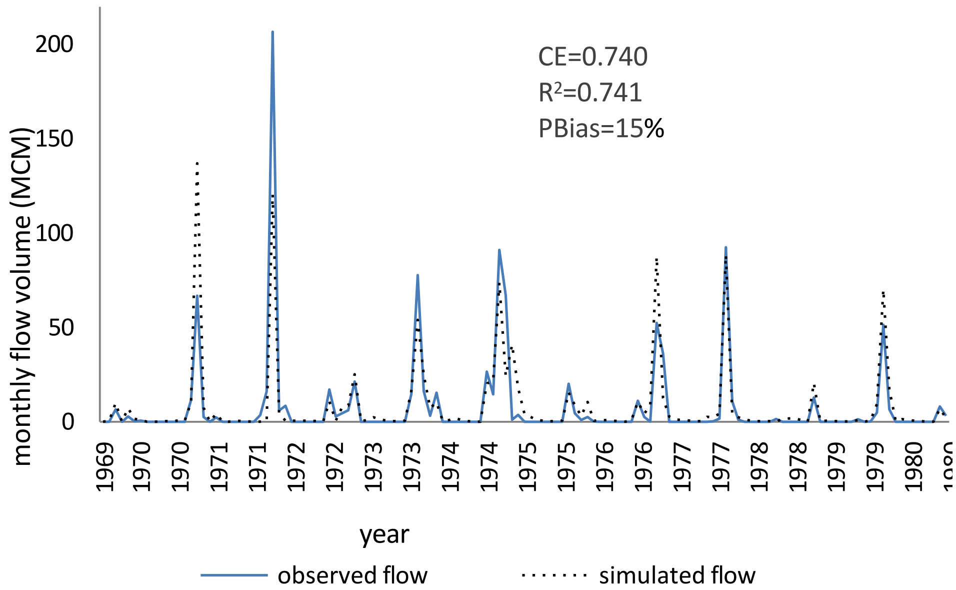

Figure 5.4: Observed and simulated monthly flows for Motloutse

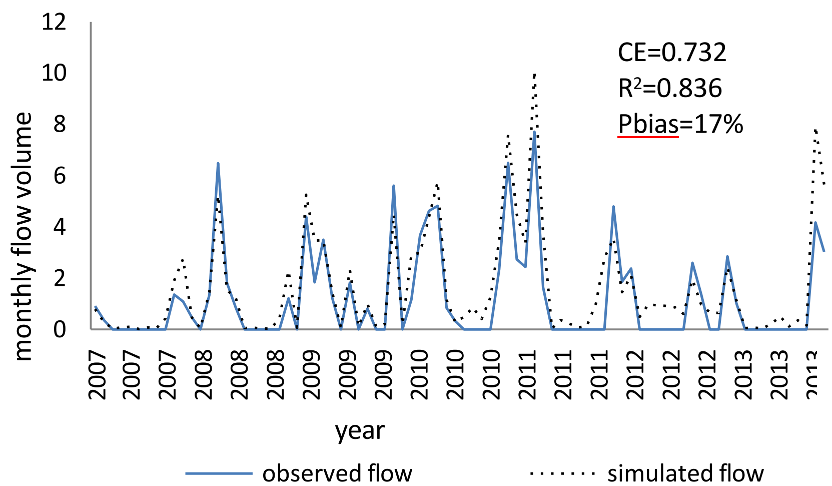

Figure 5.5: Observed and simulated monthly flows for Notwane

A good calibration performance is exhibited for the Shashe sub-basin (Figure 5.6) The respective CE, R^2 and percent bias values obtained during the calibration process are 0.849, 0.871 and 14% suggests acceptable simulations.

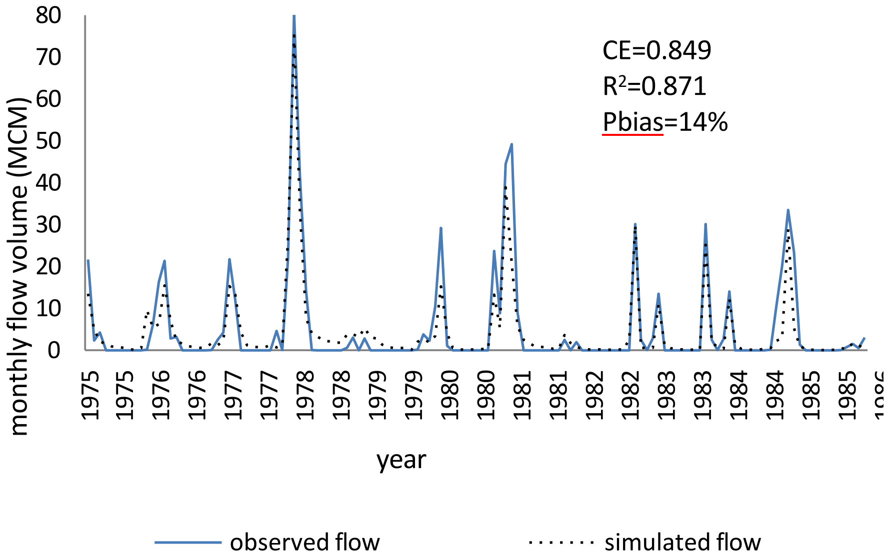

Figure 5.6: Observed and simulated monthly flows for Shashe

Model Validation

The timeseries plots showing the validation results for the respective sub-basins are given in Figures 5.7 to 5.9. The model performance statistics for the validation process were presented in Table 5.2, with R^2 and CE values ranging from 0.5 to 0.9 thereby showing a good performance. The percentage bias results range from 0.85 and 19% for all the sub-basins.

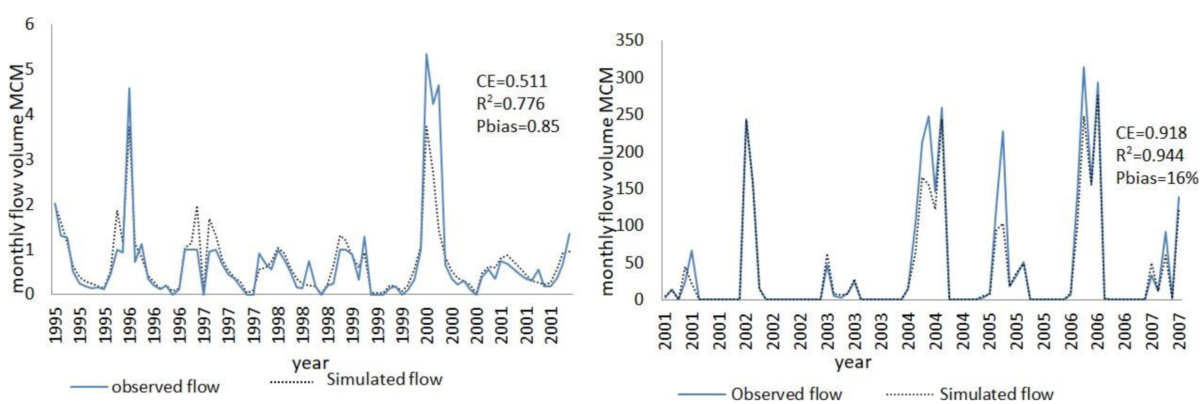

Figure 5.7: Observed and simulated monthly flows for Bonwapitse (left) and Lotsane (right)

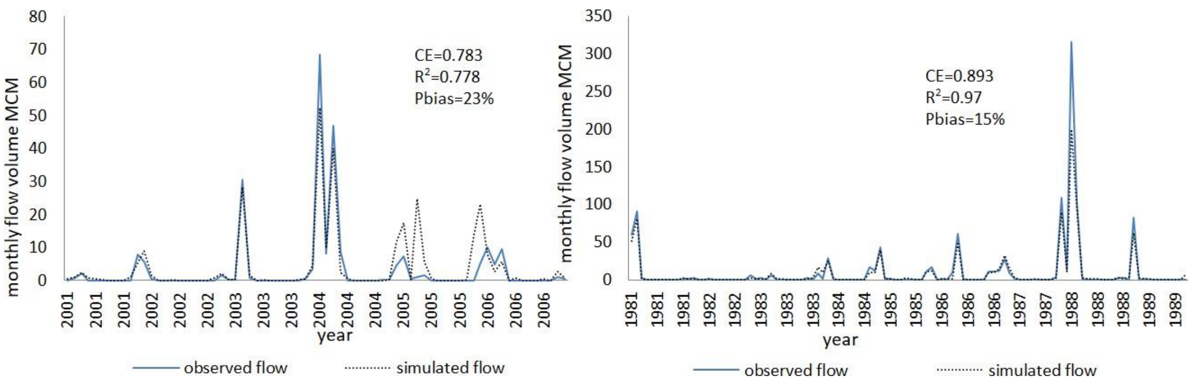

Figure 5.8: Observed and simulated monthly flows for Mahalapye (left) and Motloutse (right)

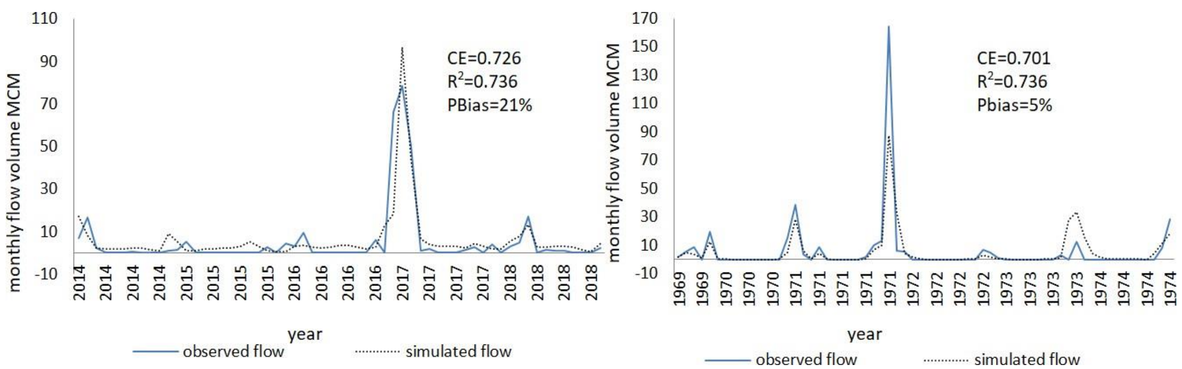

Figure 5.9: observed and simulated monthly flows for Notwane (left) and Shashe (right)

5.2.1 Discussion

The aim of this chapter was to apply the calibration process to develop a hydrological baseline for the Limpopo sub-basins located in Botswana. The resultant baseline can then be applied to assess hydrological changes due to climate variability and climate change and even various water use scenarios. The modified Pitman model was used for this purpose. The Pitman model is a conceptual semi-distributed monthly rainfall-runoff model that reflects different components of the runoff generation process at the basin scale and is based on basic hydrology principles. To perform the calibration process, physical basin characteristics were used to generate initial parameter bounds which were then subjected to an uncertainty framework of the model to generate a parameter space that could inform and refine the manual calibration process.

The physical basin characteristics have a direct influence on the physical basin parameters. Such properties were used in this study to inform the parameter space when generating the initial parameter ranges therefore it can be assumed that hydrologically sensible relationships have been developed. For example, the ST parameter considers soil properties in the unsaturated components. The moisture available in the soil is dependent on the soil's porosity and its depth while the unsaturated zone capacity is influenced by the storativity and depth of the fractured zone. As such the study resulted in high ST values for deep, well drained soils with gentle slopes which are characteristic of the Shashe sub basin while low ST values resulted from shallower soils which are usually found at steeper headwater basins. It is through the fractured rock systems that some aquifers exist, which is characteristic of Southern Africa aquifers. They have low primary permeability and large spatial variations in ground water features (Kapangaziwiri, 2008). However, with the presence of Karoo sediments which are good aquifers such as Lebung and Ecca, the GW parameter for some of the sub basins remained high. The permeability of these geological features determines the ease of water to pass through thereby directly influencing the soil moisture content.

The objective performance statistics for both the calibration and validation processes have indicated the capability (CE>0.5, PBIAS <20 and R^2>0.5 (Mwelwa, 2004; Krause, et al., 2005) of the modified Pitman model to represent the hydrological characteristics of the Limpopo sub-basins in Botswana. However, the modelling process was not made any easy because of the extremely low flows that characterise semi-arid environments, these flows proved difficult to simulate. Based on the modelling experience, it was observed that high flows were particularly sensitive to changes in the moisture storage parameter (ST) and the interception parameters (PI1 and PI2). At the same time the low flows were very susceptible to slight changes in the groundwater storage parameter (GW). The calibration experience also indicated that in semi-arid environments lower streamflows are more sensitive than the higher streamflows.

In general, model performance for the calibration process was better in the northern sub-basins compared to the southern sub-basins. For example, the CE for Shashe in the north was 0.849 while that for the Notwane sub-basin in the south was 0.732. Normally the Shashe catchment receives more rainfall than Notwane and generally in Botswana more rainfall is received in the north compared to the south. Although rainfall is not linearly transformed to streamflow this study showed that the calibration process was much easier when there is a considerable amount of streamflow compared to there being minimal or no flows at all.

Although an uncertainty framework was applied to generate the initial parameter space and minimise uncertainty from parameterisation, it should be acknowledged that the modelling process will be fraught with predictive uncertainty to some extent. Possible sources of uncertainty include the nature of the input data and limitations in model conceptualisation (Liu and Gupta, 2007). Input data uncertainty may arise from measurement errors in rainfall, evaporation and the observed streamflow. The quality of the input data may also be affected by infrequent monitoring, short time series as well as sparse and diminishing measuring networks (Vrugt et al., 2005). This situation is characteristic of the sub-basins that were examined in this study. Since the study relied initially on physical basin characteristics and other data sources to generate the parameter bounds, it is possible that due to subjectivity the data may have been misinterpreted in some cases. Also some of the datasets were not sufficient enough in terms of quality and the length of the timeseries.

5.3 Climate change impacts on basin hydrology

This section presents the expected changes in the temperature, precipitation and monthly mean streamflow in the future period of 2025 to 2050 as result of future climate change scenarios. The changes are evaluated relative to the long-term historical amounts and calculated as percent deviations of the future climate from the historical means. Worth noting is the fact that normally the wet season in Botswana extends from November through April while the dry season is from May through October.

5.3.1 Temperature change

Increased temperatures intensify the effects of evapotranspiration which in turn will affect a basin's water balance. The anticipated changes in temperature in the future for all the sub-basins and for all the GCMs are presented in Figure 5.10. A general increase in mean monthly temperature with an average of 5% is expected for the Bonwapitse sub-basin, however, the months January and October are an exception where a slight decrease in temperature of not more than 3% may be expected. The Lotsane sub-basin may experience a general increase in temperature of 4% average while the same GCM's predict decrease in temperature for the months of January and August. The temperature varies from 14.3°C to 26.7°C, with an average of 21.8°C .

A general increase in temperature with an average of 4% is predicted for the Mahalapye sub-basin with temperatures varying from 15.3°C to 29.2°C and an average of 22.6°C. Temperature decrease is observed for the months of January and Augus.t Overall and across all GCMs temperatures in the Motloutse sub-basin may increase on average by 3% while slight decreases may occur during the months of January, August, September and December. Temperature varies from 14.6°C to 26.5°C with an average of 21.8°C. For the Notwane sub-basin temperatures are expected to increase with an average of 6% across all GCMs except for the months of January, August and December where slight decreases may occur but not exceeding -5%. For the Shashe sub basin an average increase of 3% is expected with temperatures varying from 14.6°C to 25.5°C with an average of 21.2°C. The temperatures within the basin vary from 12°C to 26.4°C with an average of 20.8°C. The future temperature is expected to increase on overall by values not exceeding 16% while the temperature may decrease minimally (≤5%) for the months of January, August, September, November and December. Temperatures may change by 1.5 °C on average.

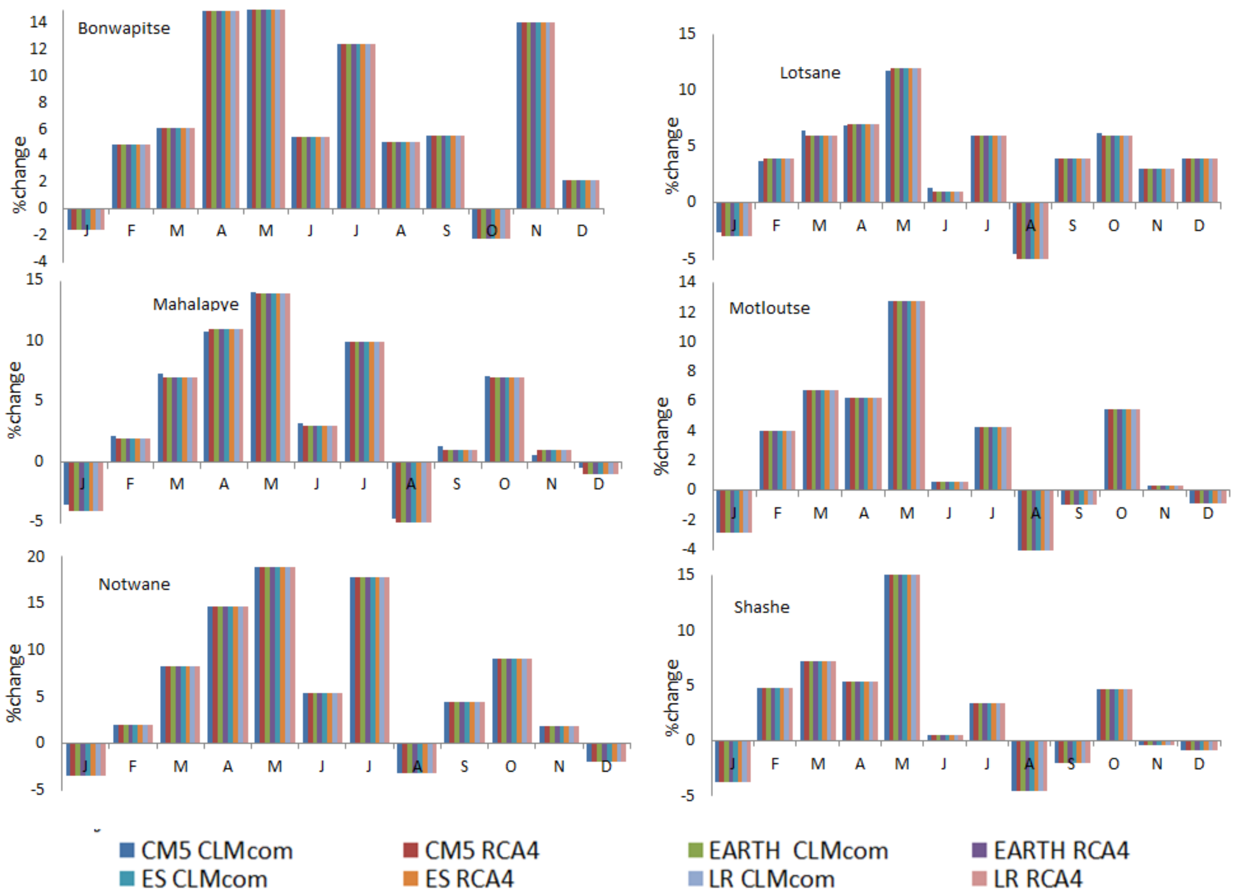

Figure 5.10: Predicted changes in future (2025 to 2050) temperature by different GCMs for the Limpopo sub-basins

5.3.2 Precipitation change

Figure 5.11 shows the expected changes in precipitation as a result of climate change in the future period of 2025 to 2050. Generally, there is a mixed direction of change in precipitation, whereby precipitation is expected to increase in some months and decrease in some months. It is expected by all GCMs that the wet season months of January to April may experience a decrease in rainfall of up to 20% on average. However, for all the sub-basins decreases in precipitation of more than 50% are predicted by ES CLMcom, ES RCA4. The dry season months in the study area extend from May to October and it is observed that these months show a considerable change (positive and negative) in precipitation. However, given that these are dry months with barely any precipitation, any slight increase or decrease in precipitation will induce a marked difference relative to the base value yet in essence the change is very small or negligible in magnitude and can therefore be ignored. ES CLMcom, ES RCA4 and EARTH CLMcom GCM's predict changes of more than 50% both negative and positive.

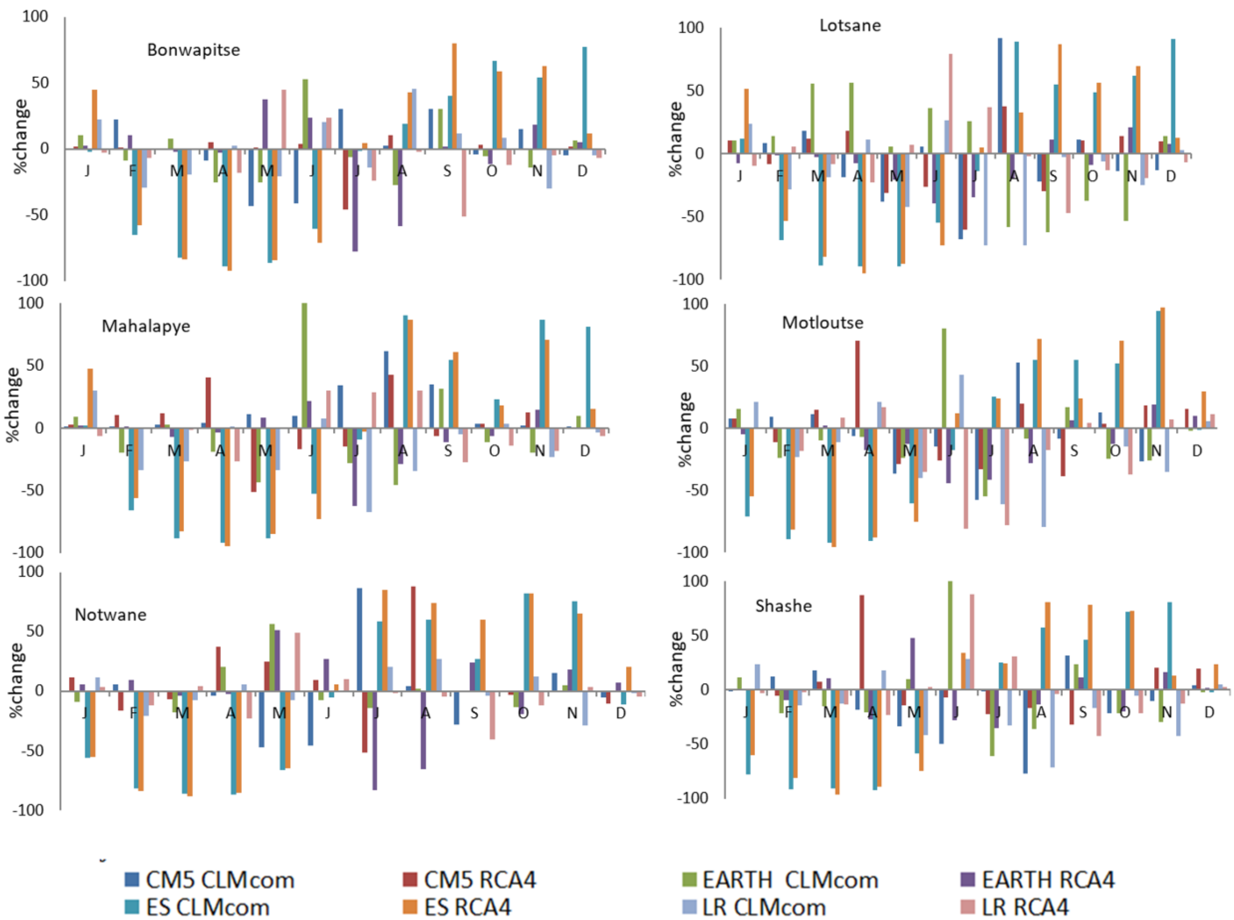

Figure 5.11: Predicted changes in future precipitation of 2025 to 2050 by different GCMs for the Limpopo sub-basins

Although with varying magnitudes, precipitation is generally expected to decrease during the wet season months of January to April. For all the sub-basins the models ES CLMcom and ESRCA4 predict large decreases in future precipitation amounts that may exceed 50% while average decreases in precipitation of not more than 20% are simulated by the other GCMs.

The Bonwapitse sub basin shows a decrease in precipitation for the EARTH RCA4, ES CLMcom and ES RCA4 models with an anticipated decrease of 50% on an average for the months of February through August. However, a general increase of 20% is expected for the sub basin for the months May through January. ES CLMcom and ES RCA4 models show the highest changes both in the negative and positive % changes during the months of February through June and August through November respectively.

An average decrease in precipitation of about 25% is generally expected for the Lotsane sub-basin. However, the months of September through April may experience increases in precipitation but not exceeding 15%. The ES CLMcom and ES RCA4 models predicted the highest percentage changes in both directions.

For the Mahalapye sub-basin the months of February through July may experience a decrease in precipitation within an approximate range of -20% to -80 % with the ES CLMcom and ES RCA4 models showing the highest changes. In addition, a general increase in precipitation from the months of August through January within a range of 10% to 80%.

The Motloutse sub basin depicts a general decrease in precipitation with the ES CLMcom, ES RCA4, LR CLMcom and LR RCA4 models showing the highest negative changes within a range of -50% to -90% for the months of January through August.

For the Notwane sub basin, an average decrease in precipitation of about 20% is expected for the months of January through May. The highest percent decrease is expected by the ES CLMcom and ES RCA4 models. However, an average increase around 15% is expected for the months of July through December with the CM5 CLMcom, ES CLMcom and ES RCA4 models showing the highest positive changes.

A general decrease in precipitation is predicted for the Shashe sub basin. An average decrease of 25% is anticipated for the months of January through August with the CM5 CLMcom, ES CLMcom and ES RCA4 models showing the highest negative changes. An average increase of 20% is expected for the Shashe sub basin for the months June through December.

5.3.3 Changes in future streamflow flow

Streamflow is used when assessing or predicting the availability of water in a catchment. Under the context of climate change streamflow is likely to be impacted by increased temperatures and high evapotranspiration rates. The predicted changes in future streamflow due to climate change are presented in Figure 5.12. A mixed direction of change and varying magnitudes of change in streamflow are expected by the different GCMs and across the different sub-basins. Streamflow is expected to decrease during the months of January through April. For all the sub-basins the models ES CLMcom and ESRCA4 predict large decreases in future streamflow amounts that may exceed 50%.

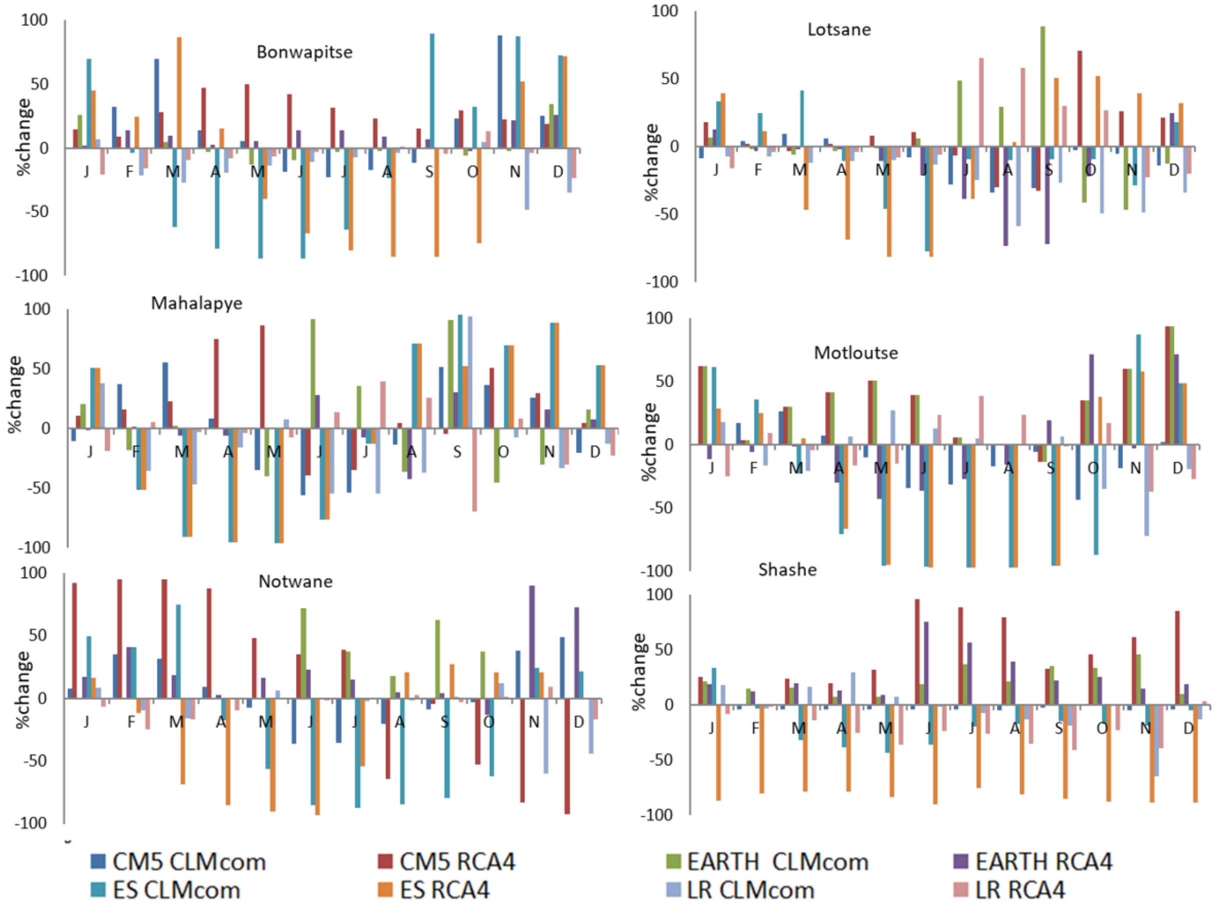

Figure 5.12: Predicted changes in future streamflow of 2025 to 2050 by different GCMs for the Limpopo sub-basins

The Bonwapitse sub basin depicts a general increase in streamflow with an average of 14% that is anticipated for the months of September through March. An average streamflow decrease of 9% is expected for the sub-basin for the months of March through October.

For the Lotsane sub basin the months of May through October may experience a general decrease in streamflow within an approximate range of 20% to 50%. While for the months of July through March an increase in streamflow with approximate range of 15% to 25% may be experienced. A general decrease in streamflow is observed with an average of 6%.

For the Mahalapye sub-basin the months of February through August may experience a decrease in streamflow with an average of range 7% the ES CLMcom and ES RCA4 models showing the highest changes. However, for the months of August through January an increase in streamflow is anticipated within an average of 5%.

The Motloutse sub basin depicts a general decrease in streamflow with ES CLMcom and ES RCA4 models showing the highest % change. A general decrease of 8% on average is anticipated for the months of April through November. An increase in streamflow with a change of 3% on average for the months of January through December is anticipated by other GCM's.

For the Notwane sub basin a general decrease in streamflow averaging about 23% is anticipated for the months of January through December with the EARTH RCA4 model showing the highest change. However, an increase in streamflow estimated at 16% on average is predicted by the other GCM's for the months June through March.

The Shashe sub basin depicts a general decrease in streamflow with an average of 4% anticipated with ES CLMcom and ES RCA4 models showing the highest % change with ES CLMcom and ES RCA4 models showing the highest % change. Other models depict an average increase in streamflow of 5%.

5.3.4 Discussion

The impacts of future climate change on water resources in the Limpopo sub-basin have been assessed using different GCMs. In general, a mixed direction of change as well as differences in magnitude of change in precipitation and streamflow were observed among the different GCMs. These differences may be attributed to uncertainty and to the fact that the different GCMs are premised on different assumptions. The future changes in temperature are, however, predicted to be uni-directional compared to precipitation and streamflow, thus making the prediction of temperature to be more certain. The ability of GCMs to predict temperature with more certainty than precipitation is attributed to the fact that the models perform better at larger scale atmospheric dynamics than the smaller scale surface dynamics such that the models are limited in their ability to incorporate and reproduce important aspects of the hydrologic cycle (Solomon et. al, 2007).

The effects of temperature and consequently evapotranspiration on water resources and the water balance are felt more in dry and arid regions of the world where a slight increase may result in marked evaporative losses which will in turn generate a smaller runoff. On average temperature is predicted to increase by 1.5°C across all sub-basins and by all GCMs. This increase in temperature concurs with the reports by USAID (2016) that in southern Africa by the year 2050 the mean monthly temperature may rise by 2.5°C while a change of 5.0°C is expected by end of the century. The increases in temperatures are likely to result in intense heat waves and high rates of evaporation which may consequently decrease the streamflow (ASSAR, 2015)

It has been observed in this study that wet season months may get drier while dry season months were expected to be wetter. The decrease concurs with some previous studies done. Nkemelang et al. (2018) reported a 6% decrease in annual rainfall as a result of 1.5°C increase in global temperatures together with a 9% and 12% decrease at 2°C and 3°C temperature rise respectively. It should also be noted that dry season months have little to no rainfall at all such that just a slight amount of rainfall will make a significant change but with respect to negligible initial amounts.

The results of this study showed a mixed direction of change of streamflow in the future under different scenarios of climate change. Some months are projected to have increased streamflow while the amount of streamflow may decrease in other months. It should be noted that the semi-arid and dry conditions in the study area may render the streamflow to be sensitive to any changes in rainfall. According to Zhu and Ringler (2010) a 26% reduction in streamflow is expected within the Limpopo River and a global temperature increase of 1.5°C Climate change is expected to increase the frequency of extreme hydrological events and according to Nkemelang et al. (2018) some increases in streamflow may be attributed to flood events that may occur. Even though less rainfall is expected its intensity may increase, for instance at 1.5°C heavy rainfalls are anticipated to increase by 1-4% while extremely heavy events are expected to increase by 4-12% (ASSAR, 2015;).

5.4 Drought Analysis

Given that the area under study is inherently semi-arid in nature and characterised by high natural climatic variability, there is unavoidably a high chance of occurrence of periodic droughts. Proper management of water resources require early warning systems which can be informed by prediction and analysis of droughts. Under this section an analysis of historical droughts is performed using the Standardised Precipitation Evapotranspiration Index (SPEI) for the period 1960-2000. A preliminary assessment of drought conditions in the future (2025- 2050) under the context of climate change is also performed using SPEI and the Standardized Streamflow Index (SSI). These two indices are also compared against each other as a way of further validating the hydrological calibration process and as a means of gaining confidence in the application of the calibrated model. In all cases hydrological drought is generated at the twelve-month timescale. SSI was generated from the streamflow which was predicted by the calibrated hydrological model under future climate change scenarios using different GCM outputs. On the other hand, the input datasets for SPEI are composed of long term timeseries of observed precipitation and evapotranspiration data sets. The Bonwapitse sub-basin has been selected as a case example for assessing future droughts, this selection was based on a good hydrological model calibration performance and a reasonably long streamflow time series. The SSI was generated following a normalisation method (Kermen et al., 2018) that is statistically similar to that used for SPEI which transforms the monthly streamflows into z-scores (Vicento-Serrano et al., 2012). The classifications of SPEI and SSI are presented in Table 5.4.

Table5.4: Classifications of SSI and SPEI (Vicento-Serrano et al., 2012; Nalbantis and Tsakiris, 2009)

Category	SPEI values	SSI values
Extremely wet	≥ 2	≥ 2
Very wet	1.5 to 1.99	-
Moderately wet	1 to 1.49	-
Normal		0 to ∞
Near normal	-0.99 to 0.99	-
Slight drought	-	-1 to 0
Moderate drought	-1.00 to -1.49	-1.00 to -1.5
Severe drought	-1.5 to -1.99	-1.5 to -2.0
Extreme drought	≤ - 2	≤ - 2

5.4.1 Historical drought analysis

Figures 5.13(a –f) show the historical droughts time series for the six sub basins while Table 5.5 shows the drought categories based on the intensities. In general, and for all the sub-basins, there is a tendency to alternate between wet and dry conditions, which signify the variable nature of the prevailing climatic conditions.

The results in Figure 5.13a indicate that the Bonwapitse sub-basin experienced moderate and severe droughts with a few droughts in the extreme category during the period of assessment. Droughts occurred during the years; 1962-1966, 1973, 1984, 1988, 1990, 1992-1996, 1998-1999, 2002, 2009-2010. Moderate droughts occurred in the years; 1964, 1966, 1990, 1992-1994, 2009 and 2010; severe droughts were observed in 1962, 1988, 1998 and 2001 and extreme droughts occurred during 1963, 1965 and 1973.

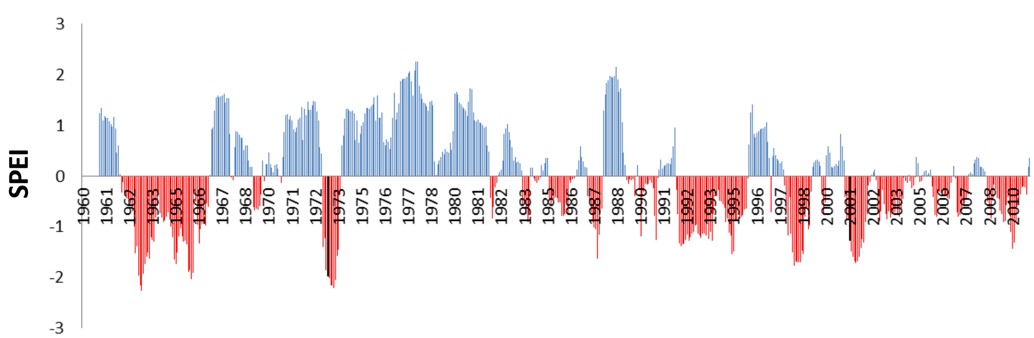

Figure 5.13(a) SPEI showing historical droughts in the Bonwapitse sub-basin

Figure 5.13(b) shows that Lotsane sub basin is more susceptible to severe droughts. The sub basin experienced severe droughts during the years 1964, 1991, 1993 and 2001-2002.

Moderate droughts were observed for the years; 1962-1963, 1965 and 2004 while the extreme droughts occurred during the years; 1972, 1997 and 2000.

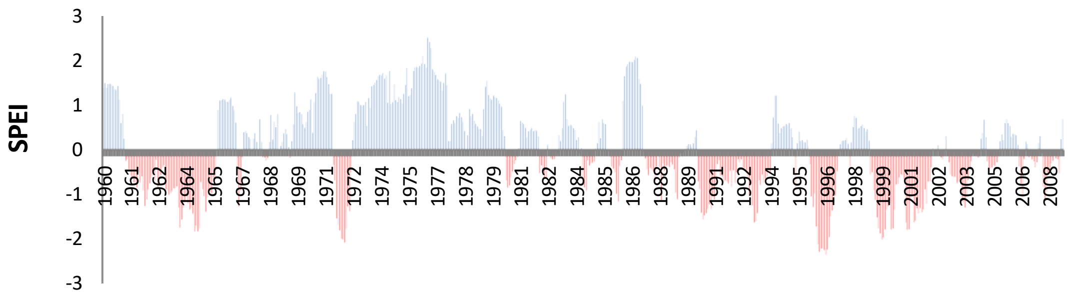

Figure 5.13 (b) SPEI showing historical droughts in the Lotsane sub-basin

As shown in Figure 5.13c, Mahalapye sub basin experienced moderate droughts during the years; 1964-1965, 1969, 1980, 1984-1985, 1995, 1999, 2001, 2003 and 2009 while severe droughts occurred in 1970, 1989-1990, 2000, 2007-2008 and extreme droughts were observed for the years 1987-1988 and 2004.

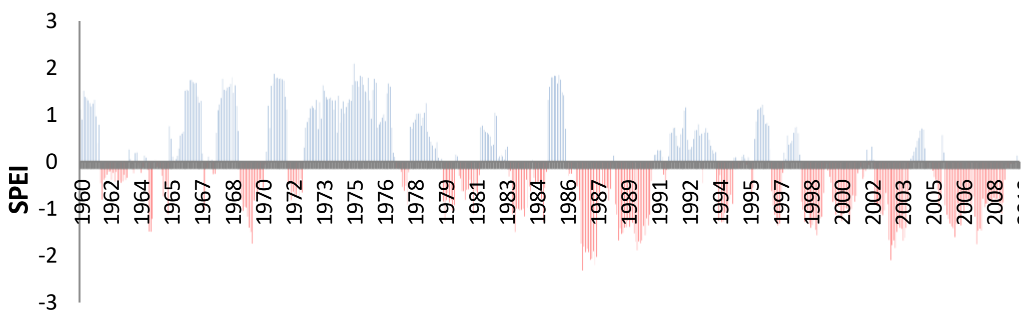

Figure 5.13 (c) SPEI showing historical droughts in the Mahalapye sub-basin

The Motloutse sub basin (Figure 5.13d) experienced moderate droughts during the years; 1962, 1964, 1968, 1982, 1986, 1990, 1992, 1997, 2008-2010 and severe droughts in 1965, 1987, 1992, 1995, 2001-2003 and 2005 while extreme droughts occurred during the years; 1973 and 1998.

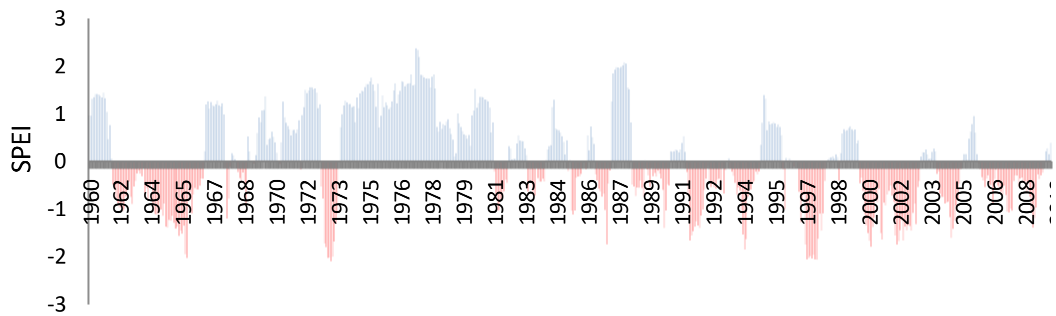

Figure 5.13 (d) SPEI showing historical droughts in the Motloutse sub-basin

Figure 5.13 (e) indicates that moderate droughts are more common in the Notwane sub basin, having occurred during the years; 1962, 1965-1966, 1969, 1990, 1993, 2001-2003, 2005 and 2009-2010 while the severe droughts occurred for the years; 1963-1964, 1992, 1998, 2007 and 2008. An extreme drought occurred for a brief period in 1995.

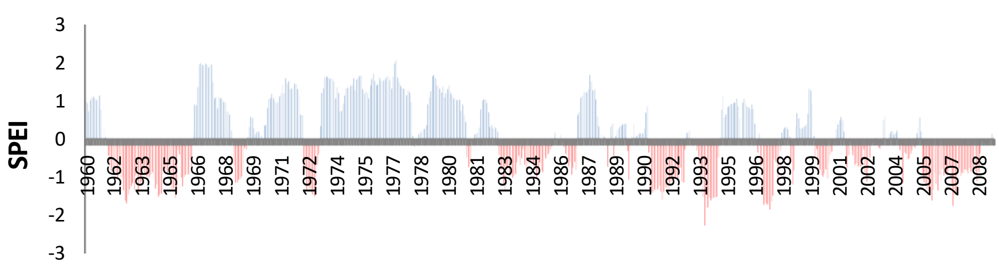

Figure 5.13 (e) SPEI showing historical droughts in the Notwane sub-basin

For the Shashe sub-basin, Figure 5.13(f) shows that moderate droughts occurred in 1964, 1982, 1987, 1994, 1998, 2001, 2005 and 2009. Severe droughts occurred in 1973, 1987, 1992, 1995, 1998 and 2002-2003 while a brief extreme drought was observed in 1965.

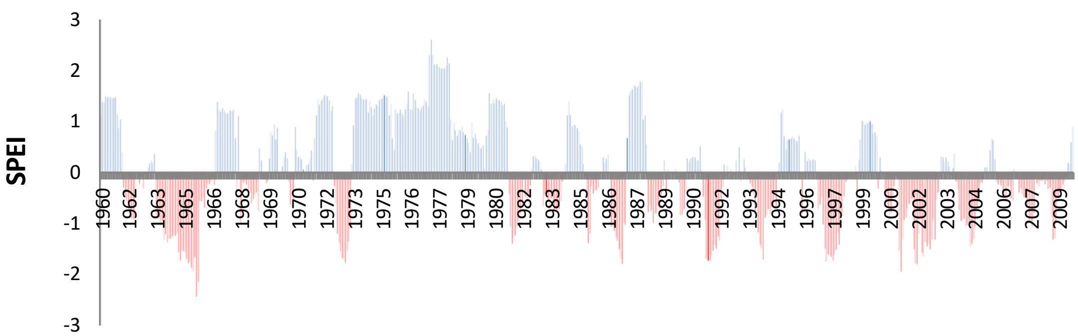

Figure 5.13 (f) SPEI showing historical droughts in the Shashe sub-basin

Table 5.5 shows that across all sub-basins, moderate droughts were the most common followed by severe droughts. Extreme droughts were less common and of a short duration. The drought period 1962-1963 is common to all sub-basins except for Mahalapye while the 1964-1965, 2001 and 2009 droughts were experienced in all sub-basins. The longest drought occurred in the Bonwapitse sub basin from 1962 to 1966. The results show that the Mahalapye, Motloutse and Notwane experienced more droughts than the other sub-basins. Although less frequent than the other drought classes the highest number of extreme droughts was observed in the Bonwapitse, Lotsane and Mahalapye sub-basins. The results also indicate a tendency of the droughts to recur from year to year thus increasing the frequency of occurrence, this is highly evident in the Notwane sub-basin.

Table 5.5: Drought years and drought categories of SPEI for the six sub basins

Sub-basin	Year		
	Moderate Drought	Severe Drought	Extreme Drought
Bonwapitse	1964, 1966, 1990, 1992-1995, 2009, 2010	1962, 1988, 1998,2001	1963, 1965 ,1973
Lotsane	1962-1963, 1965, 2004	1964, 1991, 1993, 2001-2002	1972,1997, 2000
Mahalapye	1964-1965, 1969, 1980, 1984-1985, 1995, 1999, 2001, 2003, 2009	1970, 1989-1990, 2000, 2007-2008	1987-1988, 2004
Motloutse	1962, 1964, 1968, 1982, 1986, 1990, 1992, 1997, 2008-2010	1965, 1987, 1995, 2001-2003, 2005	1973, 1998
Notwane	1962, 1965-1966, 1969, 1984-1985, 1990, 1993, 2001-2003, 2005, 2009-2010	1963-1964, 1992, 1998, 2007, 2008	1995
Shashe	1964, 1982, 1987, 1994, 1998, 2001, 2005, 2009	1973, 1987, 1992, 1995, 1998, 2002-2003	1965

5.4.2 Predicting drought under future climate change

The temporal variations of the SSI and SPEI drought indices for Bonwapitse as an example sub-basin are presented in Figures 5.14(a-h). For all the GCMs and for both drought indices in the future, droughts of varying categories are expected for the years 2025, 2026, 2027, 2028, 2029, 2031, 2032, 2033, 2034, 2036, 2038, 2039, 2040, 2041, 2042, 2043, 2044,

2046, 2047, 2048, 2049 and 2050. However, as observed for the historical droughts, only a few extreme droughts are expected while the moderate drought category is expected more than 50% of the time in the near future period. In Figure 5.14 a, the model CM5 RCA4 predicts the same pattern of droughts by both SPEI and SSI. However, there is a noted difference in the magnitude of the drought between the two indices. In general, SPEI predicts more intense droughts than SSI.

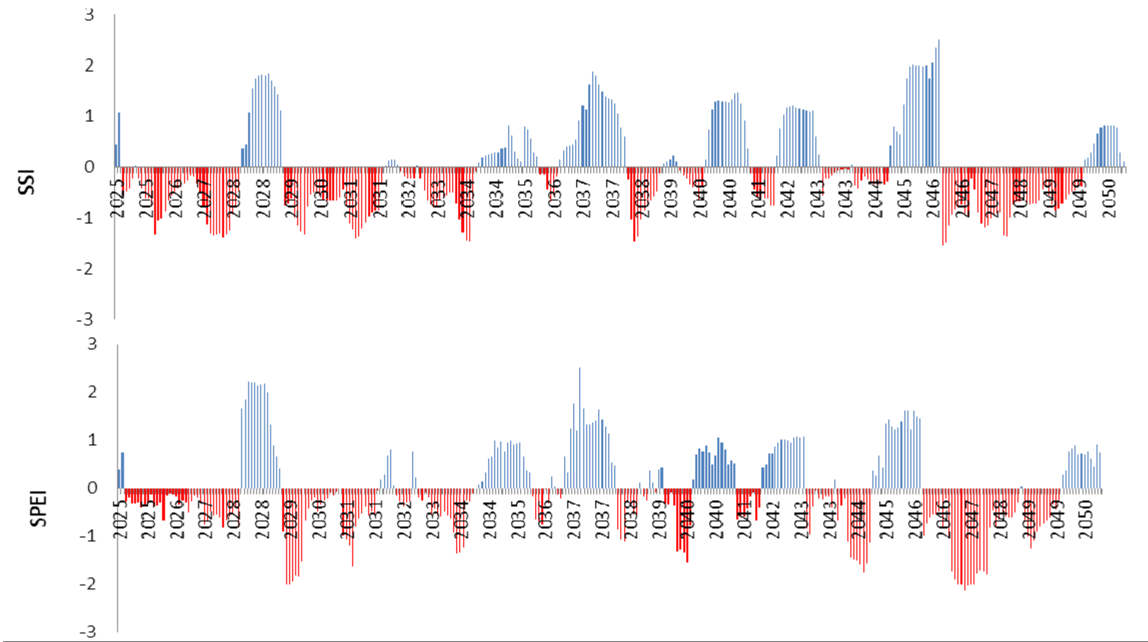

Figure 5.14(a): Temporal variations of future SSI and SPEI for Bonwapitse under CM5 RCA4

Both indices predict a similar pattern of dry and wet conditions by Earth CLMcom (Figure 5.14 b). However, prior to 2039 SSI predicts drought while SPEI indicates near normal conditions. After 2039 both indices predict droughts in the same order of magnitude.

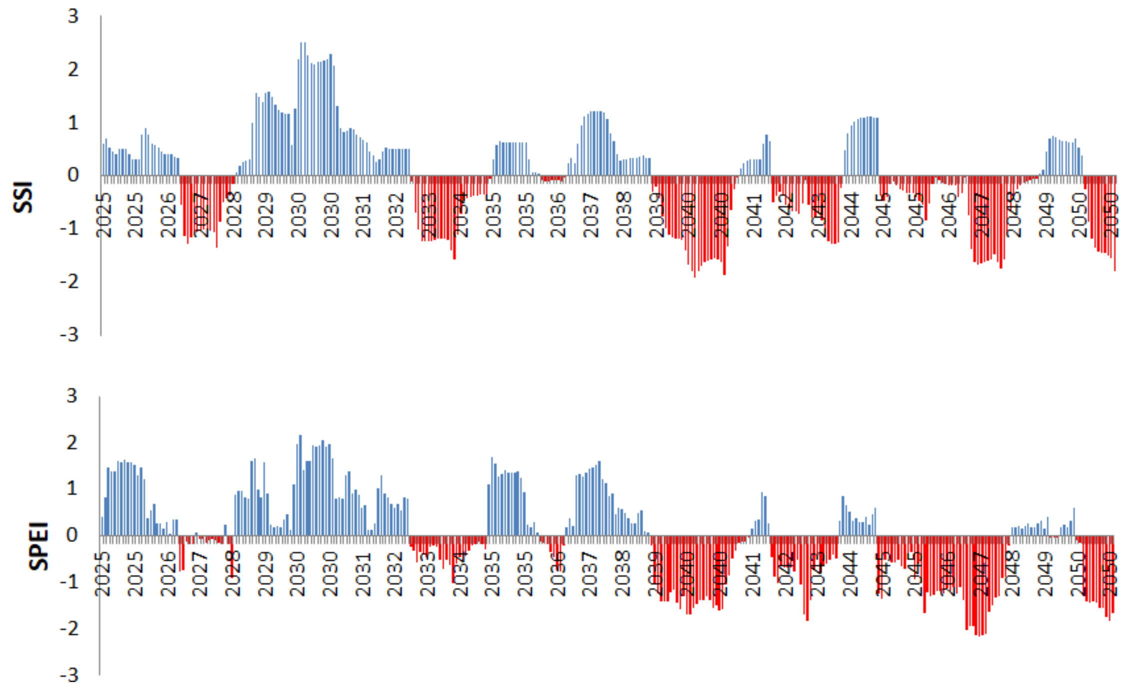

Figure 5.14 (b): Temporal variations of future SSI and SPEI for Bonwapitse under Earth CLMcom

Figure 5.14c also shows the same pattern of dry conditions by both indices. For the period up to the year 2040 near normal to mildly dry conditions are postulated while after 2040 both indices predict droughts in the moderate to severe categories. However, the droughts are more intense and prolonged for SPEI compared to SSI.

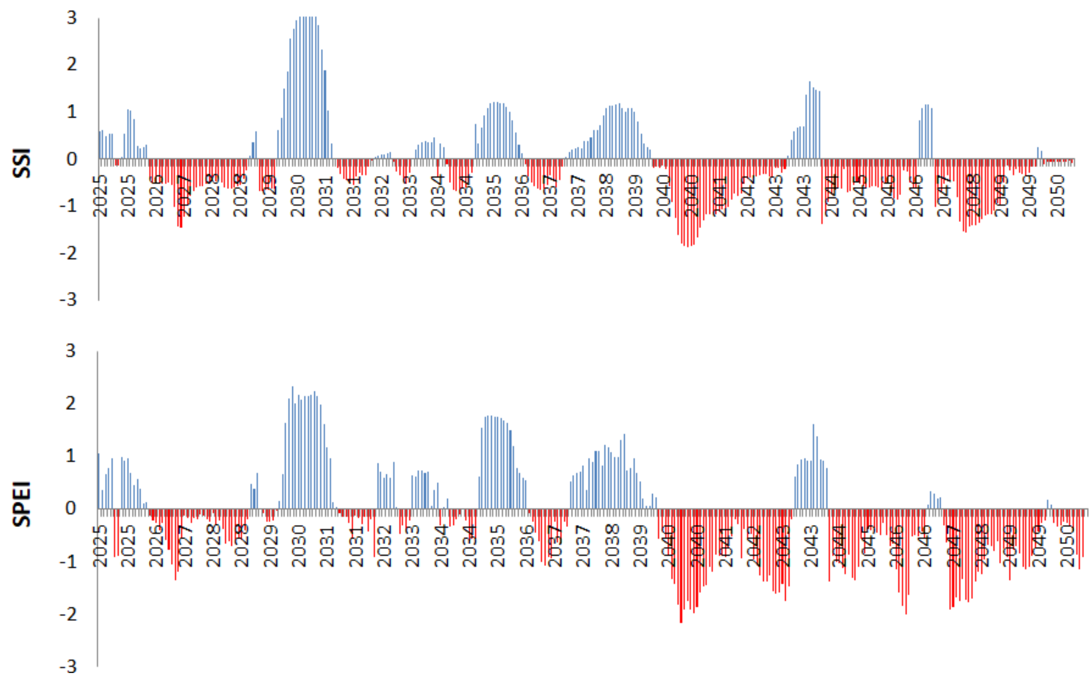

Figure 5.14(c): Temporal variations of future SSI and SPEI for Bonwapitse under Earth RCA4

For ES CLMcom model (Figure 5.14 d) the indices both a show similar pattern. However a difference in magnitude of drought between the two indices is also observed as SPEI predicted more intense droughts than SSI. Figure 5.14e also shows the same pattern of dry and wet conditions by both indices up to 2038. From 2039 there are slight mismatches in the direction (+ve or -ve) of the index for some of the years, however these have no effect both indices indicate near normal conditions.

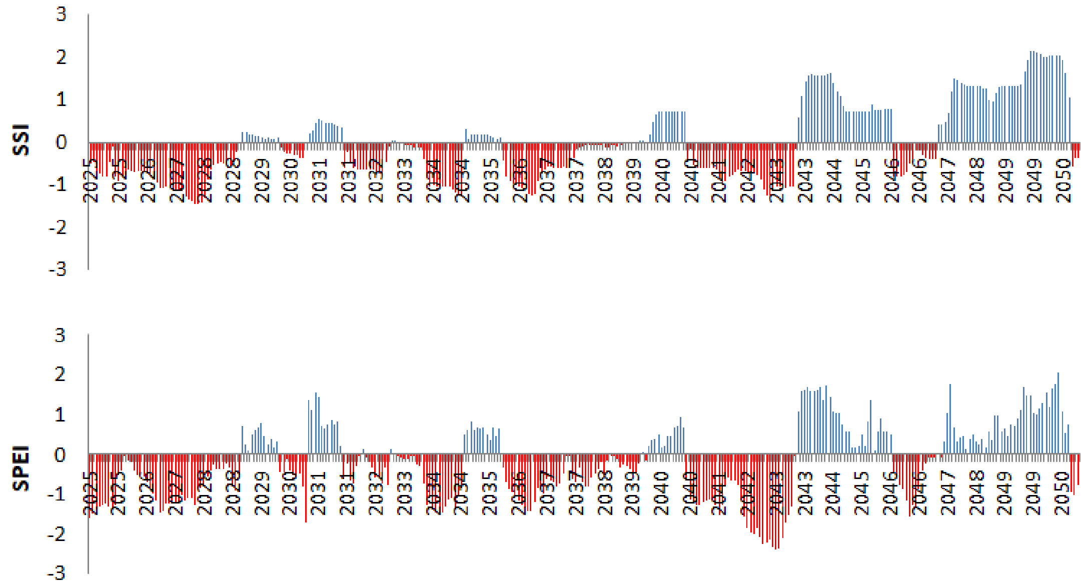

Figure 5.14 (d): Temporal variations of future SSI and SPEI for Bonwapitse under ES CLMcom

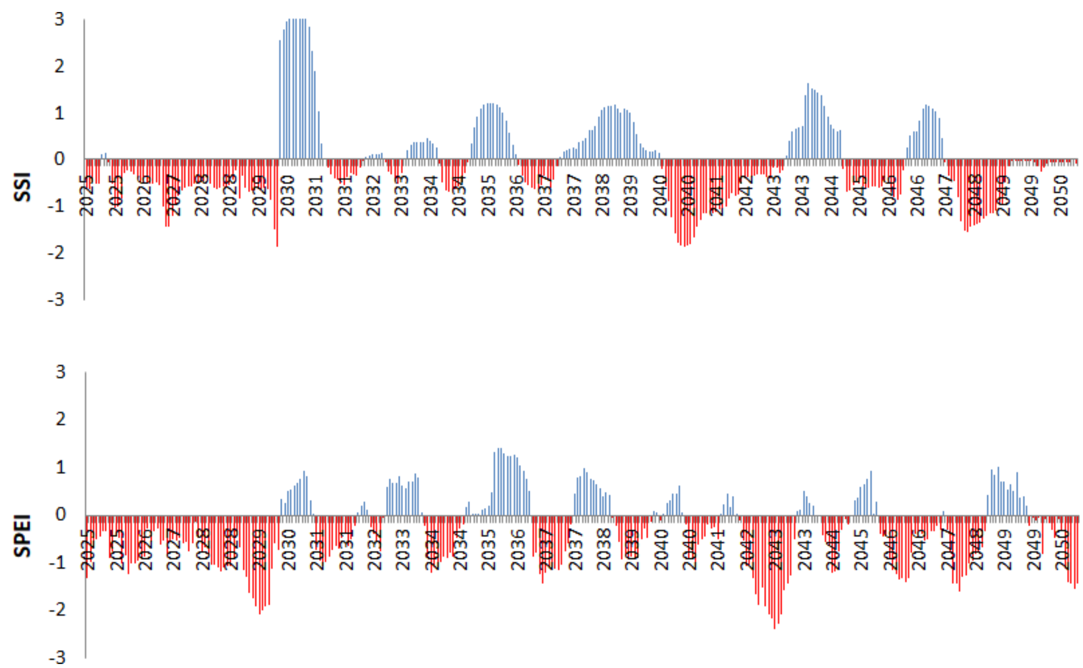

Figure 5.14 (e): Temporal variations of future SSI and SPEI for Bonwapitse under ES RCA4

For the LR CLMcom model (Figure 5.14 f), there is a very close agreement in the direct of the index and drought category between the SPEI and SSI. Both indices predict normal to near normal conditions or slight drought (by SSI) for most of the time during the future period studied. Fewer droughts are predicted by this GCM for both indices. SSI predicts moderate droughts for the years 2037, 2038 and 2049. On the other hand, more droughts in the moderate category are expected by SPEI during the years2031, 2034, 2040, 2042-2043, 2044,

2046 and 2049.

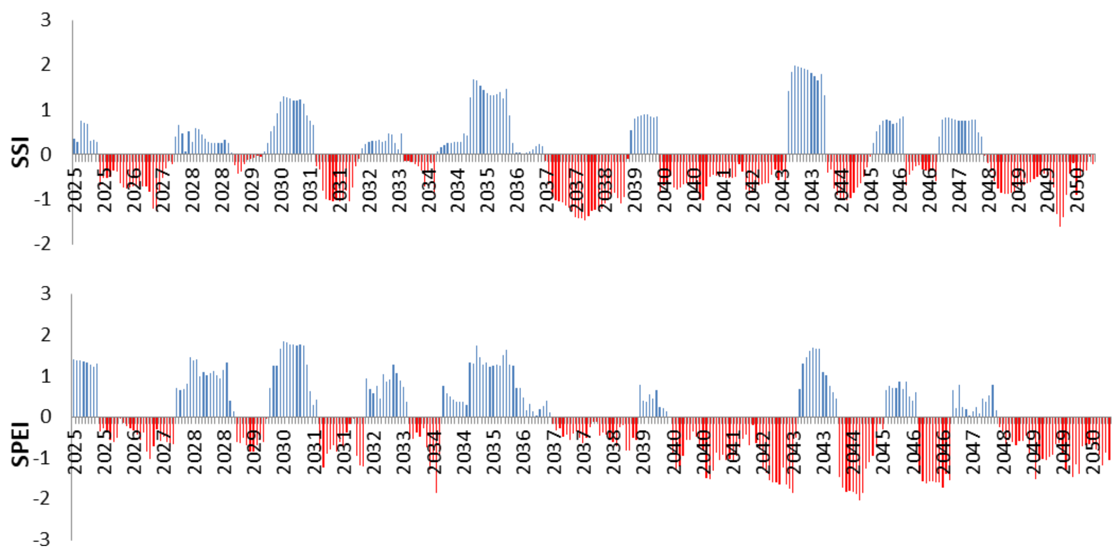

Figure 5.14 (f): Temporal variations of future SSI and SPEI for Bonwapitse under LR CLMcom

Figure 5.14g shows a similar pattern of dry conditions by both indices. However, a difference is magnitude of droughts is observed. For example, for the year 2032, SSI predicted extreme droughts while SPEI indicates near normal conditions with a slim chance of an extreme drought. The LR RCA4 model predicts a very close pattern of occurrence of droughts and magnitude between SSI and SPEI as shown in Figure 5.14h.

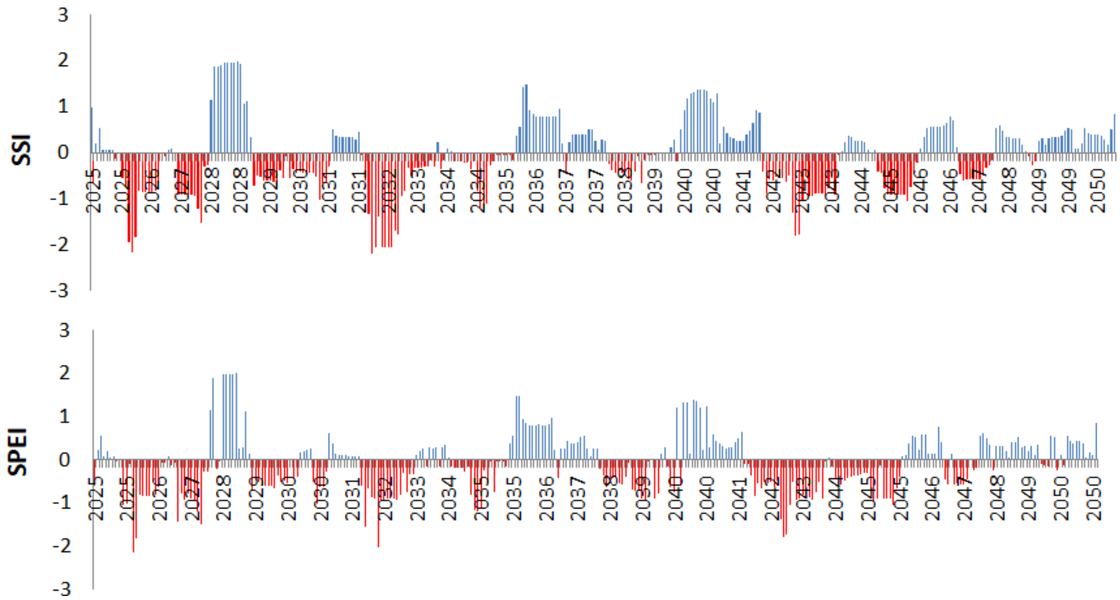

Figure 5.14 (g): Temporal variations of future SSI and SPEI for Bonwapitse under CM5 CLMcom.

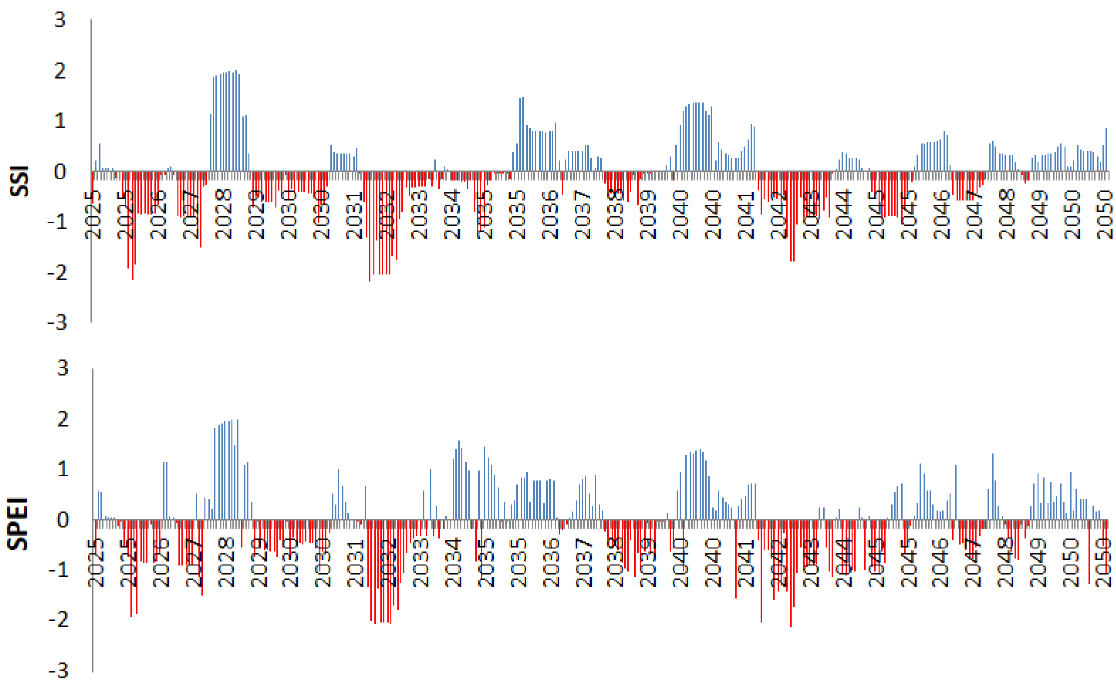

Figure 5.14(h): Temporal variations of future SSI and SPEI for Bonwapitse under LR RCA4

Figures 5.15-5.16 and Tables 5.5 and 5.6 show percentages of drought categories across the Bonwapitse sub basin for the period of 2025-2050 from SSI12 and SPEI 12. The total number of occurrences for the respective drought categories predicted by individual models over the total number of droughts occurrences with respect to their categories for all the models was expressed as a percentage to get the presented values. The ES RCA4 and LR CLMcom models predicted most of the dry periods under SPEI compared to other models. The CM5 CLMcom and LR RCA4 models predict severe droughts while moderate droughts are largely expected. With exception of the CM5 CLMcom and CM5 RCA4, all the other models predicted more droughts under SPEI compared to the droughts generated by SSI.ES RCA4 model predicted the highest moderate droughts at 29% under SPEI. A high percentage of 50% was predicted for SSI under the extreme drought category from the CM5 CLMcom and LR RCA4 models. Drought occurrence from the CM5 CLMcom ranges between 0 and 50% under SSI, with extreme droughts having the highest occurrence while there is none in the moderate drought category. LR RCA4 model drought occurrence ranges from 4% to 50%, with extreme droughts having the highest occurrence while moderate droughts have the lowest occurrence and severe droughts occurring at 22%.

Table 5.6: Drought percentages under SSI

	CM5 CLMcom	CM5 RCA4	EARTH CLMcom	EARTH RCA4	ES CLMcom	ES RCA4	LR CLMcom	LR RCA4
Moderate	0	21	10	14	21	14	14	4
Severe	33	11	0	22	0	11	0	22
Extreme	50	0	0	0	0	0	0	50

Table 5.7: Drought percentages under SPEI

	CM5 CLMcom	CM5 RCA4	EARTH CLMcom	EARTH RCA4	ES CLMcom	ES RCA4	LR CLMcom	LR RCA4
Moderate	0	7	7	15	15	29	22	7
Severe	11	11	17	11	0	11	22	17
Extreme	18	9	9	9	18	9	0	18

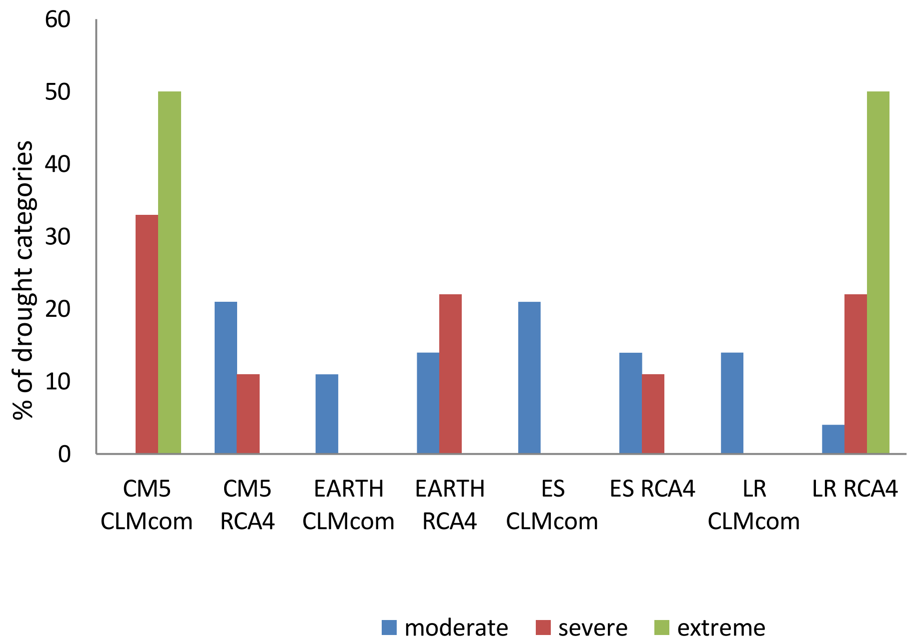

Figure 5.15: Percent of drought categories out of total expected droughts under each GCM

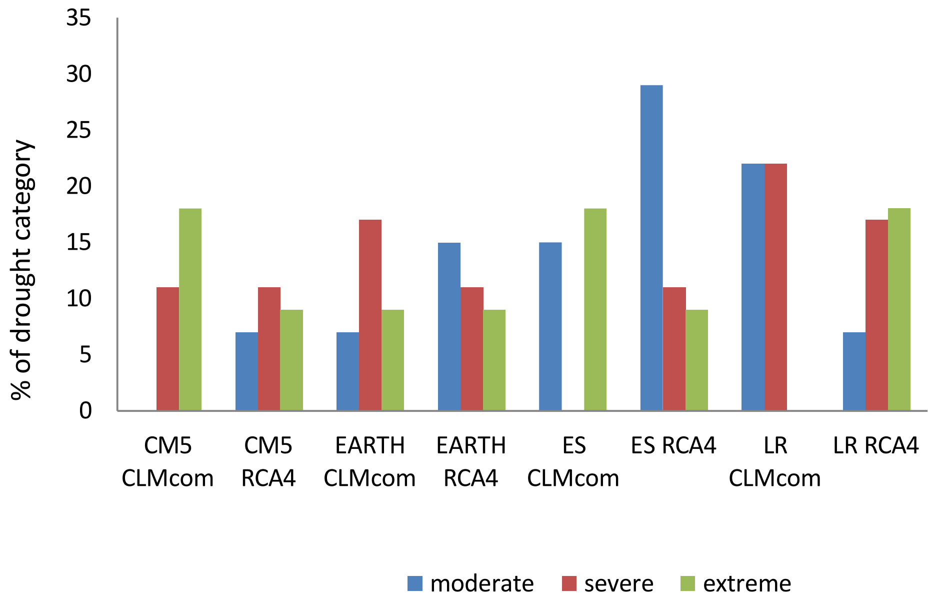

Figure 5.16: Percentages of SPEI drought categories in the future

4.3 Correlation of SSI and SPEI

Based on drought frequency and severity, the correlations between SSI and SPEI for the Bonwapitse sub-basin are presented in Figure 5.17.

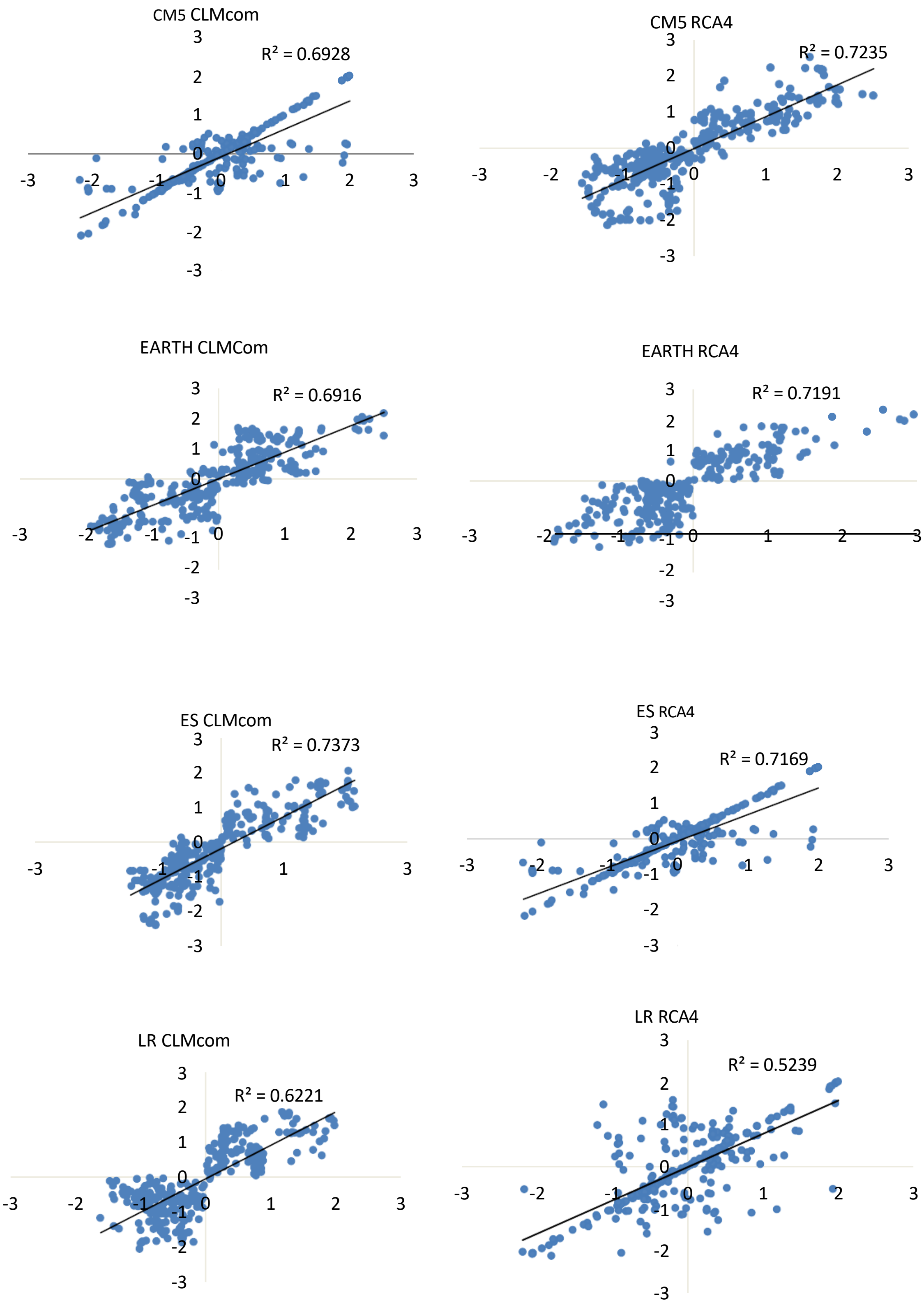

Figure 5.17: Correlation of SSI and SPEI for the different GCMs

The direction of the indices whether positive (wet) or negative (dry), coincides most of the times during the period of assessment for SSI and SPEI. All GCMs produce a positive correlation between SSI and SPEI. A reasonable agreement between the two indices is observed for all GCMs as indicated by the coefficient of determination value above 0.5 (R^2 >0.5) (Krause et al., 2005). The R^2 values are 0.7373, 0.7235, 0.7191, 0.7169, 0.6928, 0.6916, 0.6221 and 0.5239 for the ES CLMcom, CM5 RCCA4, EARTH RCA4 ES RCA4, CM5 CLMcom, EARTH CLMcom, LR CLMcom, and LR RCA4 models respectively.

5.4.4 Discussion

This study revealed a recurring pattern of historical droughts in alternation with wet events in the study area over the period 1960-2000. This occurrence is reflective of the inherently variable climate that prevails in Botswana and in the southern African region (Hulme et al., 2001). Tsheko (2003) also indicated the effect of spatial and temporal variability of the wet and dry conditions in Botswana in different sub-basins across Botswana where, for example, the Mahalapye sub-basin was found to have rainfall reliability below 0.5 and thus rendered prone to droughts. Historically moderate droughts were observed to be the most common across all the sub-basins. Other studies (e.g. Batisani, 2011; Byakatonda, 2018) concur that Botswana is more prone to moderate droughts. Also worth noting is the shortened return period between droughts thus frequency of occurrence of droughts is increased. This observation has also been noted by Davies et al. (2017) who also reported on the vulnerability of Botswana to recurrent droughts throughout the 1990s and 2000s.

Preliminary analysis of droughts under the context of climate change scenarios as carried out by this study indicates that droughts may persist into the future and thus likely to be exacerbated by the increased temperature due to climate change. A significant increase in droughts going into the future has also been predicted by Davies et al. (2017), particularly in Northern and Central Botswana. These droughts may be exacerbated by the increased temperatures which are likely to accelerate the rates of evapotranspiration. This is turn may have a negative effect on the catchment water balance. According to Moses (2017) droughts can be attributed to changing weather patterns caused by heat build-up on the earth's surface which consequently decreases the amount of rainfall received in a region. It should, however, be noted that the different GCMs predicted different magnitudes of drought and in a few cases ill matched times of occurrence. This can be explained by the fact that GCMs are uncertain. Uncertainty in climate change prediction can be attributed to a number of factors, for example uncertainty in projecting the greenhouse gas (GHG) emission/concentration scenario (Webster and Sokolov, 1998; Giorgi, 2010).

Both the SSI and SPEI predicted the same pattern of droughts in the future period of 2025-2050, this is evidenced by the positive correlations that were observed between the two indices. There was no significant difference between the indices at the 95% confidence interval. In terms of validating the calibrated hydrological model, the statistically significant correlations between SSI and SPEI suggest that the calibrated model can be reliably used to represent the hydrological responses in the study area. This observation is inferred from the fact that SSI an index derived from data obtained from simulations with the calibrated model produced results that agreed with those of SPEI whose index was generated from station observed data. The findings also reveal that precipitation plays a substantial role in explaining hydrological droughts, and that temperature has a considerable impact on water scarcity as indicated by the more droughts that were predicted under SPEI. The differences in magnitude of SSI and SPEI can be attributed to the fact that in addition to precipitation and evapotranspiration other components of the hydrological cycle such as soil moisture content, infiltration and even groundwater recharge are included as input variables to the prediction of streamflow while only precipitation and evapotranspiration are the only variables for the calculation of SPEI.

Therefore, some differences should be expected since SPEI is a climatologically based drought index while SSI is based on all the components of the hydrological cycle. These results indicated that better conclusions and a better picture on droughts can be obtained when different indices are used in combination. Also, worth noting is the fact that relationship between streamflow and precipitation is not perfectly linear as such the magnitudes of change of the two variables cannot be expected to be the same (Salimi et al., 2021).

Chapter 6

Conclusion and recommendation

In arid and semi-arid regions, limited water resources impose significant impacts on human livelihoods, the environment and the economy. At the same time water resources are under continuous threat from various developments that are on an increasing trend, growing population, this is in addition to the threats of inherent climatic variability and global climate change. Studies that continuously review catchment hydrological processes and the ensuing hydrological events are therefore important in providing early warning information that can be used to inform water resources decision making. Effective management of water resources requires solutions that are tailored for the local scale. Large catchments are characterised by spatial and temporal variability in climate while at the same time there may be different hydrological responses to climate from basin to basin. Physical basin characteristics also vary between the catchments. Understanding all these factors at different temporal and spatial scales especially at the sub-basin level ensures effective adaptation and management strategies. Therefore, it is important to apply a sub-basin response to the effective management of water resources.

Hydrological data availability especially streamflow is important when allocating water resources in a catchment. However, most sub-basins are data sparse or ungauged. This is due partly to inconsistent monitoring because of insufficient resources. Limited and sparse hydrological data adds onto the challenges for future hydrological predictions under different climate change and development scenarios. The focus of this study was therefore to set up a hydrological model at the sub-basin scale for the Limpopo sub-basins located in Botswana. This study derives its strength in that it is centered on the individual sub-basins of the Limpopo in Botswana rather than focusing on a generalised overview of the Limpopo in Botswana basin. This is important particularly given that for example, the northern and southern sub-basins in Botswana receive different amount of annual rainfall. Also worth considering is that each sub-basin may have unique characteristics that differentiate it from the other sub-basins. Focussing on local solutions that are tailor made specifically for each sub-basin will go a long way in reducing the risk of making decisions that are based on generalised or insufficient information. The calibrated model can then be used as a hydrological baseline for the respective sub-basins. It can also be used to assess the various hydrological responses to climate variability and climate changes as well as to various water use and management scenarios at the appropriate spatial scale. To fulfil the objective of the study and given that some areas have limited hydrological data, this study adopted the use of global data sets to complement the local station observed data as inputs to the hydrological model

The Pitman semi-distributed hydrological model was successfully set up and calibrated for the study area. The statistical objective functions used to assess the performance of the calibrated and model validation resulted in R2 and CE values above 0.5 while the percent bias did not exceed 20% in all cases. Given that hydrological modelling is fraught with uncertainty, an uncertainty framework was incorporated in this study, where prior parameters ranges based on physical basin properties were assigned. Incorporation of the basin physical properties gives confidence that relevant features are incorporated into the model while at the same time they can be used to guide some of the parameter values. Based on the fact that the climate and hydrological processes are not stationary, it makes sense to acknowledge uncertainty in hydrological modelling so that regrettable water resources management decisions are avoided (Todd et al., 2010). When uncertainty is incorporated, a range of likely outcomes are generated thus allowing flexible decision making. Basing decisions on a single outcome is futile because the resultant prediction may be in variation with the manner in which the future climate may unfold.

These results suggest that the calibrated model can adequately represent the hydrological response characteristics of the Limpopo sub-basins in Botswana. To further ascertain the validity of the calibrated model in the study area, two drought indices were compared, wherein, the SSI was generated from streamflow data simulated by the calibrated model while SPEI is largely dependent on temperature in the form of evapotranspiration as well as precipitation. Despite slight differences in magnitude, the two indices agreed as to the nature of droughts to be anticipated in the near future period. Therefore, this is further testimony that the calibrated hydrological model is suitable for the study area and even under the context of future climate change. Results also indicated that due to future climate change the study area may warm up by 3°C by the year 2050. Increased temperatures tend to elevate the rates of evapotranspiration within catchments with consequent decrease in the amount of water that may be available for the different water uses. A general decrease in rainfall and streamflow is also expected. However, the predictions show a mixed direction of change and magnitude no clear indication as to how or by how much these changes will occur. This signifies that GCMs are also fraught of uncertainty in addition to hydrological model uncertainty. As such water resources management and planning for the future should be carried out under conditions of uncertainty.

This study revealed that droughts are likely to persist into the near future and they may be aggravated by the effects of climate change. Moderate droughts are the most common drought category in all the sub-basins while extreme droughts are less frequent. Irrespective of the severity of the drought, droughts will amplify the negative water resources impacts that are already being felt by virtue of a semi-arid climate and high climatic variability that characterise the study area. It is therefore expected that there may be increased stress on limited water resources, which may also increase suffering on a population that is heavily dependent on rainfed agriculture for sustenance. Also reduced availability of water may have negative impacts on human health and the environment. It is encouraged to put in place well informed and timely drought monitoring and prediction strategies that will negate the impacts of climate change and drought on water and food security. Although different indices are available to monitor droughts it should be appreciated that each has its own advantages and disadvantages compared to the other indices. The SSI and SPEI agreed most of the times and for all GCMs.

Observations of this study show that different indices can agree on the nature of droughts, however, given that each index may have different types of input data and sometimes incorporate different components of the hydrological cycle, this study recommends the use of different indices to complement each other to have more confidence in the predictions. Worth noting is that it was not the aim of this study to provide a detailed assessment of the difference between the historical and future droughts. It is recommended that a future study can look more into the difference in evolution and characteristics of droughts between the past and the future under the context of climate change.

To avert the impacts of drought, Mekuria and Mekonnen (2018) suggested that crops should be diversified for example, by using more drought resistant crop varieties like maize beans and cowpeas, planting early maturing crop varieties such as groundnuts and the white grained maize hybrid. It was also recommended to plant early or late when the chances of reoccurring drought within a season are low. Long term mitigation strategies like rainwater harvesting during rainy days, water recycling and lobbying for water transfer from transboundary watercourses should be explored. Planning and adaptation strategies for water resources should also be included within development strategies for agriculture, infrastructure, and energy sectors. To improve freshwater security, new scientific findings, advancements in theoretical understanding and analytical methods, as well as a better comprehension of how people and institutions respond to all the information in hand, are all required. Thus scientific researches involving all stakeholders should be carried out in order to come up with relevant theoretical and practical information to aid in decision making regarding drought management.

Finally, it has been revealed by this study that both hydrological model prediction and GCM predictions are uncertain. Predictive uncertainty in hydrological modelling arises mainly from model structural uncertainty, input data uncertainty and parameter uncertainty. On the other hand, the sources of GCM uncertainty include limited knowledge of the global climatic processes and their feedbacks, the downscaling techniques used in reducing the GCM scale to match the regional scale, the bias-correction approaches used in trying to match the GCM rainfall baseline with the historically observed rainfall and the manner in which the transformed data are transferred to the hydrological model as well as the choice of the GCM. All these uncertainties complicate the efforts of trying to obtain reliable predictions for the future and do not provide the exact quantities of hydrological variables in the future. Therefore, the results of this study must be treated as an approximate indication of what the future may be like and should only be used as a guide when making plans for basin management in the future.

References

Abramowitz, M., Irene, A., Stegun, I.A. (Eds.), 1965. Handbook of Mathematical Functions with Formulas, Graphs, and Mathematical Tables. National Bureau of Standards Applied Mathematics Series 5. Library of Congress Catalog Card Number: 64-600°6 5.

Agarwal, A., de los Angeles, M. S., Bhatia, R., Chéret, I., Davila-Poblete, S., Falkenmark, M., & Kindler, J. *Integrated Water Resources Management. Global Water Partnership (GWP); Tack Background Papers No. 4; Global Water Partnership Technical Advisory Committee (TAC): Stockholm, Sweden, 2000* (p. 71). ISBN 91-630-9229-8.

Aghakouchak, A., & Habib, E. (2010). Application of a conceptual hydrologic model in teaching hydrologic processes. *International Journal of Engineering Education*, *26*(4), 963–973.

Ambrosino, C., Chandler, R. E., & Todd, M. C. (2011). Southern African monthly rainfall variability: An analysis based on generalized linear models. *Journal of climate*, *24*(17), 4600-4617.

An, S. I., Kim, H. J., Park, W., & Schneider, B. (2017). Impact of ENSO on East Asian winter monsoon during interglacial periods: effect of orbital forcing. *Climate Dynamics*, *49*(9), 3209-3219.

ASSAR. (2015). Understanding vulnerability and adaptation in semi-arid areas in Botswana. Adaptation to Scale in Semi-arid Regions (ASSAR).

Batisani, N., & Yarnal, B. (2010). Rainfall variability and trends in semi-arid Botswana: implications for climate change adaptation policy. *Applied Geography*, *30*(4), 483-489.

Batisani, N. (2011). The spatio-temporal-severity dynamics of drought in Botswana. Journal of Environmental Protection, 2(06), 803.

Baumberg, V., Weber, T., & Helmschrot, J. (2015, April). Assessing the Change in Rainfall Characteristics and Trends for the Southern African ITCZ Region. In EGU General Assembly Conference Abstracts (p. 1434).

Beguería, S., Vicente-Serrano, S.M., Reig, F., Latorre, B., 2014. Standardized precipitation evapotranspiration index (SPEI) revisited: parameter fitting, evapotranspiration models, tools, datasets and drought monitoring. Int. J. Climatol. 34, 3001–3023.

Belayneh, A., Adamowski, J., Khalil, B. (2016): Short-term SPI drought forecasting in the Awash River Basin in Ethiopia using wavelet transforms and machine learning methods. – Sustainable Water Resources Management 2(1): 87-101.

Bharati, L., & Gamage, N. (2010). Application of the Pitman model to generate discharges for the Lhasa Basin, China. Hydro Nepal: Journal of Water, Energy and Environment, 7, 30-34.

Binley, A.M., Beven, K.J., Calver, A. and Watts, L.G., 1991. Changing responses in hydrology: assessing uncertainty in physically based model predictions. *Water Resources Research*. **27**, 1253-1261.

Boko M, Niang I, Nyong A, Vogel C, Githeko A, Medany M, Osman-Elasha B, Tabo R, Yanda

Africa climate change 2007: impacts, adaptation and vulnerability. In: Parry ML, Canziani OF, Palutikof JP, van der Linden PJ, Hanson CE (eds) Contribution of working group II to the fourth assessment report of the intergovernmental panel on climate change. Cambridge University Press, Cambridge, pp 433–467

Botswana Climate Variability and Change: Understanding the Risks (car.org.bw)

Botswana environment statistics climate digest (2019) Retrieved from https://www.statsbots.org.bw/sites/default/files/publications/Climate%20Digest%20%202019.pdf

Boyle, D. P., Gupta, H. V., & Sorooshian, S. (2000). Toward improved calibration of hydrologic models: Combining the strengths of manual and automatic methods. *Water Resources Research*, *36*(12), 3663-3674

Britannica, T. Editors of Encyclopaedia (2016). Arenosol. Encyclopedia Britannica. https://www.britannica.com/science/Arenosol

Britannica, T. Editors of Encyclopaedia (2016, November 14). Luvisol. Encyclopedia Britannica. https://www.britannica.com/science/Luvisol

Britannica, T. Editors of Encyclopaedia (2016, June 6). Leptosol. Encyclopedia Britannica. https://www.britannica.com/science/Leptosol

Broccoli, A. J., Dahl, K. A., & Stouffer, R. J. (2006). Response of the ITCZ to Northern Hemisphere cooling. *Geophysical Research Letters*, *33*(1).

Castaings, W., Dartus, D., Le Dimet, F. X., & Saulnier, G. M. (2007). Sensitivity analysis and parameter estimation for the distributed modeling of infiltration excess overland flow. *Hydrology and Earth System Sciences Discussions*, *4*(1), 363-405.

Chen, F., Mitchell, K., Schaake, J., Xue, Y., Pan, H. L., Koren, V., ... & Betts, A. (1996). Modeling of land surface evaporation by four schemes and comparison with FIFE observations. *Journal of Geophysical Research: Atmospheres*, *101*(D3), 7251-7268.

Chiang, J. C., & Bitz, C. M. (2005). Influence of high latitude ice cover on the marine Intertropical Convergence Zone. *Climate Dynamics*, *25*(5), 477-496.

Climate Change Adaptation, (2021) retrieved from
https://www.thegef.org/what-we-do/topics/climate-change-adaptation

Climate Risk Profile: Botswana (2020): The World Bank Group

Climate(2022) retrieved from https://www.botswanatourism.co.bw/climate

Collier, P., Conway, G., & Venables, T. (2008). Climate change and Africa. *Oxford Review of Economic Policy*, *24*(2), 337-353.

Cooney, C. M. (2012). Downscaling climate models: sharpening the focus on local-level changes.

Crawford, N. H., & Linsley, R. K. (1966). Digital Simulation in Hydrology'Stanford Watershed Model 4. Stanford University, California

Dai, A., Trenberth, K. E., & Qian, T. (2004). A global dataset of Palmer Drought Severity Index for 1870–2002: Relationship with soil moisture and effects of surface warming. *Journal of Hydrometeorology*, *5*(6), 1117-1130.

Davie, T., 2008. *Fundamentals of Hydrology*. Taylor and Francis e•Library. ISBN10: 0.203.93366.4 (ebk)

Deppenmeier, A. L., Haarsma, R. J., & Hazeleger, W. (2016). The Bjerknes feedback in the tropical Atlantic in CMIP5 models. *Climate Dynamics*, *47*(7), 2691-2707.

Devac, M., & Dhanya, C. T. (2017). Sensitivity analysis of hydrological models: review and way forward. *Journal of Water and Climate Change*, *8*(4), 557-575.

Devia, G. K., Ganasri, B. P., & Dwarakish, G. S. (2015). A Review on Hydrological Models. *Aquatic Procedia*, *4*(Icwrcoe), 1001–1007. https://doi.org/10.1016/j.aqpro.2015.02.126

Dooge, J.C.I.(1959). A general theory of the unit hydrograph. *Journal of Geophysical Research.* **14**, 241-256.

Drought impact mitigation and prevention in the Limpopo River Basin: A Situational Analysis. Land and Water Discussion (2004). Food and Agricultural Organisation of the United Nations (FAO). Paper Vol.4. Food and Agriculture Orgnisation of the United Nations, Rome, Italy.

Duan, Q., Sorooshian, S. and Gupta, V.K.(1992). Effective and efficient global optimization for conceptual rainfall-runoff models. *Water Resources Research*. **28**, 1015-1031.

Environmentek, C. S. I. R. (2003). Protection and Strategic Uses of Groundwater Resources in Drought Prone Areas of the SADC Region. Groundwater Situation Analysis of the Limpopo River Basin, Summary Report. Prepared for SADC. CSIR Environmentek Report No. ENV-PC, 47.

Freeze, R. A., & Harlan, R. L. (1969). Blueprint for a physically-based, digitally-simulated hydrologic response model. *Journal of hydrology*, *9*(3), 237-258.

Freeze, R. A. (1972). Role of subsurface flow in generating surface runoff: 2. Upstream source areas. *Water Resources Research*, *8*(5), 1272-1283.

Ganoulis, J. (2009). *Risk analysis of water pollution*. John Wiley & Sons.

Giorgi, F., Jones, C., & Asrar, G. R. (2009). Addressing climate information needs at the regional level: the CORDEX framework. *World Meteorological Organization (WMO) Bulletin*, *58*(3), 175.

Gleick, P. H. (2000). *Water: the potential consequences of climate variability and change for the water resources of the United States*. Pacific Institute for Studies in Development, Environment, and Security

Gnanaseelan, C., Roxy, M. K., & Deshpande, A. (2017). Variability and trends of sea surface temperature and circulation in the Indian Ocean. In *Observed climate variability and change over the Indian Region* (pp. 165-179). Springer, Singapore.

Gnitou, G. T., Ma, T., Tan, G., Ayugi, B., Nooni, I. K., Alabdulkarim, A., & Tian, Y. (2019).

Evaluation of the Rossby Centre Regional Climate Model Rainfall Simulations over West Africa using large-scale spatial and temporal statistical metrics. Atmosphere, 10(12), 802.

Goodall, J. L., Saint, K. D., Ercan, M. B., Briley, L. J., Murphy, S., You, H., ... & Rood, R. B. (2013). Coupling climate and hydrological models: Interoperability through Web Services. *Environmental Modelling & Software*, *46*, 250-259.

Grafton, R. Q., & Hussey, K. (Eds.). (2011). *Water resources planning and management*. Cambridge University Press.

GRDC (The Global Runoff Data Center), 2003. 56068, Koblenz, Germany

Guttman, N. B. (1999). Accepting the standardized precipitation index: a calculation algorithm

1. *JAWRA Journal of the American Water Resources Association*, *35*(2), 311-322.

Hagemann, S., & Dümenil, L. (1997). A parametrization of the lateral waterflow for the global scale. Climate dynamics, 14(1), 17-31.

Heim Jr, R. R. (2002). A review of twentieth-century drought indices used in the United States. *Bulletin of the American Meteorological Society*, *83*(8), 1149-1166.

Helmenstine, Anne Marie, Ph.D. (2020, November 2). How to Calculate Percent Error. Retrieved from https://www.thoughtco.com/how-to-calculate-percent-error-609584

Hoell, A., Funk, C., Zinke, J., & Harrison, L. (2017). Modulation of the southern Africa precipitation response to the El Niño Southern Oscillation by the subtropical Indian Ocean dipole. *Climate Dynamics*, *48*(7), 2529-2540.

Hughes, D.A.(2004). Incorporating ground water recharge and discharge functions into an existing monthly rainfall-runoff model. *Hydrological Sciences Journal*. **49**, 297-311.

Hughes, D. A., Andersson, L., Wilk, J., & Savenije, H. H. (2006). Regional calibration of the Pitman model for the Okavango River. *Journal of Hydrology*, *331*(1-2), 30-42.

Hughes, D.A. and Forsyth, D.A.(2006). A generic database and spatial interface for the application of hydrological and water resource models, Comp. Geosci., 32, 1389–1402

Hughes, D.A. and Mantel, S.K.(2010). Estimating the uncertainty in simulating the impacts of small farm dams on streamflow regimes in South Africa. Hydrological Sciences Journal, 55(4), 578–592. doi:10.1080/02626667.2010.484903

Hughes, D.A., Kapangaziwiri, E. and Sawunyama, T.(2010). Hydrological model uncertainty assessment in southern Africa. J. Hydrol., 387, 221–232.

Hughes, D.A., Kingston, D. G. and Todd, M. C.(2011). Uncertainty in water resources availability in the Okavango River Basin as a result of climate change. Hydrol. Earth Syst., 15, 931–941.

Hulme, M., Doherty, R., Ngara, T., New, M. and Lister, D. (2001). African Climate Change 1900-2100. Climate Res., 17, 145–168

Huntington, T. G. (2006). Evidence for intensification of the global water cycle: Review and synthesis. *Journal of Hydrology*, *319*(1-4), 83-95.

Islam, Z. (2015). *A Review on Physically Based Hydrologic Modeling Submitted by*. (October), 46. https://doi.org/10.13140/2.1.4544.5924

IWMI (International Water Management Institute), World Water and Climate Atlas. www.iwmi.ggiar.org/WAtlas?default.aspx. Accessed 2020.

James, L.D. and S.J. Burges.(1982). Selection, Calibration, and Test- ing of Hydrologic Models. In: Hydrologic Modeling of Small Watersheds, C.T. Haan, H.P. Johnson, and D.L. Brakensiek (Edi- tors). ASAE Monograph, St. Joseph, Michigan, pp. 437-472

Johnston, P., Ziervogel, G., & Matthew, M. (2007). The uptake and usefulness of weather and climate forecast information among water resource managers in the southwest cape region of south africa. in papers and proceedings of applied geography conferences (Vol. 30, p. 380). [np]; 1998

Jones, C., Giorgi, F., & Asrar, G. (2011). The coordinated regional downscaling experiment (CORDEX). An international downscaling link to CMIP5. *CLIVAR exchanges*, *56*.

Kampf, S. K., & Burges, S. J. (2007). Parameter estimation for a physics-based distributed hydrologic model using measured outflow fluxes and internal moisture states. *Water Resources Research*, *43*(12).

Kanaujia, A., & Kumar, A. (2014). Wetlands: Significance, Threats and their Conservation GREEN Quarterly Newsletter-Directorate of Environment, 3-22.

Kapangaziwiri, E. (2008). Revised parameter estimation methods for the Pitman monthly model. *Unpublished MSc Thesis, Rhodes University, Grahamstown, South Africa (available at http://eprints. ru. ac. za/1310/)*.

King, D. M. (2009). *On the importance of input variables and climate variability to the yield of urban water supply systems* (Doctoral dissertation, Victoria University).

Kramm, G., Beier, N., Foken, T., Müller, H., Schröder, P., & Seiler, W. (1996). A SVAT scheme for NO, NO2, and O3—Model description and test results. *Meteorology and Atmospheric Physics*, *61*(1), 89-106.

Krause, P., Boyle, D. P., & Bäse, F. (2005). Comparison of different efficiency criteria for hydrological model assessment. *Advances in geosciences*, *5*, 89-97.

Landform Descriptions of the Limpopo River Basin(n.d) Retrieved from http://www.limpopo.riverawarenesskit.org/LIMPOPORAK_COM/EN/RIVER/GEOGRAPHY/BASIN_LANDSCAPE.HTM

Laprise, R. (2008). Regional climate modelling. *Journal of Computational Physics*, *227*(7), 3641-3666.

Legates, D.R., McCabe Jr. G.J. (1999)m. Evaluating the use of 'Goodness of Fit' Measures in Hydrologic and Hydroclimatic Model Validation. Water Resour. Res., 35(1), 233–241.

Lengaigne, M., Guilyardi, E., Boulanger, J. P., Menkes, C., Delecluse, P., Inness, P., ... & Slingo,

J. (2004). Triggering of El Niño by westerly wind events in a coupled general circulation model. *Climate Dynamics*, *23*(6), 601-620.

Lentswe, G. B., & Molwalefhe, L. (2020). Delineation of potential groundwater recharge zones using analytic hierarchy process-guided GIS in the semi-arid Motloutse watershed, eastern Botswana. *Journal of Hydrology: Regional Studies*, *28*, 100674.

Li, X., He, B., Quan, X., Liao, Z., & Bai, X. (2015). Use of the standardized precipitation evapotranspiration index (SPEI) to characterise the drying trend in southwest China from 1982–2012. *Remote Sensing*, *7*(8), 10917-10937.doi:10.1016/S1364-8152(01)00060-3.

Limpopo Basin Permanent Technical Committee. (2010). Joint Limpopo River Basin Study Scoping Phase: Final Report. *BIGCON Consortium*.

Liu, Y. and Gupta, H.V., 2007. Uncertainty in hydrological modelling: Towards an integrated data assimilation framework. Water Resour. Res., 43. W07401, doi: 10.1029/2006 WR 0 05756

(Lotsane Sub-basin, n.d.). Retrived from http://www.limpopo.riverawarenesskit.org/LIMPOPORAK_COM/EN/RIVER/SUB_BASIN_SUMMARIES/LOTSANE.HTM

Loucks, D.P., van Beek, E., Stedinger, J.R., Dijkman, J.P.M. and Villars, M.T.(2005). Water Resources Systems Planning and Management: An Introduction to Methods, Models and Applications: Studies and Reports in Hydrology Paris, UNESCO PUBLISHING ISBN 92-3-103998-9, 677pp.

Loucks, D. P., & Van Beek, E. (2017). *Water resource systems planning and management: An introduction to methods, models, and applications*. Springer.

Lloyd-Hughes, B., & Saunders, M. A. (2002). A drought climatology for Europe. International Journal of Climatology: A Journal of the Royal Meteorological Society, 22(13), 1571-1592.

Madsen, H., 2000. Automatic calibration of a conceptual rainfall-runoff model using multipleobjectives. Journal of hydrology, 235, issues 3-4(2000): 276-288

Marc Harris. (2015). *The Importance of Water Quality Testing.* SOLitude Lake Management Why is Water Quality Monitoring Important.

Marshall, J., Donohoe, A., Ferreira, D., & McGee, D. (2013). The ocean's role in setting the mean position of the atmosphere's ITCZ. *Clim. Dyn. http://dx. doi. org/10.1007/s00382-013-1767-z*.

McKee, T.B., Doesken, N.J. and Kleist, J., 1993. The relationship of drought frequency and duration to time scales. Proceedings of the 8th Conference on Applied Climatology. AMS, Boston, MA, pp. 179–184. McMahon, T.A., Finlayson, B.L., Haines, A. and Srikanthan R., 1987. Runoff variability: a global perspective. In The Influence of Climate Change and Climatic Variability on the Hydrologic Regime and Water Resources

(Proceedings of the Vancouver Symposium, August 1987). IAHS Publ., 168, 3–11.

Mengelkamp, H. T., Warrach, K., & Raschke, E. (1999). SEWAB–a parameterization of the surface energy and water balance for atmospheric and hydrologic models. *Advances in Water resources*, *23*(2), 165-175.

Moseki, M. L. L. (2013). The geology and tectonic setting of the Shashe-Foley-Tonota area (Central Motloutse Complex), NE Botswana (Doctoral dissertation).

Moelders, N., Raabe, A., & Beckman, T. (1999a). Technique to downscale meteorological quantities for use in hydrological models: Description and first results. IAHS Publication (International Association of Hydrological Sciences), (254), 87-96.

Mölders, N. (2001). Concepts for coupling hydrological and meteorological models.

Mölders, N., Haferkorn, U., Knappe, S., Döring, J., & Kramm, G. (1999b). Evaluation of simulated water budget by means of measurements at Brandis lysimeter station. *Tetzlaff G, GruÈnewald U (eds.)*, *2*, 67-83.

Mölders, N., & Rühaak, W. (2001). Sensitivity studies with a surface and channel runoff module cou-pled to a mesoscale atmospheric model. *Meteorologische Arbeiten aus Leipzig (VI)*.

Moore C. and Doherty J., (2005), Role of the calibration process in reducing model predictive error, Water Resources Research, 41(W05020).

Moradkhani, H. and Sorooshian, S., 2008. General review of rainfall-runoff modeling: model calibration, data assimilation, and uncertaintyanalysis. Hydrological modeling and the water cycle.Springer. 291 p. ISBN 978-3-540-77842-4.

Mosase, E., & Ahiablame, L. (2018). Rainfall and temperature in the Limpopo river basin, Southern Africa: means, variations, and trends from 1979 to 2013. *Water*, *10*(4), 364.

Moses, O. (2017). Heat wave characteristics in the context of climate change over the past 50 years in Botswana. Botswana Notes and Records, 49, 13-25.

Mwelwa, E.M., 2004. The application of a monthly time step Pitman rainfall-runoff model to the Kafue river basin of Zambia. MSc. Thesis, Rhodes University

Nachtergaele, F. (2010, August). The classification of leptosols in the world reference base for soil resources. In 19th World Congress of Soil Science, Soil Solutions for a Changing World (pp. 1-6).

Nash, J. E. and Sutcliffe, J. V., 1970. River flow forecasting through conceptual models. Part 1: A discussion of principles. J. Hydrol., 10(3), 282–290.

National Center for Atmospheric Research Staff (Eds). Last modified 08 May 2020. "The Climate Data Guide: CRU TS Gridded precipitation and other meteorological variables since 1901." Retrieved from https://climatedataguide.ucar.edu/climate-data/cru-ts-gridded-precipitation-and-other-meteorological-variables-1901.

Nielbock, M. (2017). The Intertropical Convergence Zone. arXiv preprint arXiv:1708.09324.

Nkemelang, T., New, M., & Zaroug, M. (2018). Temperature and precipitation extremes under current, 1.5 C and 2.0 C global warming above pre-industrial levels over Botswana, and implications for climate change vulnerability. Environmental Research Letters, 13(6), 065016.

Oosthuizen, N., Hughes, D. A., Kapangaziwiri, E., Mwenge Kahinda, J. M., & Mvandaba, V. (2018). Parameter and input data uncertainty estimation for the assessment of water resources in two sub-basins of the Limpopo River Basin. *Proceedings of the International Association of Hydrological Sciences*, *378*, 11-16.

Othman, N., Romali, N. S., Samat, S. R., & Ahmad, A. M. (2021, March). Calibration and validation of hydrological model using HEC-HMS for Kuantan River Basin. In *IOP Conference Series: Materials Science and Engineering* (Vol. 1092, No. 1, p. 012028). IOP Publishing.

Pabón, J. D., & Dorado, J. (2008). Intraseasonal variability of rainfall over Northern South America and Caribbean region. *Earth Sciences Research Journal*, *12*(2), 194-212

Patt, A. G., Ogallo, L., & Hellmuth, M. (2007). Learning from 10 years of climate outlook forums in Africa. *Science*, *318*(5847), 49-50.

PBA. 2007. Assessment of the Flood Hydrology of the Limpopo River. Eskom Environmental Impact Assessment for MMamabula-Delta 4 x 400Kv Transmission Power-lines. Eskom, Johannesburg, South Africa.

Pechlivanidis, I. G., Jackson, B. M., Mcintyre, N. R., & Wheater, H. S. (2011). Catchment scale hydrological modelling: A review of model types, calibration approaches and uncertainty analysis methods in the context of recent developments in technology and applications. *Global Nest Journal*, *13*(3), 193–214.

Peters, G. (2016). Identifying and valuing the functions of floodplains. In *The 2016 Floodplain Management Association National Conference* (pp. 1-16).

Pianosi, F., Sarrazin, F. and Wagener, T. (2015). A Matlab toolbox for Global Sensitivity Analysis. Environmental Modelling & Software, 70. http://dx.doi.org/10.1016/j.envsoft.2015.04.009

Potopová, V., Štěpánek, P., Možný, M., Türkott, L., & Soukup, J. (2015). Performance of the standardised precipitation evapotranspiration index at various lags for agricultural drought risk assessment in the Czech Republic. *Agricultural and Forest Meteorology*, *202*, 26-38.

Raucher, R.S., 2011. The Future of Research on Climate Change Impacts on Water: a Workshop Focusing on Adaptation Strategies and Information Needs. Tech. Rep., Water Research Foundation

Razavi, S., & Gupta, H. V. (2015). What do we mean by sensitivity analysis? The need for comprehensive characterisation of “global” sensitivity in E arth and E nvironmental systems models. *Water Resources Research*, *51*(5), 3070-3092.

Refsgaard, J.C.,1996. Terminology, modelling protocol and classification of hydrologic model codes. Distributed Hydrologic Modelling, edited by Michael B. Abbott and Jens C. Refsgaard, 41-54.

Riahi, K., Rao, S., Krey, V., Cho, C., Chirkov, V., Fischer, G., ... & Rafaj, P. (2011). RCP 8.5—

A scenario of comparatively high greenhouse gas emissions. Climatic change, 109(1), 33-57.

Saltelli, A., Tarantola, S., Campolongo, F., & Ratto, M. (2004). *Sensitivity analysis in practice: a guide to assessing scientific models* (Vol. 1). New York: Wiley.

Santhi, C., Arnold, J. G., Williams, J. R., Dugas, W. A., Srinivasan, R., & Hauck, L. M. (2001). Validation of the swat model on a large rwer basin with point and nonpoint sources 1. *JAWRA Journal of the American Water Resources Association*, *37*(5), 1169-1188.

SARDC, 2008, Southern African Environment Outlook. SADC, SARDC, IUCN, UNEP,Gaborone/Harare, Nairobi, 56pp.

Sausen, R., Schubert, S., & Dümenil, L. (1994). A model of river runoff for use in coupled atmosphere-ocean models. *Journal of Hydrology*, *155*(3-4), 337-352.

Schulze, R. E. (2005). Setting the scene: the current hydroclimatic "Landscape" in Southern Africa. *Climate Change and water Resources in Southern Africa: Studies on Scenarios, Impacts, Vulnerabilities and Adaptation. Pretoria: WRC*, *1430*(1), 05.

Sharma, K. D., Sorooshian, S. and Wheater, H., 2008. Hydrological Modelling in Arid and Semi-Arid Areas. New York : Cambridge University Press. 223 p. ISBN-13 978-0-511-37710-5.

Shiklomanov, I. A. (1998). A summary of the monograph World Water Resources. *A new appraisal and assessment for the 21st Century. UNEP: Society and Cultural Organization*

Sitoe, S., & Qwist-Hoffman, P. (2013). Limpopo River Basin Monograph.

Sitterson, J., Knightes, C., Parmar, R., Wolfe, K., Avant, B., & Muche, M. (2018). An overview of rainfall-runoff model types.

SMEC/EHES, 2006. National Water Master Plan Review: Volume 4 Groundwater Resources. Government of Botswana: Department of Water and Sanitation, Gaborone.

Solomon, S., Qin, D., Manning, M., Alley, R. B., Berntsen, T., Bindoff, N. L., & Wratt, D. (2007). Technical summary. Climate change: the physical science basis. In: Solomon, Susan, Qin, Dahe, Manning, Martin,Marquis, Melinda, Averyt, Kristen, Melinda, M., Tignor, B., LeRoy Miller Jr., Henry, Chen,Zhenlin (Eds.), Contribution of Working Group I to the Fourth Assessment Report of theIPCC. Cambridge University Press, Cambridge, UK and New York, NY

Song, X., Zhang, J., Zhan, C., Xuan, Y., Ye, M., & Xu, C. (2015). Global sensitivity analysis in hydrological modeling: Review of concepts, methods, theoretical framework, and applications. *Journal of hydrology*, *523*, 739-757.

Sorooshian S. and Gupta V.K., (1995), Model Calibration, Computer models of watershed hydrology, edited by Singh, V.P., Water Resources Publications, USA.

Tallaksen, L. M., & Van Lanen, H. A. (Eds.). (2004). Hydrological drought: processes and estimation methods for streamflow and groundwater.

Tan, Y., Guzman, S. M., Dong, Z., & Tan, L. (2020). Selection of effective GCM bias correction methods and evaluation of hydrological response under future climate scenarios. Climate, 8(10), 108.

Terray, P. (2011). Southern Hemisphere extra-tropical forcing: a new paradigm for El Niño-Southern Oscillation. *Climate dynamics*, *36*(11-12), 2171-2199.

Tessema, S. M. (2011). Hydrological modeling as a tool for sustainable water resources management: a case study of the Awash River Basin. In *Trita-LWR. LIC NV - 2056*. Retrieved from http://kth.diva-portal.org/smash/get/diva2:416594/FULLTEXT01.pdf%0Ahttp://urn.kb.se/resolve?urn=urn:nbn:se:kth:diva-33617

Teutschbein, C. (2013). *Hydrological modeling for climate change impact assessment: transferring large-scale information from global climate models to the catchment scale* (Doctoral dissertation, Department of Physical Geography and Quaternary Geology, Stockholm University).

Thornthwaite, C.W., 1948. An approach toward a rational classification of climate. Geogr. Rev. 38, 55–94.

Tirivarombo, S. (2012). Climate variability and climate change in water resources management of the Zambezi River basin (Doctoral dissertation, Rhodes University).

Tirivarombo, S., Osupile, D., & Eliasson, P. (2018). Drought monitoring and analysis: standardised precipitation evapotranspiration index (SPEI) and standardised precipitation index (SPI). *Physics and Chemistry of the Earth, Parts A/B/C*, *106*, 1-10.

Todd, M. C., Taylor, R. G., Osborn, T., Kingston, D., Arnell, N.W., and Gosling, S. N. (2010). Quantifying the impact of climate change on water resources at the basin scale on five continents a unified approach, Hydrol. Earth Syst. Sci. Discuss., 7, 7485–7519.

Törnros, T., & Menzel, L. (2014). Addressing drought conditions under current and future climates in the Jordan River region. *Hydrology and Earth System Sciences*, *18*(1), 305-318.

Tsheko, R. (2003). Rainfall reliability, drought and flood vulnerability in Botswana. Water Sa, 29(4), 389-392.

Tumbo, M., & Hughes, D. A. (2015). Uncertain hydrological modelling: application of the Pitman model in the Great Ruaha River basin, Tanzania. Hydrological Sciences Journal, 60(11), 2047-2061.

Uhlenbrook, S., Roser, S., & Tilch, N., 2004. Hydrological process representation at the meso-scale: the potential of a distributed, conceptual catchment model. Journal of Hydrology, 291(3-4), 278-296.

United Nations Development Programme, 2012. Botswana Water Sector Policy Brief Reflecting on the Challenges of Attaining a Green Economy1 for Botswana, Gaborone: United Nations Development Programme.

USAID (2015). Risk Vulnerability & Resilience in the Limpopo River Basin. Climate Change, Water and Biodiversity – a synthesis. URL:https://www.climatelinks.org/sites/default/files/asset/document/Risk,%20Vulnerability%20and%20Resilience%20in%20the%20Limpopo%20River%20Basin%20-%20A%20Synthesis_0.pdf

Van Loon, A. F. (2015). Hydrological drought explained. Wiley Interdisciplinary Reviews: Water, 2(4), 359-392.

Van Vuuren DP, Den Elzen MGJ, Lucas PL, Eickhout B, Strengers BJ, Van Ruijven B, Wonink S, Van Houdt R (2007) Stabilizing greenhouse gas concentrations at low levels: an assessment of reduction strategies and costs. Clim Chang 81:119–159

Van Vuuren, D. P., Edmonds, J., Kainuma, M., Riahi, K., Thomson, A., Hibbard, K., ... & Rose, S. K. (2011). The representative concentration pathways: an overview. *Climatic change*, *109*(1), 5-31.

Vaze, J., Jordan, P., Beecham, R., Frost, A., Summerell, G., 2012. Guidelines for rainfall-runoff modelling: Towards best practice model application. pp. 47.

Vegetation in the Basin(n.d) Retrieved from http://www.limpopo.riverawarenesskit.org/LIMPOPORAK_COM/EN/RIVER/GEOGRAPHY/VEGETATION_IN_THE_BASIN.HTM

Vellinga, M., & Wood, R. A. (2002). Global climatic impacts of a collapse of the Atlantic thermohaline circulation. *Climatic change*, *54*(3), 251-267.

Vicente-Serrano, S. M., Beguería, S., & López-Moreno, J. I. (2010). A multiscalar drought index sensitive to global warming: the standardized precipitation evapotranspiration index. *Journal of climate*, *23*(7), 1696-1718.

Vrugt, J.A., Gupta, H.V., Bouten, W. and Sorooshian, S., 2003. A Shuffled Complex Evolution Metropolis algorithm for optimization and uncertainty assessment of hydrologic model parameters. *Water Resources Research*, **39**, 1201.

Vrugt, J.A., Diks, C.G.H., Gupta, H.V., Bouten, W., Jacobus, M. and Verstraten, J.M, 2005. Improved treatment of uncertainty in hydrologic modeling: Combining the strengths of global optimization and data assimilation. Water Resour. Res., 41. W01017, doi: 10. 10 2 9/2004WR003059.

Wagener T., Wheater H.S. and Gupta H.V., (2004), Rainfall-Runoff Modelling in Gauged and Ungauged Catchments. Imperial College Press, London, UK, 1-306 pp.

Wagener, T. and Wheater, H.S.(2006). Parameter estimation and regionalization for continuous rainfall–runoff models including uncertainty. Journal of Hydrology, 320 (1–2), 132–154.doi:10.1016/j.jhydrol.2005.07.015

Wang, Q., Shi, P., Lei, T., Geng, G., Liu, J., Mo, X., ... & Wu, J. (2015). The alleviating trend of drought in the Huang-Huai-Hai Plain of China based on the daily SPEI. *International Journal of Climatology*, *35*(13), 3760-3769.

Weedon, G. P. G. Balsamo, N. Bellouin, S. Gomes, MJ Best, and P. Viterbo, 2014: The WFDEI meteorological forcing data set: WATCH Forcing Data methodology applied to ERA-Interim reanalysis data. *Water Resour. Res*, *50*, 7505-7514.

Wise, M., Calvin, K., Thomson, A., Clarke, L., Bond-Lamberty, B., Sands, R., ... & Edmonds, J. (2009). Implications of limiting CO2 concentrations for land use and energy. Science, 324(5931), 1183-1186.

Wheater, H., Sorooshian, S., & Sharma, K. D. (Eds.). (2007). *Hydrological modelling in arid and semi-arid areas*. Cambridge University Press.

Wheater, H. S. (2008). Modelling hydrological processes in arid and semi-arid areas: an introduction to the workshop. *Hydrological modelling in arid and semi-arid areas*, 1-20.

White, K. L., & Chaubey, I. (2005). Sensitivity analysis, calibration, and validations for a multisite and multivariable SWAT model. *Journal of the American Water Resources Association*, *41*(5), 1077–1089. https://doi.org/10.1111/j.1752-1688.2005.tb03786.x

Wilby, R. L., C. W. Dawson, and E. M. Barrow (2002), SDSM - a decision support tool for the assessment of regional climate change impacts, Environ Modell Softw, 17(2), 145–157, Wang, L., D'odorico, P., Ringrose, S., Coetzee, S., & Macko, S. A. (2007). Biogeochemistry of Kalahari sands. *Journal of Arid Environments*, *71*(3), 259-279.

Wilby, R. L., P. G. Whitehead, A. J. Wade, D. Butterfield, R. J. Davis, and G. Watts (2006), Integrated modelling of climate change impacts on water resources and quality in a lowland catchment: River Kennet, UK, J Hydrol, 330(1- 2), 204–220, doi:10.1016/j.jhydrol.2006.04.033

Winker, T.(1980). Sand Rivers of Botswana. A Reconnaissance of the Major Sand Rivers. Department of Water and Sanitation, Gaborone.

Yan, Y. Y. (2005). Intertropical convergence zone (ITCZ). *Encyclopedia of World Climatology*, 429-432.

Yang, W., Andréasson, J., Phil Graham, L., Olsson, J., Rosberg, J., & Wetterhall, F. (2010). Distribution-based scaling to improve usability of regional climate model projections for hydrological climate change impacts studies. *Hydrology Research*, *41*(3-4), 211-229.

Zakaria, Z., Gairola, S., & Shariff, N. M. (2010). Effective microorganisms (EM) technology for water quality restoration and potential for sustainable water resources and management.

Zeinalie, M., Bozorg-Haddad, O., & Chaplot, B. (2021). Modeling and Simulation in Water Resources Management. In Essential Tools for Water Resources Analysis, Planning, and Management (pp. 1-31). Springer, Singapore.

Zhu, T., & Ringler, C. (2010). Climate change implications for water resources in the Limpopo River Basin (No. 961). International Food Policy Research Institute (IFPRI)